Glacier Sensitivity and Regional Climate: Past and Present

Summer Burton Rupper

A dissertation
submitted in partial fulfillment of the
requirements for the degree of

Doctor of Philosophy

University of Washington

2007

Program Authorized to Offer Degree:
Earth and Space Sciences

University of Washington
Graduate School

This is to certify that I have examined this copy of a doctoral dissertation by

Summer Burton Rupper

and have found that it is complete and satisfactory in all respects,
and that any and all revisions required by the final
examining committee have been made.

Chair of the Supervisory Committee:

_____
Gerard Roe

Reading Committee:

_____
Gerard Roe

_____
Eric J. Steig

_____
David Battisti

_____
Alan Gillespie

Date: March 15, 2007

In presenting this dissertation in partial fulfillment of the requirements for the doctoral degree at the University of Washington, I agree that the Library shall make its copies freely available for inspection. I further agree that extensive copying of the dissertation is allowable only for scholarly purposes, consistent with "fair use" as prescribed in the U.S. Copyright Law. Requests for copying or reproduction of this dissertation may be referred to ProQuest Information and Learning, 300 North Zeeb Road, Ann Arbor, MI 48106-1346, 1-800-521-0600, to whom the author has granted "the right to reproduce and sell (a) copies of the manuscript in microform and/or (b) printed copies of the manuscript made from microform."

Signature_____

Date_____

University of Washington

Abstract

Glacier Sensitivity and Regional Climate: Past and Present

Summer B. Rupper

Chairs of the Supervisory Committee:
Assistant Professor Gerard Roe
Associate Professor Eric Steig
Earth and Space Sciences

This study develops a surface energy- and mass-balance model with which to understand the interactions between glaciers and climate on regional-scales. This model is applied to Central Asia because of the diverse climate regimes and glacier history. The model is used to understand the sensitivity of equilibrium line altitudes (ELAs) to modern interannual climate variability, and to reconcile patterns of ELA changes with climate changes during the early Holocene and Last Glacial Maximum (LGM) in Central Asia. Patterns in the present day climate give rise to patterns in the dominant ablation mechanisms at the ELA. In turn the patterns in ablation give rise to patterns in glacier sensitivity to climate changes. In particular, ELAs in melt-dominated regions are most sensitive to interannual variability in temperature. ELAs in sublimation-dominated regions are most sensitive to interannual variability in precipitation. The patterns of glacier advance and retreat during the early Holocene and LGM, in the melt-dominated regions, are both due to the patterns in temperature change. Glaciers in sublimation-dominated regions are highlighted as being acutely sensitive to even small changes in numerous atmospheric variables. For present day, Holocene, and LGM, changes in clouds are important in all regions through their influence on the shortwave and longwave radiative fluxes, which dominate the surface energy balance at the ELA. This work highlights the importance of a systematic analysis of the sensitivity of glaciers to changes in climate.

TABLE OF CONTENTS

LIST OF FIGURES

LIST OF TABLES

ACKNOWLEDGEMENTS

The author wants to express sincere appreciation for the continuing support of my advisors and friends, Gerard Roe and Eric Steig. I want to thank Gerard for the many hours of stimulating conversations, both on the phone and in front of the computer, as well as the late night pool games, without which this dissertation would not have been possible or as much fun. I'd like to thank Eric for his encouragement and never ending enthusiasm, and for opening his home to my family and me. I thank my mom, dad, Steve, Mary, brothers, sisters- and brothers-in-law for providing support, love, and encouragement throughout graduate school. I want to thank my children, Abigail and Eli, for providing much needed distractions from my graduate work and for teaching me the most important lessons in life – such as the fact that the foam under the carpet tastes better than the carpet itself, there are several ways to tie shoe laces, it will someday be possible to fly to the stars in a pink airplane, and ducks aren't the only things that quack. I especially want to thank my husband, Adam, for his patience and love, and for always believing in me (and for teaching our children that ducks aren't the only things that quack).

DEDICATION

To my husband, children, and parents.

Chapter One

AN INTRODUCTION TO THE INTERACTIONS BETWEEN GLACIERS AND CLIMATE

1.1 Motivation

Glaciers are excellent recorders of properties of the atmosphere, retreating and advancing in direct response to changes in accumulation and ablation. Thus histories of glacier variability are some of the most useful records of paleoclimate. In many parts of the world the glacier history is the primary descriptor of the climate history beyond the instrumental record, particularly where glacier deposits are widespread and confidently dated. Indeed, the history of advance and retreat of mountain glaciers and ice caps have played a central role in the description of the earth's climate history (e.g., Porter, 1977; Porter, 1985; Gillespie and Molnar, 1995; Lowell et al., 1995; Kaufman et al., 2004). These very observations first prompted the realization that the earth had undergone dramatic swings in climate many times during the Pleistocene epoch.

This dissertation focuses on the climate and glacier histories in Central Asia. There is a remarkable temporal and spatial pattern of glacier advances and retreats across Asia during the last glacial cycle (~100,000 years) (e.g., Gillespie and Molnar, 1995). These glacier changes are not synchronous with the high-latitude

ice sheets, which have been used to describe the pacing and sequencing of ice ages world wide. The observations in Central Asia, therefore, challenge the global applicability of such sequencing, suggesting instead a large degree of regional variability. Yet, researchers have historically focused on global-scale changes in climate, and on making associations between widely separated proxy climate records. This is perhaps, at least in part, due to sparse data sets of an array of proxy variables that only indirectly reflect climate variables. The further back in time, the more sparse the data tends to be. For example, debates over the global nature of such paleoclimatic events as the Little Ice Age, Medieval Warm Period, and the Younger Dryas are ongoing (Lowell et al., 1995; Broecker, 2003; Roe and Steig, 2004; Wunsch, 2006), highlighted by the inclusion of a section in the IPCC report (2001) entitled "Was there a Little Ice Age and a Medieval Warm Period."

Patterns in climate change should be expected from modern observations and modeling. Indeed, the idea that climate variability tends to be expressed in spatial patterns is central to modern climate dynamics. The classic example of this is the El Niño Southern Oscillation (ENSO). Shifts in the pattern in tropical sea-surface temperatures from year to year associated with ENSO give rise to global changes in climate, but manifested differently in different regions. For example, patterns in precipitation arise in response to ENSO variability through shifts in the locations of storm tracks and monsoonal circulations (e.g., Ropelewski and

Halpert, 1987; Bradley et al., 1987; Dai and Wigley, 2000). Climate model simulations that include a doubling of CO_2 predict spatial and temporal patterns in climate change in response to a uniform increase in anthropogenic greenhouse gas emissions. For example, these models predict that temperature increases will be greatest at high latitudes and over continents when CO_2 emissions are doubled (IPCC, 2001). Thus different climatic responses to what is generally thought of as a uniform forcing are evident in modern climate variability, as well as model simulations of future climate scenarios. Spatial patterns in climate change should extend to past climates as well. There are several instances where this has to be the case. For example, while the Laurentide and Fenno-Scandinavian ice sheets covered large parts of North America and Europe, there is little evidence for substantial ice over Siberia or Alaska. This is most likely the result of large spatial patterns in and regional sensitivity to accumulation and/or temperature (e.g., Pollard, 2000). The challenge therefore, is to reconcile the glacier histories with the mechanisms driving them in order to understand both the regional nature of such changes, and the global applicability of the regional climate history.

The above discussion highlights the potential importance of glacier changes as climate indicators, past and present. Despite their obvious importance, there is still much ambiguity as to which atmospheric variables glaciers are most sensitive to, and how that sensitivity may change from one region to the next. For example, Casal et al. (2004) suggest that monsoonal precipitation is the primary

influence on the glacier mass balance (accumulation minus ablation) during the Holocene in the southern and central regions of the Tibetan Plateau. Oerlemans and Fortuin (1992) state that, in general, the mass balance of glaciers in wetter regimes (such as the monsoonal regions of the Himalaya) is more sensitive to changes in temperature than those in drier regions. Along these lines, a detailed study of the sensitivity of glacier AX010 in the Nepalese Himalaya to changes in climate suggests that that particular glacier is sensitive to both changes in temperature and precipitation (Kaystha et al., 1999). Yet most studies attribute the advance of glaciers in the southern Himalaya during the early Holocene to an increase in monsoonal precipitation only (Benn and Owen, 1998; Finkel et al., 2003; Owen et al., 2003). These studies are just an example of some of the ambiguity about glacier-climate interactions in the published literature. A working knowledge of how glaciers respond to changes in climate requires an understanding of which atmospheric variables have the greatest influence on glacier mass balance, and how that may change for different climate regimes. Several approaches have been used to estimate glacier ablation and the link between changes in mass balance and climate. A very general discussion of these approaches follows. A more detailed discussion of the various techniques and how this dissertation expands upon previous work is included in Section 1.2.

Most studies that focus on a regional sensitivity of glaciers to changes in climate use simplified representations of ablation. Typically ablation is assumed to be

proportional to some measure of summertime temperature (e.g., Braithwaite, 1995; Casal et al., 2004; Zhang et al., 2006). Such ablation parameterizations are appealing in their simplicity and the results from using them can be easily interpreted. However, this simplified approach to estimating ablation neglects sublimation as well as other potentially important atmospheric variables such as wind speed, relative humidity, and cloudiness. These variables are thought to be of particular importance in lower-latitude, high-altitude glaciers (e.g., Hasternath, 1992; Molg and Hardy, 2004). In addition to the above assumptions, this type of approach also requires use of a melt factor that relates the measure of summer temperature to the ablation rate, and which is an empirically-determined parameter. Yet studies of different glaciers suggest melt-factors commonly vary from place-to-place by about a factor of two (e.g., Paterson, 1999), and less commonly by as much as five (Kayastha et al., 2002; Zhang et al., 2006).

Moreover it is not, of course, temperature *per se* that causes ablation, but rather it is heat. Therefore a more physically based approach is to perform a self-consistent calculation of the energy balance at the glacier surface. Such models have the advantage that all the relevant atmospheric variables are included, and that both sublimation and surface melting are a product of the calculation. Thus the relative importance of different atmospheric variables and different ablation processes can be clearly evaluated and understood. These models have been applied successfully to single glaciers and basins, and have been used to

understand the relationship between a glacier and the local climate (e.g., Kayastha et al., 1999; Molg and Hardy, 2004).

This dissertation examines climate-glacier interactions on a regional scale. It creates a framework with which to reconcile the regional changes in climate with the observed glacier responses. This framework includes the development of a glacier mass-balance model that integrates the relevant physics of a surface energy-balance model, but adapted for use at spatial scales much larger than single basins. This model, in combination with a simpler mass-balance model, is then applied to Central Asia. Spatial patterns in modern climate, glacier histories, and simulations of past climates dominate the region of Central Asia.

The rest of this chapter provides an introduction to the components of this research and background information necessary to place the results in context. Information about modeling of glacier mass balance is presented in section 1.2. On the basis of this information, the glacier-climate interactions in Central Asia are assessed using glacier mass-balance models. Section 1.3 provides background information on Central Asian glacier history. This is followed by a summary of the atmospheric circulation and climate of Central Asia in Section 1.4. Sections 1.3 and 1.4 provide justification for the use of Central Asia as a case study region. An outline of the research presented in the main body of the dissertation is provided in section 1.4.

1.2 Estimating Glacier Ablation

As mentioned above, there are several approaches to estimating glacier ablation. The most commonly utilized technique applied at a regional scale is one that assumes ablation is proportional to some measure of temperature (hereafter noted as the temperature-ablation method). This has been a useful approach in many instances. For example, Oerlemans (2005), under the assumption that temperature changes are the primary drivers of glacier fluctuations over decades to centuries, reconstructed a temperature history for many parts of the world from glacier length changes. This study provided complementary evidence on the magnitude of the current global warming, the timing that this warming began, and that this warming is global in nature. There are many other examples where this temperature-ablation method has been used to gain very useful insights into the basic relationships between glacier changes and climate (e.g., Braithwaite, 1995; Fountain et al., 1999). Specific to Central Asia, the region of interest in this dissertation, Casal et al. (2004) applied the temperature-ablation method to the Tibetan Plateau to evaluate the net annual mass balance for modern climate and periods extending back 11,000 years. They use positive degree days (PDDs; a measure of summertime temperature) and a melt factor to convert PDDs into an amount of melt. They determined that the present-day mass balance is negative over most of the plateau, with small regions of positive balance. In addition, their results show an increasingly less negative mass balance since 11,000 years ago,

suggesting that the possibility of ice sheet growth has increased since the beginning of the Holocene. Although both of these examples highlight the use of these simple temperature-ablation mass-balance models, they require tuning (melt factors) that is sensitive to location and likely to be sensitive to climate state. Without data to tune the melt factors, Casal et al. (2004) extrapolated degree day melt factors from higher latitudes to the Tibetan Plateau.

A more physically based approach to estimate ablation is that using a surface energy-balance model. These models include calculations of all relevant energy fluxes at the surface using atmospheric variables (such as temperature, wind, humidity) and surface conditions (such as the albedo and surface roughness). When the surface temperature is zero, any excess energy available is used to melt. When surface temperatures are below zero, energy from turbulent latent heat flux is used to sublimate. Thus this approach allows for a detailed diagnosis of the glacier sensitivities to atmospheric variables, and allows for an assessment of the importance of sublimation and melt. Examples where this approach has been applied to the Himalayas and the tropics are discussed below. These examples highlight the important information that surface energy-balance models provide.

Kayastha et al. (1999) formulated a mass-balance model based on the energy balance at the snow or ice surface of glacier AX010 in the Nepalese Himalaya. Their model agrees well with mass-balance measurements on the glacier surface,

within the uncertainty of the mass-balance measurements and atmospheric data used in the model. In tests of the sensitivity of the mass balance to changes in climate, they find that the mass balance is strongly sensitive to precipitation and summer air temperature and only weakly sensitive to relative humidity. This example highlights the ability of these models to test mass-balance sensitivity to many atmospheric variables. In a similar approach, Molg and Hardy (2001) estimate the energy balance on a glacier at the summit of Kilimanjaro. They use this estimate to describe the interaction between ablation and climatic forcing. They conclude that sublimation is the dominant process for the recent ablation of this glacier, despite some evidence of melt along the glacier margins and at selected sites on the glacier surface. In addition, their results corroborate others for Kilimanjaro – that these glaciers are extremely sensitive to precipitation variability, and, in particular the influence of precipitation on the albedo of the glacier surface (e.g. Hastenrath, 1994; Kaser, 2001; Kaser et al., 2004). Given that glaciers respond to both regional changes in climate as well as local conditions, it is difficult to apply the results from studies of single glaciers, such as those above, to other regions. Therefore there is a great need for a physically based approach that can be applied at a regional scale.

I adapt a self-consistent energy-balance model akin to that of Molg and Hardy (2004) and Kayastha et al. (1999) that is appropriate at a regional scale. Surface conditions, such as the albedo, must be parameterized, but the seasonality in

atmospheric variables is included. Thus the surface energy- and mass-balance (SEMB) model can be used test the sensitivity of glaciers to changes in climate at a regional scale. The results from the SEMB model are also used to assess the appropriateness of the simpler temperature-ablation method.

Both a simpler temperature-ablation scheme and the SEMB model are applied to Central Asia under conditions appropriate for present day, the mid-Holocene (6 ka), and the Last Glacial Maximum (21 ka). The results are compared to the geologic evidence of glacier advances and retreats. Thus a discussion of the glacier history in Central Asia, followed by an introduction to the modern climate dynamics and climate history of the region is warranted.

1.3 Central Asian Glacier History

Until the early 1990s it was generally assumed that alpine glacier advances in Central Asia were synchronous with those of high-latitude ice sheets (e.g., Anderson and Prell, 1993, Emeis et al., 1995, Kuhle, 1998). As more extensive and reliable numerical dates have become available, it has become evident that these advances were not even synchronous within Asia itself (e.g., Schafer et al., 2002; Wei et al., 2006), or elsewhere (e.g., Gillespie and Molnar, 1995) (Figure 1.1). Thus the glacier history in Central Asia over the last glacial cycle is a very

promising record to use in addressing the issue of global versus regional climate change.

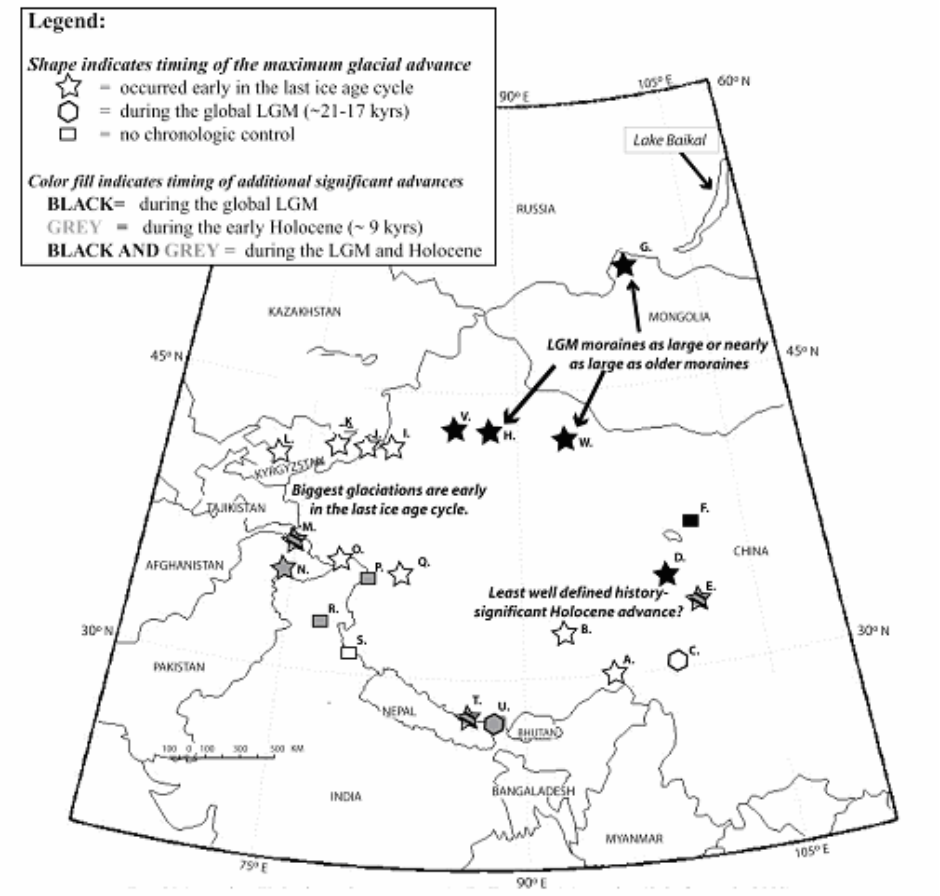

Figure 1.1: Sites in Asia where there is information related to the timing and extent of Quaternary glaciation. This figure highlights evidence for glacier advances for three specific periods: during the early Holocene, during the LGM, and prior to the LGM. Figure courtesy of Matthew Kuharic, but modified to include new data. A. Bomi Mountains (Kuharic et al., in progress) B. Tanggula Mountains (Schafer et al., 2002) C. Litang (Schafer et al., 2002) D. Nianbaoyese Mountains (Owen et al., 2003) E. Anyemaqen Mountains (Owen Et al., 2003) F Qilian Shan (Owen et al., 2003) G. Jarai and Tingis Rivers (Merle et al., 2000) H. Die Han Je Le Gou (Clark et al., 2001) I. Muzart He (Clark et al., 2001) J. Kyrgyz Front Range (Koppes et al., 2003) K. Issyk-Kul Basin (Koppes et al., 2003) L. Southern Kyrgyz Front Range (Koppes et al., 2003) M. Hunza Valley, Karakoram Mountains (Owen et al., 2002) N. Nanga Parbat (Phiips et al., 2000) O. Karakax Valley (Clark et al., 2001) P. Aksayqin Basin (Koppes et al., 2003) Q. Kunlun Mountains (Koppes et al., 2003) R. Lahul Himalaya (Owen et al., 2001) S. Garhwal Himalaya (Barnard et al., 2003) T. Everest Region (Finkel et al., 2003) U. Kanchenjunga Himal (Tsukamoto et al., 2002) V. Daxigou (Gillespie and Burke, 2000) W. Karlik Shan (Burke et al., 2003).

Glacier deposits in Central Asia have been dated using numerous different techniques including: C^{14}, thermal luminescence (TL), optically stimulated luminescence (OSL), cosmogenic radionuclides (CRN), and electron spin resonance (ESR) (e.g., Wang et al., 1981; Owen et al., 2002; Zhoa et al., 2001; Ju, 2004; and Yang et al., 2003). Where deposits have been reliably dated, glacier extent provides a snapshot in the glacial history. In particular, glaciers are known to be sensitive to climatic factors such as precipitation (usually as snow) and summer temperatures. Both the terminus and equilibrium-line altitude (ELA, where accumulation equals ablation) of the glacier rise with increased temperatures and fall with increased snowfall. Because the ELA and terminus position covary, considerable effort has been invested in recovering paleoELAs from the highest elevation of the lateral moraines, the altitude difference between the terminus and headwall (THAR), the accumulation/ablation area ratio (AAR), and other measures of glacier shape (e.g., Benn and Owen, 1998). Therefore it is, in principle, possible to infer past climate changes from ELA reconstructions.

Gillespie et al. (2003) argue for three zones in Central Asia within which glaciers have behaved differently over the last ~100 ka, as defined by the changes in ELA. In particular they focus on evidence for glacier advances within three time periods: pre-LGM (~115 – 35 ka), LGM (~22 – 18 ka), and the early Holocene (~11 – 8 ka). Although the long pre-LGM period designated here can obviously be subdivided, and information for other periods such as the Little Ice Age is

available, this simple organization is useful for understanding the broad outlines of Central Asia's glacial climate. I briefly summarize what is known about the timing and extent of glacier advances during these three time periods, with a particular focus on changes in ELA, in the three zones.

1.3.1 Western Zone

The western zone includes the Kyrgyz Tien Shan south to the Karakoram and east to central Tibet. Significant work has been done in this vast region to define the timing of Quaternary glaciations (Sites I-S, Figure 1.1). Here, the largest glacial advances occurred before the LGM at all sites where the dating is constrained. The ELA depressions that Shi (2002, his Figure 6) report range from 1000 m in the southern and western sides of the ranges to 300-500 m in the arid Tibetan Plateau. He reports these changes in ELA as "LGM" depressions. However, they most likely correspond to the early maximum advances as evidence of significant advances during the LGM throughout this zone is lacking. Abramowski et al. (2006) report pre-LGM ELA depressions for the western zone ranging between 370-380 m in the eastern Pamir and >750 and 600 m in the Alay-Turkestan Range.

Abramowski et al. (2006) report Be^{10} ages corresponding to the pre-LGM, LGM, and Holocene for glacier advances in the Pamir and the Alay-Turkestan Range.

They, however, emphasize that the largest advances throughout the region were during the pre-LGM. Owen et al. (2002) report dates for two minor valley glaciations in the Karakoram at Pakistan's northern most tip. The dates, 25.7-21.8 ka and 18.4-15.3 ka, bracket the LGM, and the glaciers were smaller than the pre-LGM advances. Near Mt. Everest, just east of the western zone (Site T), Finkel et al. (2003) report evidence of two smaller advances also bracketing the LGM. There is evidence as well that the LGM moraines in the Kyrgyz Tien Shan were actually restricted to the cirques, close to the modern glaciers (Koppes et al., 2003). At most sites in the western zone there is inconclusive evidence for large glacier advances during the LGM (Sites J-L, N-S) (e.g., Koppes et al., 2003; Phillips et al., 2000; Clark et al., 2001; Owen et al, 2001; Barnard et al., 2004). Thus it appears that there is substantial evidence of large pre-LGM advances, with deposits indicating many large valley and piedmont glaciers dating to that period, while LGM glaciers were much smaller than these earlier advances.

There is also evidence of early Holocene glacier advances extending a few kilometers from present glacier margins. The regions where dates are most reliable are in the Karakoram (10.8-9 ka), near Everest (9.2 ka), and in the Lahul Himalaya (11.4-10.6 ka) (Sites M, T, R) (Owen et al., 2001; Owen et al., 2002; Finkel et al., 2003). A more limited glacial advance dating to the early Holocene is also evident near Nanga Parbat and in the Aksayqin Basin (Sites N, P) (Phillips et al., 2000; Koppes et al., 2003).

1.3.2 Northern Zone

The area from central Mongolia to the Tien Shan of Xinjiang, China, defines the northern zone. There, large pre-LGM advances are evident but there is also evidence of LGM advances of similar extent as well. This contrasts with the western zone, where it appears that the advances early in the last ice-age cycle were far larger than at the LGM

For example, there is evidence of large advances at the LGM near the Jarai and Tingis rivers in the Darhad Basin of northern Mongolia, headwaters of the Yenisei River (Merle et al., 2000), and in the Die Han Je Le Gou drainage in the Xinjian Tien Shan (Clark et al., 2001) (Sites G, H, I). There is also evidence that glaciers advances during the LGM in western Xinjiang, Daxigou in the Tien Shan, and the Karlik Shan were at least as large as the pre-LGM advances in the region (Gillespie et al., 2001; Burke et al., 2003) (Site V, N). However, direct evidence of a major early Holocene advance is not clearly evident. Throughout the northern region, maximum changes in ELA values increase with latitude, from ~500 m in the Tien Shan to 1000-1200 m north of 51^{o}N (e.g., Shi, 2002). The LGM and maximum change in ELAs documented so far differ by only 25-100 m.

1.3.3 Eastern Zone

The glacial history in the eastern zone, Nepal and Tibet, is not as clearly defined as the other two zones. For example, Tsukamoto et al. (2002) define three glaciations near Kachenjunga from just three OSL dates of till, discounting a fourth sample that seemed too old (Site U). In the Tanggula Mountains, Schafer et al. (2002) define ages of two glacial advances on four surface-exposure ages, one of which they discount as being too old (Site B). In the eastern zone, several studies such as those above speculate about the timing of past glaciations using little data. There are also several studies in which dates are convincing and can be used to begin to understand the glacial history of the regions. In particular, Owen et al. (2003) demonstrate convincingly that the largest advance in the Anyemaqen and Nianbaoyeze mountains were pre-LGM (Sites A, B, D, E). However, Schafer et al. (2002) show that the largest advance at Kanchenjunga Himal and near the town of Litang occurred during the LGM (Sites C, U). Maximum changes in ELA values in eastern Tibet and the Himalaya increase from west to east as well as from north to south, ranging from 300-500 m on the plateau to >1000 m near Namche Barwa (Shi, 2002).

What distinguishes the eastern from the northern zone is substantial evidence for relatively large early Holocene advances in the east. A glacier advanced ~5 km from the present terminus in the Anyemaqen Mountain ~9 ka (Owen et al., 2003);

a glacier in the Kanchenjunga Himal advanced at least 4 km from the present day ice margin at 8-10 ka. Finkel et al. (2003) date an advance to ~9 ka at Mt. Everest. Wei et al. (2006) provide a TL date of ~10 ka for a glacier in the Kiancang Shan near Yuju Peak. It is not yet clear if there is evidence of an early Holocene advance in the Bomi Mountains, Tanggula Mountains, or at Litang.

In summary, the western zone extends from the Kyrgyz Tien Shan down to the Karakoram and across to central Tibet. In this region the largest advances occurred during the pre-LGM (30 – 70 ka) with little evidence for large advances during the LGM (e.g., Phillips et al., 2000; Clark et al., 2001; Owen et al., 2002; Finkel et al., 2003; Koppes et al., 2003; Barnard et al., 2004; Abramowski et al., 2006). In contrast, the glaciers in the northern zone (central Mongolia to the Xinjiang Tien Shan) advanced at the LGM, roughly synchronous with the high-latitude ice sheets (e.g., Merle et al., 2000; Clark et al., 2001; Shi, 2002). While there is evidence for large pre-LGM and LGM advances in the southern Himalaya around the areas of Nepal and Tibet (eastern zone), evidence for a large early Holocene (9 ka) advance distinguishes it from the more northern regions (e.g., Schafer et al, 2002; Shi, 2002; Owen et al., 2003; Wei et al., 2006) and contrasts with the rapid retreat of the high-latitude ice sheets.

The data available are still quite sparse so that patterns in the glacial history on smaller spatial scales cannot be ruled out. Nonetheless the size of the three zones

are consistent with the spatial scale expected of major climate modes, as found for both observations of the present climate and for models of past climates (discussed below and in Rupper et al., 2007). These zones are a convenient framework for characterizing the glacier and climate histories. In addition, while some uncertainty will obviously attend ELA reconstructions, as the exact position depends on the method used (i.e., accumulation area ratio, toe-headwall area ratio), it is not crucial for the changes in ELA to be reconstructed exactly for the purposes of this dissertation. The primary goal is to reconcile general regions of glacier advance and retreat with the climate changes driving them; the dating and relative changes in ELA reported here are adequate for this purpose.

1.4 Central Asian Climate

Glaciers are found on high topography throughout central Asia, and in very diverse climates: glaciers in the Himalaya are fed by the intense summer monsoon precipitation and a wintertime storm track; glaciers nestled along the eastern side of the Karakoram face the extreme dryness of the desert; and glaciers clinging to the peaks of the Mongolian Altai experience seasonal cycles in temperature as large as 40 ^{o}C. In addition to a general description of Central Asian climate, past and present, this section will also provide a description of the climate models whose output are used extensively throughout the remainder of this dissertation.

1.4.1 Present-day Climate Variability

In order to describe present day climate variability across Central Asia, adequate data, both in time and space, must be used. Weather-station data often provide the best source of information on atmospheric variables, but sufficiently long data are not available for much of Central Asia, especially the remote, high-relief regions of interest here. Another valuable source is that of the NCEP-NCAR reanalysis (Kalnay et al., 1996; Kistler, 2001). Reanalysis is a forecast model which assimilates data where available and provides output for all atmospheric variables on daily and monthly time scales. Output is available for more than 50 years on a regular 2.5^{o} grid over the entire globe. Although large uncertainties attend some of the atmospheric variables from reanalysis output, I found that the spatial pattern and seasonal cycle in the variables relevant to this research compared well with the available station data. Therefore, NCEP-NCAR reanalysis climatology, as well as information from previous studies, are used to provide a general description of present day climate variability in Central Asia, with a focus on the differences between the precipitation and temperature in the three zones discussed above.

Whereas vast amounts of research have focused on the mechanisms giving rise to climate variability in the monsoonal region of Central Asia, comparatively little has been done on climate variability at mid and high latitudes in Asia (notable

exceptions include Barnett et al., 1988; Cohen and Rind, 1990; Wang et al., 2000; Gong et al., 2002; Barlow et al., 2002; Tippett et al., 2003). Araguas-Araguas et al. (1998) provide one of the few overviews of the general circulation and climate of the entire Asian continent.

I give a synopsis of Asian climate as discussed in Araguas-Araguas et al. (1998) to provide some context with which to discuss the three separate regions that were defined by the glacier history. A characteristic feature of the regional climate is the monsoon, which is a complete reversal of weather patterns from winter to summer. The extreme temperature contrast between the ocean and land surface drives the intense monsoonal circulation. A surface low develops during the summer months, typically June through August, creating onshore flow from off the warm ocean and resulting in torrential rains in India and the southern Himalaya. During the winter months, dominantly October through June, a high pressure ridge develops over the Plateau, making subsidence the norm. The resulting dry, cold air flows out of the plateau to the north, east, and south.

One of the most prominent features of Asia is the Tibetan Plateau, which plays a crucial role in influencing and modifying the climatology of the region. Although the exact role the plateau has played in onset of monsoonal circulation in Asia remains an active area of debate (e.g., Zhisheng et al., 2000; Qiang et al., 2001; Harris, 2006), it is generally accepted that the plateau does play an important

modifying role. For example, the presence of the plateau is thought to shift the regions of intense summer low and winter high pressures and have a profound influence on the patterns of precipitation. The Tibetan Plateau also blocks the westerlies and splits the jet stream which moves to the north and south of the plateau.

Araguas-Araguas et al. (1998) list five major air masses which influence Asian climate, a result of the atmospheric circulation described above:

- polar air mass originating in the Arctic
- continental air mass originating over central Asia
- tropical-maritime air mass originating in the northern Pacific
- equatorial-maritime air mass originating the western equatorial Pacific
- equatorial-maritime air mass originating in the Indian Ocean.

These air masses and their regional extent serve to characterize the pluviometric regime of much of Asia. The three air masses that exert the greatest influence on the northern, western, and eastern zones of interest here are the Arctic polar air mass, central Asian continental air mass, and the equatorial-maritime air mass associated with the Indian monsoon. The regional variability in precipitation and temperature, two variables known to influence glaciers, depends therefore on the predominant air masses, the influence of high topography, and local factors such as the continentality of the region. This spatial variability can clearly be seen in a comparison of temperature and precipitation between the three different zones.

The western zone experiences hot summers and cold winters. Total annual precipitation is approximately 0.6 m/yr, with the maximum rainfall occurring during the late winter and spring. Most of the rain may be attributed to the weak Mediterranean storm track which maximizes in the winter and spring and is blocked from entering further into the plateau by the presence of the high topography.

In the northern zone, the winter and spring storms that develop are deflected by the ridge and down-stream trough in the jet stream. Thus, unlike the western zone, most of the precipitation in the northern zone occurs during the summer months with land-surface feedbacks providing an important influence on the amount and source of moisture (e.g., Gallimore and Kutzbach, 1989). The moisture source for the region is predominantly recycled continental moisture (Schotterer et al., 1997). The northern zone is also far from the moderating effects of the oceans and experiences a temperature range from winter to summer of up to 40 ^{o}C. The intense winter cooling is balanced dynamically by subsidence in the Siberian high-pressure system.

In contrast to both the western and northern zones, the climate of the eastern zone is dominated by the South East Asian monsoon. The surface low that develops during the summer creates onshore flow from the warm ocean resulting in the

torrential rains in India and the southern Himalaya. The high topography prevents most of the moisture from reaching the interior of the plateau. During the winter monsoon, subsidence over the plateau is the norm, creating even drier conditions in the interior. A westerly storm track, associated with the splitting of the westerlies and jet stream, is present in the winter but is relatively weak. Unlike the extremely large temperature range in the more northern areas, the temperature range in the eastern zone are relatively moderate. This is largely due to the region's close proximity to the ocean as well as its position at lower latitude.

This regional climate variability within Central Asia makes it an ideal area to both test the abilities of the new surface energy- and mass-balance model and to gain an understanding of how the sensitivity of glacier mass balance changes from one region to the next. In particular, it is reasonable to expect that these diverse climate settings are likely to respond differently to even uniform changes in climate forcing. Since glaciers respond to changes in climate, it is not surprising to find a diverse glacier history in these regions as well. The climate history of Central Asia can only be explained by considering how the complex set of climate factors discussed above varied under changes in insolation (orbitally induced), CO_2, and land-surface conditions (presence/absence of large ice sheets).

1.4.2 Holocene and LGM Climates

In the Northern Hemisphere, the mid-Holocene was a period of maximum summer insolation and increased seasonality while land surface conditions were similar to today. Modeling studies under mid-Holocene conditions show that the Indian summer monsoon increased, which resulted in increased precipitation in India and the Southern Himalayas (e.g., Joussaume et al., 1999; Bush, 2002). This increase in precipitation has been invoked as the cause of the advance of glaciers during the early Holocene (discussed above). However glaciers respond to both annual precipitation and summer (melt season) temperatures. Therefore, a glacier's response to the predicted changes in precipitation and temperature will depend on its sensitivity to both variables. None of these studies address the effect of increased summer insolation at the top of the atmosphere, which, all else being equal, would have the tendency to warm the climate. Kayastha et al. (1999) show that glacier AX010 in the Nepalese Himalayas is sensitive to both temperature and precipitation. Given this fact from the modern climate both the increase in monsoonal precipitation and the increase in summer insolation must be accounted for in understanding what the glacial history of the region reflects.

Chapter three of this dissertation reconciles the Holocene climate history with the spatial variability in glacier advances and retreats in Central Asia, using both mass-balance models discussed above and climate simulations for 6 ka (discussed

below). A detailed discussion of the climate changes during the Holocene as compared to the present day, for each of the three zones, is presented in that chapter.

In contrast to the early and mid Holocene, insolation during the LGM was closer to present day conditions. However, the large high-latitude ice sheets influenced both the planetary albedo and the general circulation of the atmosphere. Changes in the magnitude and pattern in SSTs also changed the atmospheric circulation. The exact response of the atmospheric circulation to the presence of these ice sheets and changes in SSTs depends greatly on the model used and the prescribed boundary conditions (e.g., Kageyama et al., 1999; Chiang et al., 2003). In addition to large land-surface and SST changes, CO_2 during the LGM was lower than today, providing a uniform decrease in radiative forcing relative to today. The increased albedo, modification of stationary waves by the ice sheets and resulting temperature advection downwind of the ice sheets, change in sea surface temperatures, and lower CO_2 have the potential to influence the climate of Central Asia. In Central Asia, climate models generally show a substantial cooling, with the greatest temperature decrease in the continental interior (e.g., Ganapolski et al., 1998; Weaver et al., 1998; Joussaume et al, 1999; Kageyama and Valdez, 2000). Precipitation changes vary greatly from one region to the next, and from model to model. For example, some studies show a large decrease in precipitation across the monsoon region (e.g., Joussaume et al., 1999; Braconnot

et al., 2000). Still others show a shift in the position of monsoonal influence with precipitation increasing at the LGM as compared to today in some regions (e.g., Bush, 2004). Likewise, the glacier advances and retreats in Central Asia at the LGM have been attributed to different things. In the southern Himalayas, some studies suggest that the substantial advance of glaciers at the LGM was due to an increase in precipitation (e.g., Bush, 2004), while others attribute it to a decrease in temperatures (e.g., Owen et al., 2003).

The spatial pattern in ELAs at the LGM suggests that the climate changes in response to LGM boundary conditions varied from region to region. Previous explanations of the LGM glacier history vary from study to study, and none test the sensitivity of these glaciers to possible changes in climate at the LGM. Chapter four of this dissertation reconciles the LGM climate history with the spatial pattern in glacier advances and retreats in Central Asia, using two mas-balance models (discussed above) and climate model simulations for 21 ka (discussed below). A detailed discussion of the climate changes during the LGM as compared to the present day, for each of the three zones, is presented in that chapter.

1.4.3 General Circulation Models

General circulation model (GCM) simulations provide the necessary information for comparing the present day climate to the LGM and Holocene, and climate input for the mass-balance modeling exercises. The GCMs used in this study were acquired from the Paleoclimate Model Intercomparison Project (PMIP). PMIP's main goal is to encourage the systematic study of atmospheric GCMs; assess their ability to simulate large changes in climate by comparing them to the available paleoclimate data; increase understanding of climate changes in the past; determine where model results are a robust response of the climate to changes in boundary conditions and where results are model dependent (Joussaume and Taylor, 2001). Output from the eighteen GCMs were used in this study. The suite of GCMs provide climate simulations at three time periods - present-day, 6 ka, and 21 ka – with each model using the same boundary conditions appropriate for each time period. Summaries of the boundary conditions and eighteen GCMs are presented in Tables 1.1 and 1.2, respectively. Though any given model can not be thought of as correct, agreement between models provides confidence in the results and provides a means to test how sensitive Central Asian glaciers are to possible climate changes under different boundary conditions.

Table 1.1: PMIP prescribed boundary conditions for the present day, 6 ka, and 21 ka. 8 models prescribe sea surface temperatures (SSTs), 9 compute SSTs using a mixed-layer ocean model.

		Present Day	**6 ka**	**21 ka**
SSTs	**prescribed**	control run	no change	CLIMAP reconstructions (1981)
	computed	ocean mixed-layer	not available	ocean-mixed layer
CO_2		345 ppm	280 ppm	200 ppm
Eccentricity		0.016724	0.018682	0.018994
Obliquity		23.446 degrees	24.105 degrees	22.949 degrees
Perihelion[a]		102.04 degrees	0.87 degrees	114.42 degrees
Land Albedo (ice-free)		control run	no change	no change
Ice Sheet Topography		control run	no change	Peltier reconstructions (1994)
Coastlines		control run	no change	-105 m

[a] longitude of perihelion relative to the moving vernal equinox minus 180 degrees

Table 1.2: PMIP Models: List of the 18 PMIP GCMs used in this study, grid resolution, runs available, and whether SSTs are prescribed (P) or computed (C).

Model and Version		Resolution	6 ka	21 ka
BMRC	Bureau of Meteorology Research Centre (Australia)	R21, L9	C	
CCC2	Canadian Centre for Climate Modelling and Analysis (Canada)	T32, L10	C	P,C
CCM3	NCAR Climate Community Model (USA)	T42, L18	C	
CCM1		R15, L12		C
CCSR1	Center for Climate System Research (Japan)	T21, L20	C	P
CNRM2	Centre National de Recherches Météorologiques (France)	T31,L19	C	
CSIRO	Common wealth Scientific and Industrial Research Organisation (Australia)	R21, L9	C	
ECHAM3	Max-Planck Institute for Meteorology (Germany)	T42, L19	C	P
GEN2	National Center for Atmospheric Research (USA) GENESIS model	T31, L18	C	P,C
GEN1		R15, L12		C
GFDL	Geophysical Fluid Dynamics Laboratory (USA)	R30, L20	C	C
GISS	Goddard Institute for Space Studies (USA)	72*46, L9	C	
LMD4	Laboratoire de Météorologie Dynamique (France)	48*36, L11	C	P,C
LMD5		64*50, L11	C	P
MRI2	Meteorological Research Institute (Japan)	72*46, L15	C	P,C
MSU	Moscow State University (Russia)	10*15, L3	C	P
UGAMP	UK Universities Global Atmospheric Modelling Programme (UK)	T42, L19	C	P,C
UIUC11	University of Illinois at Urbana-Champaign (USA)	72*46, L11	C	
UKMO	UK Meteorological Office Unified Model (UK)	96*73, L19	C	P
YONU	Yonseï University (Korea)	72*46, L8	C	

1.5 Dissertation goal and outline

To recap, glacier histories of advances and retreats provide a great opportunity to understand regional climate variability, especially for Northern Hemisphere landmasses. Much of the regional assessments of glacier-climate interactions to date have relied on simplified assumptions of ablation being proportional to some measure of temperature. In order to understand the global retreat of glaciers today and to reconcile histories of glacier advances and retreats with the climate mechanisms driving them, we need a framework with which to test glacier sensitivities to changes in climate. This dissertation develops such a framework and applies it to the region of Central Asia.

As discussed above, the reasons for choosing Central Asia are two-fold: first, glaciers are found in a variety of climate settings. Second, the glacier history of Central Asia is strikingly different than that of the high-latitude ice sheets (e.g., Gillespie and Molnar, 1995). Thus Central Asia provides a region where glacier sensitivities to differing climatic regimes can be estimated, simulated, and evaluated against a rich and varied glacier history. Reconciling the pattern of glacier advances and retreats with the climate mechanisms driving them will provide insight into regional patterns in climate change and the global applicability of such changes.

The rich spatial patterns of glaciers and the asynchroneity of Asian glaciers with high-latitude ice sheets prompts three questions.

- Can we understand the relative importance of accumulation and ablation in controlling mass balance of glaciers over large regions?
- Are the observed patterns of glacier response to changes in temperature and precipitation consistent with regional changes in climate?
- Do the patterns in glacier advances actually reflect patterns in climate change or are they the result of differing sensitivities to the same changes in a particular climate variable?

Though thinking about past climate changes in terms of spatial patterns might complicate the interpretation of paleoclimate records, it makes the proxies much more relevant to our understanding of modern climate. This dissertation continues in that tradition with Chapter 2 presenting the surface energy- and mass-balance model and the sensitivity of glacier mass balance to modern climate variability in Central Asia. With a working knowledge of mass balance sensitivities in hand, Chapter 3 focuses on reconciling the Holocene glacier history with the climate mechanisms driving them. Chapters 2 and 3 are written as journal articles, and, therefore, some of the motivation and discussion provided above is duplicated in their introduction sections. Chapter 4 presents the results

from applying the mass-balance models to the Last Glacial Maximum conditions. Chapter 4 reconciles the LGM glacier history with the climate mechanisms driving them. Chapter 5 is a synopsis of the conclusions of the main body of the dissertation, and further discussion of the three questions posed above and how the results of this dissertation address those questions.

1.6 Notes to Chapter One

Abramowski U, Bergau A, Seebach D, Zech R, Glaser B, Sosin P, Kubik PW, Zech W, 2006: Pleistocene glaciations of Central Asia: results from Be-10 surface exposure ages of erratic boulders from the Pamir (Tajikistan), and the Alay-Turkestan range (Kyrgyzstan). Quaternary Science Reviews, 25 (9-10): 1080-1096.

Anderson DM, Prell WL, 1993: A 300 kyr record of upwelling off Oman during the late Quaternary – evidence of the Asian southwest monsoon. Paleoceanography, 8 (2): 193-208.

Araguas-Araguas L, Froehlich K, Rozanski K, 1998: Stable isotope composition of precipitation over southeast Asia. Journal of Geophysical Research, 103 (D22): 28721-28742.

Barlow M, Cullen H, Lyon B, 2002: Drought in Central and Southwest Asia: La Nina, the warm pool, and Indian Ocena precipitation. Journal of Climate, 15: 697-700.

Barnard P, Owen L, Finkel R, 2004: Style and timing of glacial and paraglacial sedimentation in a monsoon-influenced high Himalayan environment, the upper Bhagirathi valley, Gavhwal Himalaya. Sedimentary Geology, 165: 199-221.

Barnett T, Dumenil L, Schlese U, Rockner E, 1988: The effect of Eurasian snow cover on global climate. Science, 239: 504-507.

Benn DI, Owen LA, 1998: The role of the Indian summer monsoon and the mid-latitude westeries in Himalayan glaciation: review and speculative discussion. Journal of the Geological Society, 155 (2): 353-363.

Braconnot, P., S. Joussaume, N. de Noblet, G. Ramstein, 2000: Mid-Holocene and last glacial maximum African monsoon changes as simulated within the Paleoclimate Modeling Intercomparison project. Global and Planetary Change, 26, 51-66.

Bradley R, Diaz H, Kiladis G, Eischeid J, 1987: ENSO signal in continental temperatuare and precipitation records. Nature, 327 (6122): 497-501.

Braithwaite RJ, 1995: Positive degree-day factors for ablation on the Greenland ice-sheet studied by energy-balance modeling. Journal of Glaciology, 41 (137): 153-160.

Briffa, K.R., 2000: Annual climate variability in the Holocene: interpreting the message of ancient trees. Quaternary Science Review, 19: 87-105.

Briffa, K.R., P.D. Jones, F.H. Schweingruber, S.G. Shiyatov and E.A. Vaganov, 1996: Development of a North Eurasian chronology network: Rationale and preliminary results of comparative ring-width and densitometric analyses in northern Russia. In: Tree Rings, Environment, and Humanity. Radiocarbon 1996, J.S. Dean, D.M. Meko and T.W. Swetnam (eds.). Department of Geosciences, The University of Arizona, Tucson, 25-41.

Briffa, K.R., P.D. Jones, F.H. Schweingruber and T.J. Osborn, 1998: Influence of volcanic eruptions on Northern Hemisphere summer temperature over the past 600 years. Nature, 393: 450-455.

Broecker WS, 2003: Does the trigger for abrupt climate change reside in the ocean or in the atmosphere? Science 300 (5625): 1519-1522.

Burke R, Gillespie A, Bayasgalan A, Sheinkman V, Chadwick O, 2003: Late Quaternary glaciation in northern Central Asia. XVI INQUA Congress, Programs with Abstracts, Reno, July, 156.

Bush ABG, 2002: A comparison of simulated monsoon circulations and snow accumulation in Asia during the mid-Holocene and at the Last Glacial Maximum. Global and Planetary Change, 32 (4): 331-347.

Bush ABG, 2004: Modelling of late Quaternary climate over Asia: a synthesis. Boreas, 33 (2): 155-163.

Casal TGD, Kutzbach JE, Thompson LG, 2004: Present and past ice-sheet mass balance simulations for Greenland and the Tibetan Plateau. Climate Dynamics, 23 (3-4): 407-425.

Chiang JCH, Biasutti M, Battisti DS, 2003: Sensitivity of the Atlantic Intertropical Convergence Zone to Last Glacial Maximum boundary conditions. Paleoceanography, 18(4): 1094.

Clark D, Gillespie A, Bierman P, Caffee M, 2001: Glacial asynchrony in the Kunlun Shan, northwestern Tibet. Abstracts with Programs – Geological Society of America, 33 (6): 441.

CLIMAP, 1981: Seasonal reconstructions of the Earth´s surface at the last glacial maximum. Map Series, Technical Report MC-36, Geological Society of America, Boulder, Colorado.

Cohen J, Rind D, 1990: The effect of snow cover on the climate. Journal of Climate, 4: 689-706.

Dai AG, Wigley TM, 2000: Global patterns of ENSO-induced precipitation. Geophysical Research Letters, 27 (9): 1283-1286.

Emeis KC, Anderson DM, Doose H, Kroon D, Schulzbull D, 1995: Sea-surface temperatures and the history of monsoon upwelling in the northwest Arabian Sea during the last 500,000 years. Quaternary Research, 43 (3): 355-361.

Finkel RC, Owen, L, Barnard P, Caffee M, 2003: Beryllium-10 dating of Mount Everest moraines indicates a strong monsoon influence and glacial synchroneity throughout the Himalaya. Geology, 31 (6): 561-564.

Fountain AG, Lewis KJ, Doran PT, 1999: Spatial climatic variation and its control on glacier equilibrium line altitude in Taylor Valley, Antarctica. Global and Planetary Change, 22 (1-4): 1-10.

Gallimore R, Kutzbach J, 1989: Effects of soil-moisture on the sensitivity of a climate model to earth orbital forcing at 9000-yr-BP. Climatic Change, 14 (2): 175-205.

Ganopolski, A., S. Rahmstorf, V. Petoukhov and M. Claussen, 1998: Simulation of modern and glacial climates with a coupled global model of intermediate complexity. Nature, 391: 351- 356.

Gillespie A, Burke R, Byasgalan A, 2001: Neoglaciation in Central Asia. Abstracts with Programs- Geological Society of America, 33 (6): 442.

Gillespie A, Molnar P, 1995: Asynchronous maximum advances of mountain and continental glaciers. Reviews of Geophysics, 33 (3): 311-364.

Gillespie A, Rupper S, and Roe G, 2003: Climatic interpretation from mountain glaciations in Central Asia. Geological Society of America, Abstracts with Program 35(6).

Gong G, Entekhabi D, Cohen J, 2002: Modeled northern hemisphere winter climate response to realistic Siberian snow anomalies. Journal of Climate, 16: 3917-3932.

Harris N, 2006: The elevation history of the Tibetan Plateau and its implications for the Asian monsoon. Palaeogeography Palaeoclimatology Palaeoecology, 241 (1): 4-15.

Hastenrath S, 1994: Recession of tropical glaciers. Science, 265 (5180): 1790-1791.

Intergovernmental Panel on Climate Change, 2001: The scientific basis.

Joussaume S, Taylor K, 2001: The paleoclimate model intercomparison project. Proceedings from the third PMIP workshop.

Joussaume S, Taylor KE, Braconnot P, Mitchell JFB, Kutzbach JE, Harrison SP, Prentice IC, Broccoli AJ, Abe-Ouchi A, Bartlein PJ, Bonfils C, Dong B, Guiot J, Herterich K, Hewitt CD, Jolly D, Kim JW, Kislov A, Kitoh A, Loutre MF, Masson V, McAvaney B, McFarlane N, de Noblet N, Peltier WR, Peterschmitt JY, Pollard D, Rind D, Royer JF, Schlesinger ME, Syktus J, Thompson S, Valdes P, Vettoretti G, Webb RS, Wyputta U, 1999: Monsoon changes for 6000 years ago: Results of 18 simulations from the Paleoclimate Modeling Intercomparison Project (PMIP). Geophysical Research Letters, 26 (7): 859-862.

Ju Y, 2004: Glacial advance/retreat and climate change in the middle part of North-Tianshan. Doctoral Thesis, pp34-37.

Kageyama M, Valdes P, Ramstein G, Hewitt C, Wyputta U, 1999: Northern hemisphere storm-tracks in present day and last glacial maximum climate simulations: a comparison of the European PMIP models. Journal of Climate, 12, 742-760.

Kageyama M, Valdes P, 2000: Impact of the North American ice-sheet orography on the Last Glacial Maximum eddies and snowfall. Geophysical Research Letters, 27 (10): 1515-1518.

Kalnay E, Kanamitsu M, Kistler R, Collins W, Deaven D, Gandin L, Iredell M, Saha S, White G, Woollen J, Zhu Y, Chelliah M, Ebisuzaki W, Higgins W, Janowiak J, Mo KC, Ropelewski C, Wang J, Leetmaa A, Reynolds R, Jenne R, Joseph D, 1996: The NCEP/NCAR 40-year reanalysis project. Bulletin of the American Meteorological Society, 77 (3): 437-471.

Kaser G, Hardy DR, Molg T, Bradley RS, Hyera TM, 2004: Modern glacier retreat on Kilimanjaro as evidence of climate change: Observations and facts. International Journal of Climatology, 24 (3): 329-339.

Kaser G, 2001: Glacier-climate interaction at low latitudes. Journal of Glaciology, 47 (157): 195-204.

Kaufman DS, Porter SC, Gillespie AR, 2004: Quaternary alpine glaciation in Alaska, the Pacific Northwest, Sierra Nevada, and Hawaii, in Gillespie AR, Porter SC, and Atwater BF, eds., The Quaternary Period in the United States. Developments in Quaternary Science, Volume 1, Elsevier Press, 77-103.

Kayastha RB, Ageta Y, Fujita K, 2002: Use of positive degree-day method for calculating snow/ice melting and discharge from glacierized basins in Nepal. EGS XXVII General Assembly, abstract #3520.

Kayastha RB, Ohata T, Ageta Y, 1999: Application of a mass-balance model to a Himalayan glacier. Journal of Glaciology, 45 (151): 559-567.

Kistler R, Kalnay E, Collins W, Saha S, White G, Woollen J, Chelliah M, Ebisuzaki W, Kanamitsu M, Kousky V, van den Dool H, Jenne R, Fiorino M, 2001: The NCEP-NCAR 50-year reanalysis: Monthly means CD-ROM and documentation. Bulletin of the American Meteorological Society, 82 (2): 247-267.

Koppes MN, Gillespie AR, Burke RM, Thompson SC, Clark DH, 2003: Late Quaternary glaciation in northern Central Asia. XVI INQUA Congress, Programs with Abstracts, Reno, July, p. 156.

Kuhle M, 1998: Reconstruction of the 2.3 million km (2) late Pleistocene ice sheet on the Tibetan Plateau and its impact on the global climate (vol 45, pg 71, 1998). Quaternary International, 47-8: 173-182.

Lowell TV, Heusser CJ, Andersen BG, Moreno PI, Hauser A, Heusser LE, Schluchter C, Marchant DR, Denton GH, 1995: Interhemispheric correlation of late Pleistocene glacial events. Science, 269 (5230):1541-1549.

Mann ME, 2002: The value of multiple proxies. Science, 297 (5586): 1481-1482.

Merle J, Carson R, Cady J, Hinz N, 2000: Quaternary geology of the Tengis_Shishid Gol region, Khovsgo, Mongolia. Anonymous Abstracts with Programs- Geological Society of America, 33 (3): 67.

Molg T, Hardy DR, 2004: Ablation and associated energy balance of a horizontal glacier surface on Kilimanjaro. Journal of Geophysical Research, 109 (D16): Art. No. D16104.

Oerlemans J, 2005: Extracting a climate signal from 169 glacier records. Science, 308 (5722): 675-677.

Oerlemans J, Fortuin J, 1992: Sensitivity of glaciers and small ice caps to greenhouse warming. Science, 258 (5079): 115-117.

Owen LA, Gualtieri L, Finkel RC, Caffee MW, Benn DI, Sharma MC, 2001: Cosmogenic radionuclide dating of glacial landforms in the Lahul Himalaya, northern India: defining the timing of Late Quaternary glaciation. Journal of Quaternary Science, 16 (6): 555-563.

Owen LA, Kamp U, Spencer JQ, Haserodt K, 2002: Timing and style of Late Quaternary glaciation in the eastern Hindu Kush, Chitral, northern Pakistan: a review and revision of the glacial chronology based on new optically stimulated luminescence dating. Quaternary International, 97-8: 41-55.

Owen LA, Finkel RC, Haizhou M, Spencer JQ, Derbyshire E, Barnard PL, Caffee MW, 2003: Timing and style of Late Quaternary glaciation in northeastern Tibet. Geological Society of America Bulletin, 115 (11): 1356-1364.

Paterson, 1999: Physics of Glaciers. Pergamon/Elsevier Science Inc.

Peltier W, 1994: Ice-age paleotopography. Science, 265 (5169): 195-201.

Phillips WM, Sloan VF, Shroder JF, Sharma P, Clarke ML, Rendell HM, 2000: Asynchronous glaciation at Nanga Parbat, northwestern Himalaya Mountains, Pakistan. Geology, 28 (5): 431-434.

Porter SC, 1977: Present and past glaciation threshold in the Cascade Range, Washington, U. S. A.: topographic and climatic controls, and paleoclimatic implications. Journal of Glaciology, 18, 101-116.

Porter SC, Orombelli G, 1985: Glacier contraction during the middle Holocene in the western Italian Alps – evidence and implications. Geology, 13(4): 296-298.

Qiang XK, Li ZX, Powell CM, Zheng HB, 2001: Magnetostratigraphic record of the Late Miocene onset of the East Asian monsoon, and Pliocene uplift of northern Tibet. Earth and Planetary Science Letters, 187 (1-2): 83-93.

Roe GH, Steig EJ, 2004: Characterization of millennial-scale climate variability. Journal of Climate, 17 (10): 1929-1944.

Ropelewski C, Halpert M, 1987: Global and regional scale precipitation patterns associated with the El-Nino Southern Oscillation. Monthly Weather Review, 115 (8): 1606-1626.

Rupper SB, Roe G, and Gillespie G, 2007: Spatial patterns of Holocene glacier advance and retreat in Central Asia. In preparation.

Schafer JM, Tschudi S, Zhao ZZ, Wu XH, Ivy-Ochs S, Wieler R, Baur H, Kubik PW, Schluchter C, 2002: The limited influence of glaciations in Tibet on global climate over the past 170 000 yr. Earth and Planetary Science Letters, 194 (3-4): 287-297.

Schotterer U, Frohlich K, Gaggeler HW, 1997: Isotope records from Mongolian and alpine ice cores as climate indicators. Climatic Change, 36 (3-4): 519-530.

Shi Y, 2002: Characteristics of late Quaternary monsoonal glaciation on the Tibetan Plateau and in East Asia. Quaternary International, 97-8: 79-91.

Tippett M, Barlow M, Lyon B, 2003: Statistical correction of Central Southwest Asia winter precipitation simulations. International Journal of Climatology, 23: 1421-1433.

Tsukamoto S, Asahi K, Watanabe T, Rink WJ, 2002: Timing of past glaciations in Kanchenjunga Himal, Nepal by optically stimulated luminescence dating of tills. Quaternary International, 97-8: 57-67.

Wang J, 1981: Ancient glaciers at the head of Urumqui River, Tian Shan. Journal of Glaciology and Cryopedology, 3, 55-63.

Wang B, Wu R, Fu X, 2000: Pacific-East Asian teleconnectoin: How does ENSO affect East Asian climate? Journal of Climate, 13: 1517-1536.

Weaver AJ, Eby M, Augustus FF, Wiebe EC, 1998: Simulated influence of carbon dioxide, orbital forcing and ice sheets on the climate of the Last Glacial Maximum. Nature, 394 (6696): 847-853.

Wei Z, Zhijiu C, Yanghua L, 2006: Review of the timing and extent of glaciers during the last glacial cycle in the bordering mountains of Tibet and in East Asia. Quaternary International, 154-155: 32-43.

Wunsch C, 2006: Abrupt climate change: An alternative view. Quaternary Research, 65 (2): 191-203.

Yang JP, Ding YJ, Chen RS, Liu SY, Lu AX, 2003: Causes of glacier change in the source regions of the Yangtze and Yellow rivers on the Tibetan Plateau. Journal of Glaciology, 49 (167): 539-546.

Zhang Y, Shiyin L, Yongjian D, 2006: Observed degree-day factors and their spatial variation on glaciers in western China. Annals of Glaciology, 43, 301-306.

Zhisheng A, Kutzbach JE, Prell WL, Porter SC, 2001: Evolution of Asian monsoons and phased uplift of the Himalayan Tibetan plateau since Late Miocene times. Nature, 411 (6833): 62-66.

Zhoa J, Zhou S, Cui J, Jiao K, Ye Y, Xu L, 2001: ESR dating of glacial tills at the headwaters of the Urumqui River in the Tianshan Mountains. Journal of Glaciology and Geocryology, 24, 737-743.

Chapter Two

GLACIER CHANGES AND REGIONAL CLIMATE: A MASS AND ENERGY BALANCE APPROACH

2.1 Introduction and Motivation

Geological reconstructions of previous glacier extents reveal climate variations in the past. In many parts of the world, reconstructed histories of glacier extents form the primary record of past climate changes (e.g., Porter, 1977; Porter, 1985; Gillespie and Molnar, 1995; Lowell et al., 1995; Kaufman et al., 2004). Many researchers argue these histories reflect global-scale climate changes, such as the little ice age and the Younger Dryas (e.g., Grove and Switzer, 1994; Denton and Hendy, 1994; Lowell et al., 1995; Bradley, 2000). The conclusions and interpretations about such global connections in the climate system rest on assumptions of how sensitively glaciers respond to characteristic climate variations.

Despite their obvious importance, there is still much ambiguity about how glaciers respond to climate. At face value, glaciers appear to be among the most straightforward natural recorders of climate: a glacier simply reflects the difference between accumulation of snow and ablation (i.e., mass loss). However, numerous environmental factors control accumulation and ablation: avalanches or

wind-blown snow, rain versus snow, surface albedo variations, hillside shading, and cloudiness are just some of the examples (e.g., Paterson, 1999; Kayastha et al., 1999). Moreover if climate changes are based on the change in a glacier's terminus position, glacier dynamics are also part of the signal.

Where glaciers within an entire region are behaving in the same way (i.e., advancing or retreating synchronously), there can be confidence that local factors specific to any single glacier are not dominating the response, and that regional-scale climate variations are at work. This regional-scale approach is the approach I pursue in this study.

Several methods have been employed to explore the link between glacier mass balance and climate, and at a variety of scales ranging from single glaciers and basins to whole complexes of glaciers across large regions (e.g., Braithwaite, 1995; Wagnon et al., 2003; Kessler et al., 2006). The larger the scale, the simpler the approach to estimating ablation tends to be. For example, at scales larger than a single basin, ablation is typically assumed to be proportional to some measure of summertime temperature (e.g., Fountain et al., 1999; Braithwaite et al., 2003; Oerlemans, 2005). Such ablation parameterizations are appealing in their simplicity and the results from using them can be easily interpreted. However, this simplified approach to estimating ablation neglects sublimation as well as other potentially important atmospheric variables such as wind speed, relative

humidity, and cloudiness. For example, Oerlemans' (2005) reconstructions of temperature from glacier length changes assume that, in the aggregate, the 169 mid- and low- latitude glaciers used in the study are responding only to changes in ablation, and that changes in ablation are due to changes in temperature; all other atmospheric variables are neglected. In addition to the above assumptions, this type of approach also requires use of a melt factor that relates the measure of summer temperature to the ablation rate. This melt factor is an empirically determined parameter. Yet studies of different glaciers suggest melt factors vary from place to place by about a factor of two (e.g., Paterson, 1999), and even up to five (Kayastha et al., 2002; Zhang et al., 2006).

Moreover it is not, of course, temperature *per se* that causes ablation, but rather it is heat. Therefore a more physically based approach to modeling ablation is to perform a self-consistent calculation of the energy balance at the glacier surface. Such ablation models have the advantage that all the relevant atmospheric variables are included, and that both sublimation and surface melting are a product of the calculation. Thus the relative importance of different atmospheric variables for ablation can be clearly evaluated and understood. Mass balance models that calculate ablation using the energy balance approach have been applied successfully to single glaciers and basins to understand the relationship with the local climate (e.g., Kayastha et al., 1999; Plummer and Phillips, 2003; Molg and Hardy, 2004). For example, a detailed study of the sensitivity of a

glacier in the Nepalese Himalaya suggests that this particular glacier is sensitive to changes in both temperature and precipitation (Kayastha et al., 1999). To complicate things even further, several studies suggest that the observed retreat of tropical glaciers is sensitive to subtle changes in moisture-related variables, such as cloudiness, relative humidity, and precipitation (e.g., Hastenrath, 1994; Kaser et al., 2004; Molg and Hardy, 2004), and not directly related to increasing temperatures. These examples highlight the need for a better understanding of how glacier-climate interactions vary from region to region. With this in mind, there are two questions which need to be addressed. Firstly, can we understand the relative importance of accumulation and ablation in controlling mass balance of glaciers at regional scales? Secondly, how do the observed patterns of glacier response reflect regional changes in climate?

This chapter presents a surface-energy and mass-balance model that is a framework within which to address these questions. The model is driven by the regional climate of Central Asia. The reasons for choosing Central Asia are two-fold: first, glaciers are found throughout Asia in a variety of climate settings, allowing for diverse tests of the model's abilities; and second, the glacier history of Central Asia is strikingly different than that of the high-latitude ice sheets (e.g., Gillespie and Molnar, 1995), and requires explanation (Rupper et al., 2007). This paper focuses on the presentation of the model and on evaluating the relationship between spatial patterns of climate change and spatial patterns of glacier response.

This study aims to address the first-order climate controls on regional-scale glacier mass balance. The surface energy- and mass-balance model is able to capture the regional differences in glacier mass balance, and is in agreement with case studies done at individual glaciers. An analysis of the energy fluxes reveals the causes of these regional differences, and sensitivity tests highlight where the cause of glacier changes can likely be understood confidently and other regions where greater uncertainty exists. The caveats and limitations of the model are the focus of the discussion, as well as what studies might further improve our understanding of the sensitivity of glaciers to changes in climate.

2.2 Glaciers and Climate

The equilibrium-line altitude (or ELA) is defined here as the altitude on a glacier where annual accumulation equals annual ablation, and it is considered to be one of the most useful glaciological measures for reconstructing climate changes (e.g., Porter, 1975; Fountain et al. 1999; Paterson, 1999). All else being equal, if the ELA lowers the glacier advances; if it rises, the glacier retreats. Whereas other glacier characteristics such as length depend on ice dynamics, geometry of the bed, and myriad other factors, the ELA is most directly related to climate, reflecting a simple balance between accumulation and ablation (e.g., Paterson,

1999; Fountain et al., 1999). The ELA therefore provides a common measure whereby changes can be compared directly from one region to another.

The surface energy- and mass-balance (SEMB) model used in this paper determines the ELA for a given set of climate variables. As a case study, the model is applied to understanding the ELAs of glaciers across Central Asia.

2.2.1 Central Asian Glaciers

The glacier history across Central Asia has been characterized in terms of the reconstructions of paleo-ELAs. Gillespie et al. (2003) identify three regions that capture the spatial and temporal variability of the glaciers in Central Asia during the last glacial cycle. These three zones have distinctly different glacier histories and each is different again from that of North America, Europe, Greenland, and Antarctica (Gillespie et al., 2003; Rupper et al., 2007). The three regions are shown in Figure 2.1. The western zone extends from the Kyrgyz Tien Shan down

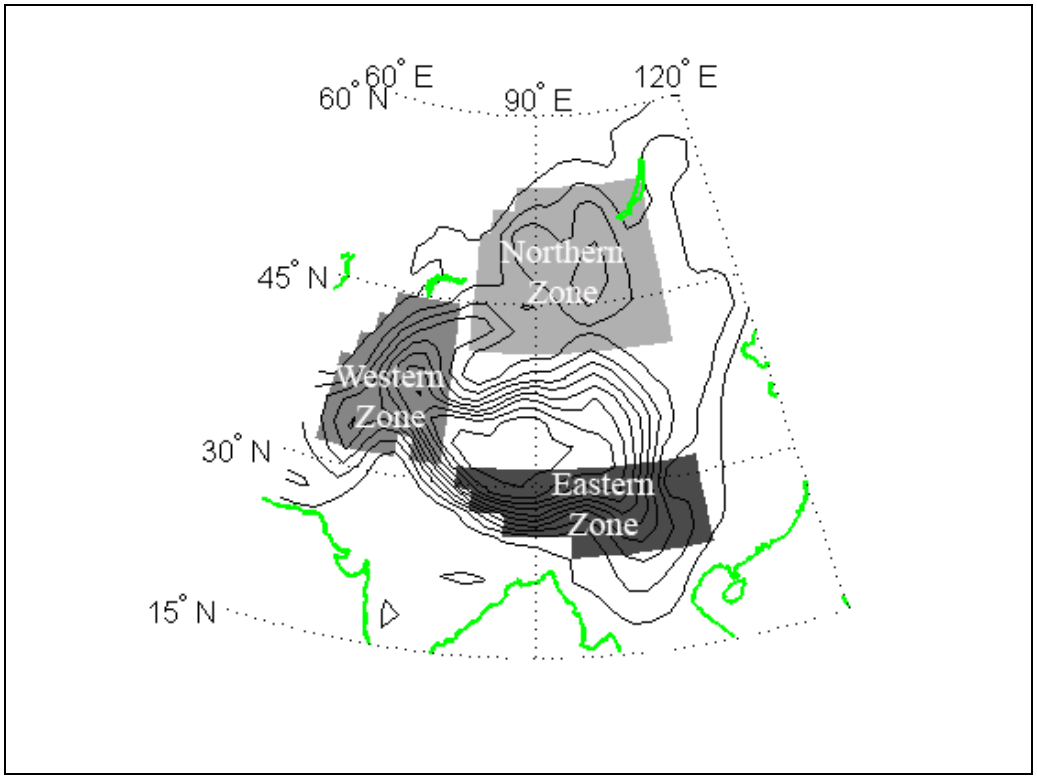

Figure 2.1: Shaded areas of gray represent the general outline of the eastern, western, and northern zones, as defined by the glacier history. These are the regions over which statistics are calculated for each zone (Tables 2.3 and 2.4). Contours are the 500 m NCEP-NCAR reanalysis elevations; zero contour not shown. Coast lines are in gray.

to the Karakoram and into central Tibet. The northern zone includes the regions of the Tien Shan in Xinjiang province, China and the mountainous areas of central Mongolia. Finally, the eastern zone includes the portion of the Himalaya around Nepal and eastern Tibet. I demonstrate in the sections that follow that the size of each of these zones corresponds approximately to the spatial scale expected of patterns in regional climate in the modern climate, so it is perhaps not surprising that the glacier history also varies on these spatial scales (Gillespie and Molnar, 1995; Rupper et al., 2007).

2.2.2 Central Asian Climate Variability

Glaciers are found on high topography throughout Central Asia, and in very diverse climates: glaciers in the Himalaya are fed by the intense summer monsoon precipitation and a wintertime storm track; glaciers nestled along the eastern side of the Karakoram face the extreme dryness of the desert; and glaciers clinging to the peaks of the Mongolian Altai experience seasonal cycles in temperature as large as 40 °C. Modern interannual climate variability can be used to test the sensitivity of these glaciers to typical changes in climate (e.g., using standard deviations), and how that sensitivity changes across these diverse climates.

I focus first on characterizing this regional variability in the modern climate, using the NCEP-NCAR reanalysis dataset (Kalnay et al., 1996; Kistler et al., 2001). The two atmospheric quantities I consider are total precipitation and positive degree days (PDDs – explained in the next paragraph). I analyze total precipitation instead of snowfall because of the coarse resolution of the reanalysis (2.5° x 2.5°) dataset. Topography is strongly smoothed at this resolution, and so rain at the surface elevation of a reanalysis grid point would likely not be rain at the ELA of a glacier within that grid point. In the development of the SEMB model in Section 2.3, I assume that all precipitation falling at the ELA is snow. A fully consistent accounting of the difference between rain and snow at the ELA

would also involve calculating the refreeze of rain within the snowpack and the resulting heat input. I can neglect these effects given my focus on regional scales and first-order questions. The implications for the conclusions are addressed in sensitivity studies in Section 2.5, and in the discussion in Section 2.6.

The second quantity I consider is positive degree days (PDDs). PDDs are the sum of daily mean air temperatures (T_a) that are above zero:

$$PDD = \sum H(T_a), \qquad 2.1$$

where H is 0 for $T_a \leq 0$ and T_a for $T_a > 0$; the sum is taken over the calendar year. Thus PDD has units of °C days. The number of PDDs in a year is frequently used as an indicator of ice and snow melt over the year. In simple treatments total ablation is assumed to be proportional to PDDs, the constant of proportionality is known as the melt factor, and calibrated to observed melt at glaciers (e.g., Hoinkes and Steinacker, 1975; Braithwaite, 1995). The method is sometimes modified to include different melt factors for snow and ice, and to allow for percolation and refreeze of meltwater within the snowpack (Casal et al., 2004; Zhang et al., 2006).

The regional, as well as temporal, variability in Asian climate is illustrated in Figure 2.2. The figure shows total annual precipitation anomalies (m/yr) and

positive degree day (PDD) anomalies for each year from 1948 to 2006 for each of the three zones using the NCEP/NCAR reanalysis data set (Kalnay et al., 1996).

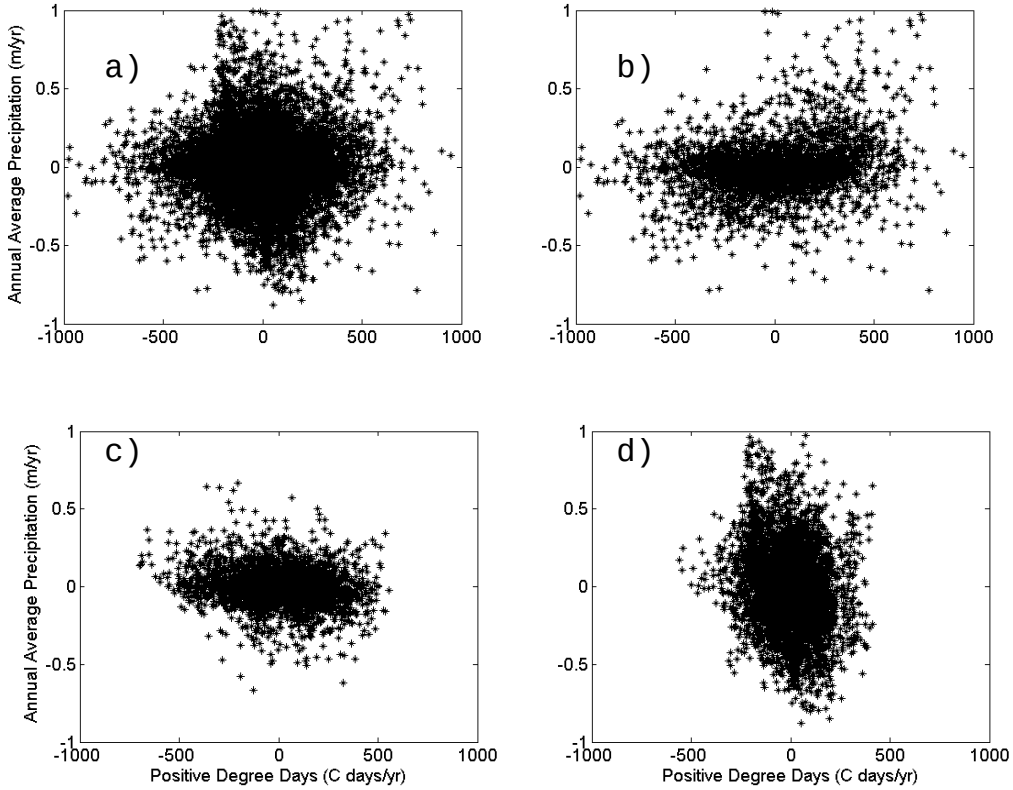

Figure 2.2: Scatter plots of annual average precipitation anomalies (m/yr) versus positive degree day anomalies (^{o}C days/yr) for each grid point in the NCEP reanalysis data set for the years 1948 to 2006. a) Central Asia, b) the western zone, c) the northern zone, and d) the eastern zone. The different shape to the scatter in each region demonstrates the differences in climate variability. Means and standard deviations averaged over each of the three zones are provided in Table 2.3.

Lumping all three regions together, panel a, the plot looks like there is no pattern. Separately, however, it is clear that each zone has different climate variability (panels b c, and d). The eastern zone is dominated by variations characteristic of monsoonal climates, high precipitation variability and low PDD variability. The

northern zone is the most continental climate, with low precipitation rates and hence low precipitation variability, contrasting with high PDD variability. In the western zone both PDD and precipitation variability is high. Thus the figure highlights the important point that there are significant regional differences in the climate variables that glaciers care about.

This regional climate variability within Central Asia makes it an ideal setting to understand how the sensitivity of glaciers changes in different climatic regimes. I want to evaluate how these variations in regional climate variability translate into the glacier response. The following section describes the energy-balance modeling framework used to achieve this.

2.3 Surface Energy- and Mass-Balance Model

I emphasize here that my main goal is to understand how the ELA *changes* in response to climate *changes*. It matters less, therefore, that the absolute ELA is in close agreement with observations. It is only necessary that the model correctly reflect the most important terms in the energy balance at the ELA. If it does this, the model can be used to evaluate the relative sensitivity of the ELA to changes in atmospheric variables. A particular strength to framing the approach in this way is that, while the absolute ELA is very sensitive to model parameters (i.e., albedo,

surface roughness, etc), the change in ELA for a change in climate is insensitive to the magnitude of the parameters (Appendix B).

This SEMB model has two nested balance algorithms, a surface energy balance and a mass balance. By definition, the ELA is the elevation at which these two balances both apply. For specified climate inputs, the model solves for the elevation at which a snow-covered surface would be in energy and mass balance. In other words, I ask the question "if there were a glacier within a given reanalysis grid point, what would the elevation of its ELA be?" The surface energy-balance model is described first.

2.3.1 Surface Energy-Balance Model

The surface energy-balance model follows closely the approach taken by Kayastha et al. (1999), Wagnon et al. (2003), and Molg and Hardy (2004) but modified such that it is suitable for application to a larger region.

The basic surface energy-balance equation used is

$$Q_m = S + L + Q_s + Q_l + Q_g, \qquad 2.2$$

where: Q_m is the energy available for melting the snow/ice surface; S is the net shortwave radiation flux absorbed at the surface; L is the net longwave radiation flux; Q_s is the sensible heat flux; Q_l is the latent heat flux; and Q_g is the heat conduction at the glacier surface. Q_g is a small term in the seasonal energy balance (e.g., Calanca and Heuberger, 1990; Kayastha et al., 1999; Ohmura, 2001), and so is neglected from here on. As noted earlier, I assume that all precipitation falls as snow at the ELA, thus the heat flux supplied by precipitation is zero. I take the sign convention that downward fluxes are positive. Tables 2.1 and 2.2 list all variables and parameters used in the equations, in the order they appear in the text. For clarity only the main equations are discussed in the body of the text. Refer to Appendix A for a fuller discussion of equations and parameters used.

Table 2.1: Model parameters and constants, their values where appropriate, and units for all equations described in Section 2.3 and Appendix A.

	Parameters and Constants	Value	Units
α	Albedo of the glacier surface	0.6	
σ	Stefan-Boltzmann constant	5.67×10^{-8}	$W\ m^{-2}\ K^{-4}$
ε	Emissivity of the glacier surface	1	
C_1	Longwave emissivity constant	0.5 to 0.9	hPa^{-1}
c_p	Specific heat of air at constant pressure	1010	$J\ kg^{-1}\ K^{-1}$
ρ_o	Density of air at standard sea level	1.29	$kg\ m^{-3}$
p_o	Pressure of air at standard sea level	1013	hPa
L_v	Latent heat of vaporization	2.514	$MJ\ kg^{-1}$
L_s	Latent heat of sublimation	2.848	$MJ\ kg^{-1}$
L_m	Latent heat of fusion	.334	$MJ\ kg^{-1}$
t	time		months
k	von Karman constant	0.4	
z	Measurement level above the surface of wind, humidity, and temperature	2	m
z_{om}	Scalar roughness length of momentum	0.5	mm
z_{oh}	Scalar roughness length of temperature	0.5	mm
z_{ov}	Scalar roughness length of humidity	0.5	mm
g	Gravitational constant	9.8	$m\ s^{-2}$
A	Constant	17.67	°C
B	Constant	243.5	°C
H	Scale height	8	km
Z	Elevation		km

Table 2.2: List of the model variables and units used in the equations described in Section 2.3 and Appendix A.

	Variables	**Units**
$\mathbf{T_a}$	Monthly mean air temperature at the ELA	°C
$\mathbf{T_s}$	Monthly mean surface temperature at the ELA	°C
$\mathbf{e_a}$	Evaporation vapor pressure of the air	hPa
$\mathbf{D_s}$	Turbulent-transfer coefficient for stable conditions	
p	Pressure of air at the ELA	hPa
$\mathbf{e_s}$	Saturation vapor pressure at the surface	hPa
$\overline{\mathbf{T}}$	Mean annual air temperature	°C
$\mathbf{T_{amp}}$	Amplitude in the seasonal cycle of air temperature	°C
$\mathbf{D_n}$	Transfer coefficient for neutral stability	
v	wind speed	$m\ s^{-1}$
$\mathbf{v^*}$	Friction velocity	$m\ s^{-1}$
Ri	Bulk richardson number	
RH	Relative humidity	%
Z	Height of the ELA	m
ps	Pressure of air at the surface	hPa

2.3.2 Shortwave Radiation

The shortwave radiation absorbed by the glacier surface, S, is dependent upon the incident shortwave (S↓) and the albedo (α):

$$S = S\downarrow (1 - \alpha). \qquad 2.3$$

While in reality albedo varies both in space and time, it is unrealistic to know it for all glacier surfaces across the large region of interest, and impossible to know

the albedo of past glaciers. Albedo in this model is, therefore, set to be equal to an albedo of 0.6, which is intermediate between that of pure ice and that of fresh snow (e.g., Paterson, 1999). The effect of albedo variations is evaluated in Sections 2.5 and 2.6. Since albedo is held fixed, both the regional and temporal variability in absorbed shortwave radiation in the model is governed only by the impact of cloudiness on the incoming shortwave radiation.

The absorbed shortwave radiation is balanced by a combination of the longwave radiation, sensible heat, latent heat, and subsurface heat fluxes.

2.3.3 Longwave radiation

Net longwave radiation is equal to the sum of the outgoing and incoming longwave radiation,

$$L = L\uparrow + L\downarrow. \qquad 2.4$$

$L\uparrow$ is calculated using the Stefan-Boltzmann law

$$L\uparrow = \sigma \varepsilon_s T_s^4, \qquad 2.5$$

and is therefore a function only of the surface temperature (T_s). Emissivity (ε_s) of the snow/ice surface is assumed to be equal to one and σ is the Stefan-Boltzman constant. $L\downarrow$ is controlled largely by the air temperature above the surface, but is also dependent on radiative properties of the atmosphere itself, especially atmospheric humidity and clouds.

There are many empirical formulas employed to calculate incoming longwave radiation. I follow the equation for incoming longwave radiation in mountainous terrain suggested by Duguay (1993) in a review of radiation modeling. This equation relies on a combination of air temperature (T_a), humidity, and empirical constants:

$$L\downarrow = \sigma T_a^4 (C_1 + C_2 e_a). \qquad 2.6$$

e_a is the vapor pressure of the near-surface air (2m) and is dependent upon the air temperature at the ELA and the prevailing relative humidity. The longwave down was determined in two ways. First, values for C_1 and C_2 were assumed to be equal to the average reported for individual glaciers, 0.55 and 0.017, respectively (e.g., Duguay, 1993; Molg and Hardy, 2004). For the level of approach taken and the uncertainty in the atmospheric variables, the contribution from $C_2 e_a$ is negligible (typically less than 5%). This suggests that the humidity is not as important as other radiative properties of the atmosphere, such as clouds. Second,

for the standard case I present here, the monthly mean C_1 is determined using the NCEP downwelling radiation at the surface, which yields similar values to Duguay (1993). This calibrated C_1 is therefore the emissivity of the lower troposphere in the longwave band, and is therefore dependent on temperature, cloudiness, et cetera.

2.3.4 Sensible and Latent Heat Fluxes

A commonly employed method for calculating turbulent heat fluxes is the so-called "bulk" method based on the Monin-Obukhov similarity theory. The expression for the sensible heat flux is

$$Q_s = D_s c_p \rho_o \frac{p}{p_o} (T_a - T_s). \qquad 2.7$$

T_s and T_a are the surface temperature and near surface air temperature respectively. C_p is the specific heat at constant pressure; ρ_o is the density of air at sea level. D_s is the turbulent transfer coefficient. This coefficient is dependent upon wind speed, roughness lengths, and a correction for buoyant versus mechanical mixing. p/p_o is the atmospheric pressure at the ELA divided by atmospheric pressure at standard sea level. It reflects the fact that the atmosphere's ability to carry heat is dependent on its density.

The expression for latent heat is

$$Q_l = D_s \rho_o \frac{1}{p_o} L_{v,s} (e_a - e_s). \qquad 2.8$$

If the surface temperature is zero or above, then the latent heat of vaporization (L_v) is used; below zero that for sublimation (L_s) is used. e_s is the vapor pressure at the surface. It is assumed to be saturated and is therefore only dependent upon the surface temperature. Since saturation vapor pressure is an exponential function of temperature (e.g, Wallace and Hobbs, 2005), the latent heat flux depends on T_a, T_s, and relative humidity.

2.3.5 Mass Balance and Seeking the ELA

The surface energy-balance model is combined with a mass-balance model and solved for the elevation of the equilibrium line. To facilitate discussion of the algorithms, described in the next paragraphs, one more constraint from the reanalysis data needs to be addressed. The ELA is an annual mean property. In order to close the equations, and get a unique value for the ELA, the relationship between the temperatures at each time step in the annual cycle must be prescribed:

$$T_a = \bar{T}(z) + T_{amp} \cos(2\pi \frac{t}{12}), \qquad 2.9$$

and $\bar{T}$ is the mean annual 2m air temperature at the ELA. The amplitude of the annual cycle in air temperature, $T_{amp,}$ is prescribed using the reanalysis output.

The model calculates the energy available for melt (Q_m) every month from Equation 2.2, following the method of e.g., Kayastha et al. (1999). Using an iterative solver, T_s converges toward a value such that all fluxes are balanced (i.e., Q_m is equal to zero). If the resulting T_s is greater than zero, then T_s is reset to zero and Q_m is recalculated. This recalculated Q_m represents the energy available for melt. Melt is then equal to Q_m x L_m^{-1} for months where T_s equals 0 ^oC. Additionally, evaporation occurs when T_s equals 0 ^oC and $e_a<e_s$; and is calculated as Q_l x L_v^{-1}. When T_s is less than 0 ^oC and $e_a<e_s$ sublimation occurs at a rate of Q_l x L_s^{-1}. The total ablation per month is then the sum of the monthly sublimation, evaporation, and melt.

In the mass balance iterative algorithm, the model seeks the elevation at which the $\bar{T}$ results in a total annual ablation (calculated using the surface energy-balance method above) that exactly equals the total annual accumulation. In the mass balance portion of the model, the $\bar{T}$ is sought for which ablation equals accumulation. Once this $\bar{T}$ is found, the climatological lapse rate is applied to

determine the elevation of the ELA. The final model output includes monthly 2m air temperature, surface temperature, all energy balance terms, sublimation, melt, and evaporation at the equilibrium line for a given set of climate variables and model parameters.

In the next sections, I discuss the results of applying the model to Central Asia, which climate variables are most influential on glacier mass balance, and how that changes for differing regions.

2.4 Surface Energy- and Mass-Balance Model Results

I briefly recap the procedure. The basic goal is to characterize how regional patterns of climate variability translate into regional patterns of ELA sensitivity. Taking NCEP/NCAR reanalysis output, I ask the question "if there were a glacier within a given reanalysis grid point, what would the elevation of its ELA be?" In other words, using the SEMB model I solve for the elevation at which a snow-covered surface would be in mass and surface energy balance.

2.4.1 Equilibrium-line altitudes

There is a pattern in the ELAs calculated from the NCPE-NCAR climatology using the SEMB model (Figure 2.3). Despite the coarse resolution of the

reanalysis output and the uncertainty in model parameters, I show that this general pattern in the modeled ELAs is reasonable. In particular, Figure 2.4a shows a high resolution digital elevation model (DEM) with colors marking peaks that would intersect the modeled ELAs. Figure 2.4b shows the same DEM and ELA intersection, but with bright pink dots marking actual glaciers. The ELAs are more extensive than the actual glaciers in the interior of the plateau. This is likely due to the coarse resolution of the NCEP-NCAR climatology, which allows for greater penetration of the monsoonal rains into the Tibetan Plateau. However, Figure 2.4 shows that the model is predicting glaciers to exist in broadly the same regions where glaciers exist today.

I emphasize that my primary interest is in how patterns in climate *change,* lead to patterns of ELA *change*, and so I am less interested in simulating the climatological mean ELA. However it is at least reassuring that the SEMB model reproduces broadly where glaciers are found in the current climate.

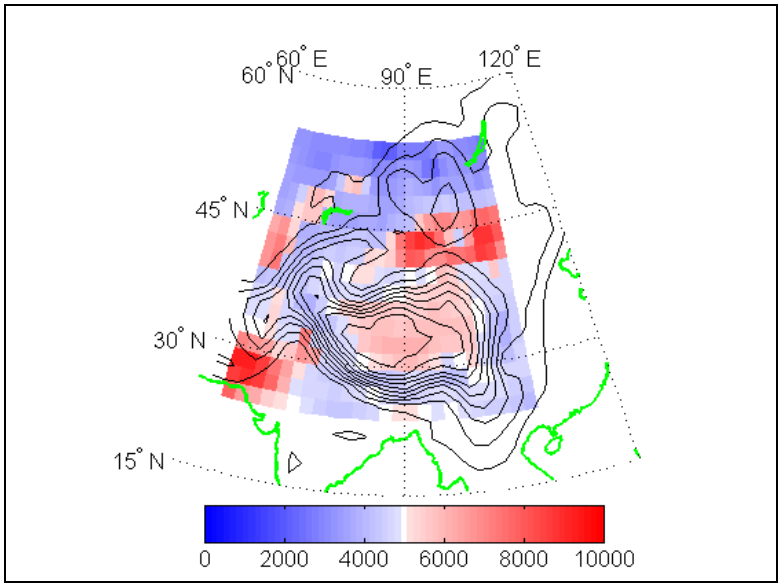

Figure 2.3: Colors are the elevation of the equilibrium line calculated using the SEMB model.

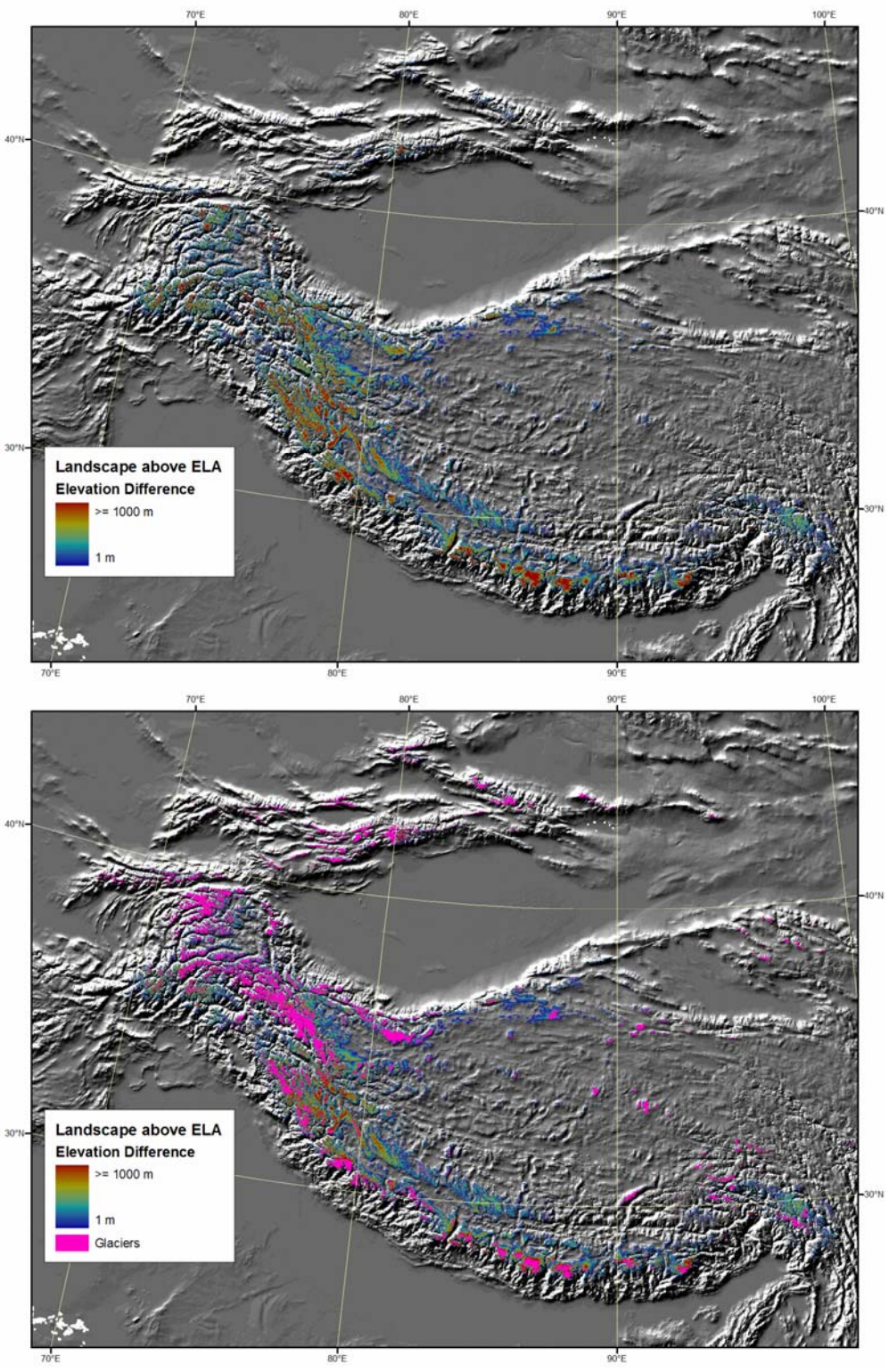
70°E
80°E
90°E
100°E
40°N
30°N
Landscape above ELA
Elevation Difference
>= 1000 m
1 m
Glaciers

Figure 2.4: Gray scale is a high resolution DEM of Central Asia. Colored shading from blue to red highlights those regions where and by how much the topography intersects the modeled ELAs. In the lower panel, locations of actual glaciers are highlighted in pink. This is not intended to be a test of the model skill.

2.4.2 Sublimation or Melt?

Most studies which look at glacier mass balance on a regional scale use simple mass balance schemes such as the PDD method for calibrating ablation. In so doing, they ignore the possible contribution of sublimation, clouds, etc. One of the advantages of applying a self-consistent surface energy balance approach is the ability to assess the relative importance of sublimation and melt in the ablation process, and an assessment of when and where one process dominates over another.

In addition to spatial patterns in the ELAs, there are also spatial patterns in the dominant ablation processes. The fractional contribution of melt to the total ablation at the ELA calculated from the NCEP-NCAR climatology is shown in Figure 2.5. There are places where ablation occurs almost entirely by melt and others by sublimation. In particular, a qualitative comparison of the pattern in the fractional contribution of melt (Figure 2.5) to the spatial pattern in annual-average precipitation (Figure 2.9a) indicates that, at the ELA, melt dominates where precipitation is high and sublimation dominates where precipitation is low.

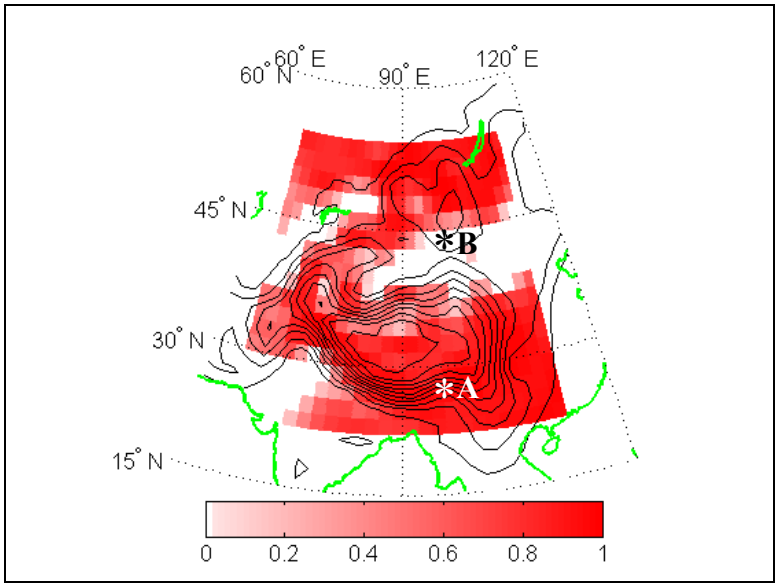

Figure 2.5: Fractional contribution of melt to the total ablation, at the equilibrium-line altitude. Output is from the surface energy- and mass-balance model. White areas are regions where sublimation accounts for the total ablation; red regions are melt-dominated areas. Note the spatial pattern in dominant ablation mechanisms across the region. This pattern is reminiscent of the pattern in annual average precipitation (Figure 2.10a). Points A and B denote grid points where seasonal cycles in climate and energy balance terms are presented in Figures 2.7 and 2.8.

The relationship between the ablation pattern and precipitation pattern is highlighted in Figure 2.6. The scatter plot shows melt dominating in regions where precipitation is greater than ~0.5 m/yr and sublimation dominating in regions where precipitation is less than ~0.25 m/yr. The reason for this general relationship between ablation and precipitation can be seen from a comparison of the seasonal cycle in the surface temperature and energy balance. The rapid transition between melt and sublimation is not diagnosed here, but is discussed further in Section 2.6.

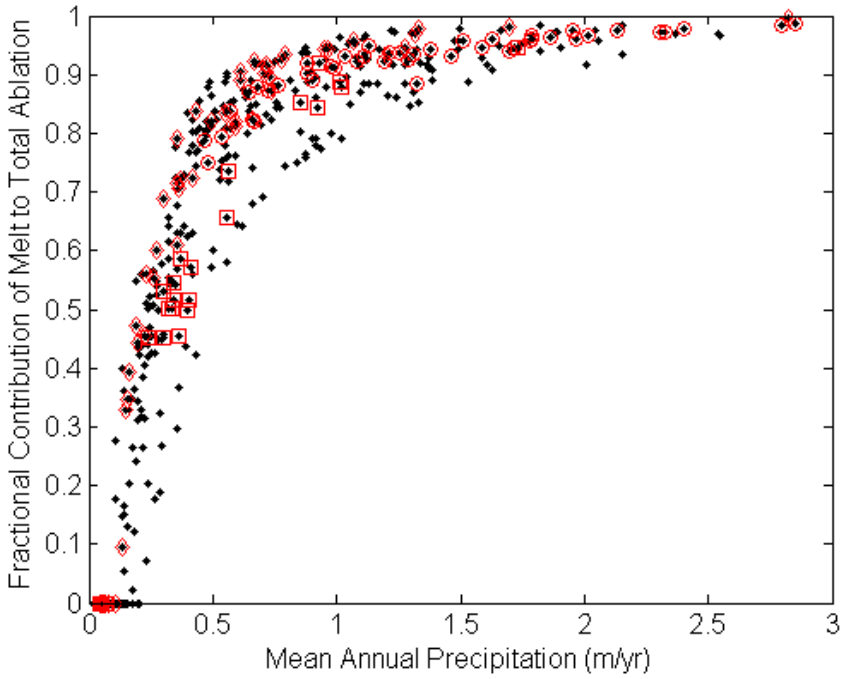

Figure 2.6: Mean annual precipitation versus fractional contribution of melt to total ablation at each NCEP-NCAR reanalysis grid point across Central Asia. Shapes highlight those points that fall within the three zones: eastern zone (circles), western zone (squares), and northern zone (diamonds).

2.4.3 Seasonal Cycle in Climate and Energy Balance Terms

I contrast the surface energy and mass balances at the ELA for two reanalysis grid points, one in the melt-dominated region and one in the sublimation region. They are denoted by A and B, respectively, in Figure 2.5.

First, for grid point A in the melt dominated region, the total precipitation is 3.5 m/yr, and peaks strongly during the summer monsoon (Figure 2.7, top panel). To melt this depth of ice takes a flux of approximately ~50 W m^{-2} averaged over the

year. In contrast, because the energy required to sublimate is 8.5 times greater than that to melt, it would require approximately ~425 W m^{-2} to sublimate the total accumulation. It is therefore much more efficient for the system to melt the 3.5 m/yr. At the ELA, in order to balance this amount of accumulation, the SEMB model determines that the surface temperature must be equal to 0 ^{o}C for approximately five months (i.e., the length of the melt season), shown in the top panel of Figure 2.7. Therefore the annual-mean surface temperature at the ELA must be higher, and so results in an ELA that is lower.

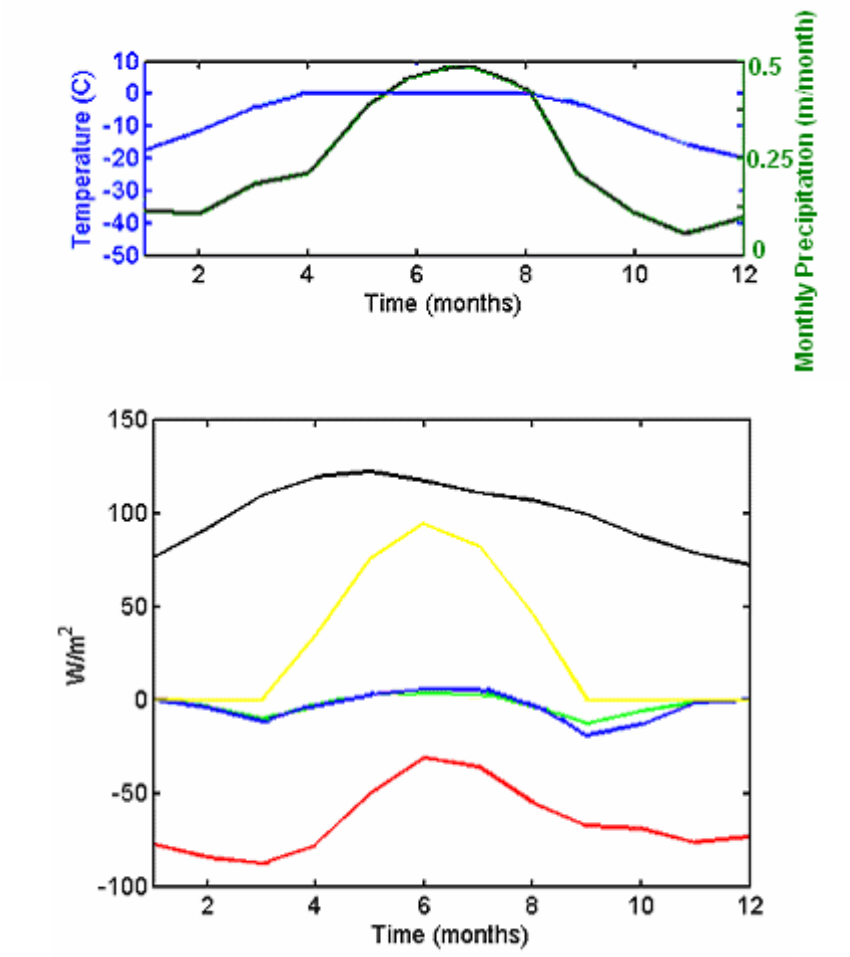

Figure 2.7: Seasonal cycle in climate and energy balance components at grid point A (Figure 2.5) in a melt-dominated region. Top panel is the seasonal cycle in surface temperature at the modeled ELA (blue) and total monthly precipitation (green). Bottom panel is the seasonal cycle in net shortwave radiation (black), net longwave radiation (red), turbulent sensible heat flux (green), turbulent latent heat flux (blue), and excess energy flux available for melt (yellow) at the modeled ELA.

The different energy fluxes in the seasonal cycle are shown in the bottom panel of Figure 2.7. For the five month period for which T_s equals zero, there is an imbalance in the energy fluxes, which provides the excess energy available for melt. This energy flux used for melting is approximately equal to the difference between net shortwave and net longwave radiation fluxes. These three terms

dominate the energy balance throughout the year. The turbulent sensible and latent heat fluxes are small in comparison to the radiative fluxes. During the other seven months of the year the energy fluxes are in balance and surface temperatures remain below zero, and melt cannot occur. Instead, the turbulent latent heat flux, which is negative through those seven months, implies sublimation. Some sublimation does occur because the turbulent latent heat flux is negative when $T_s<0$; overall, however, melt is much higher than sublimation, accounting for 99.5% of the total annual ablation. These results are summarized in Table 2.3, with values of the energy balance components averaged over the melt season and sublimation season separately.

The seasonal cycle and seasonal averages of the energy balance terms compare well with studies on individual glaciers in melt dominated regions of Central Asia (e.g., Calanca and Heuberger, 1990; Kayastha et al., 1999). These studies also show that melt dominates in regions where precipitation is high, and that the radiative fluxes dominate the energy balance at the surface.

Table 2.3: All values are the mean for the eastern, western, and northern zones (Figure 2.1). The table includes the mean ELA (m) and melt contribution to total ablation (fraction) at the ELA. Also included in the table are the mean and standard deviation (σ) in annual precipitation (P), summertime solar insolation (S), summertime wind speed (V), summertime relative humidity (RH), and summertime air temperature (T_a). Summertime is the mean for June, July, and August. The change in ELA for one standard deviation changes in P, S, V, and RH are also shown. The change in ELA for changes in all atmospheric variables composited over years when mean summer time temperatures are one standard deviation above the mean is also included.

	Units	East	West	North
Modeled ELA	m	4880	4625	4648
Melt Fraction	--	0.85	0.60	0.40
Mean P	m yr^{-1}	1.6	0.6	0.4
σP	m yr^{-1}	0.7	0.2	0.1
dELA for σP	m	-130	-136	-554
Mean S	W m^{-2}	283	358	311
σS	W m^{-2}	10	9	9
dELA for σS	m	78	69	81
Mean RH	%	89	45	58
σRH	%	2	5	4
dELA for σRH	m	2	3	-11
Mean V	m s^{-1}	1.6	1.4	1.1
σV	m s^{-1}	0.4	0.6	0.7
dELA for σV	m	4	2	-14
Mean T_a	^{o}C	15	17	16
σT_a	^{o}C	0.7	1.6	1.1
dELA for anomalously warm summers	m	225	265	210

The dominance of radiative fluxes throughout the year at grid point A (Figure 2.7b, Table 2.3), and in all regions where melt dominates, suggests that the ELA in melt-dominated regions will be most sensitive to climate variables that control the radiative fluxes: cloudiness, air temperature, surface temperature, and the

longwave constant (C_1 in Equation 2.6). While C_1 is a measure of the emissivity of the lower troposphere in the longwave band, I show in Section 2.3.3 that the influence of humidity on longwave down is small. Therefore the ELA is less likely to be sensitive to changes in relative humidity and wind since they only directly influence the latent and sensible heat fluxes, which are small in comparison to the other energy components. A detailed discussion of the sensitivity of the ELAs to changes in precipitation and ablation is provided in Section 2.5.

In contrast, at a grid point B, where sublimation dominates, the total annual precipitation is extremely low, approximately 15 cm/yr (Figure 2.8, top panel). This takes a flux of only ~2 W m^{-2} to melt. By comparison sublimating the same amount of mass would consume ~16 W m^{-2}. With such low accumulation rates, melting cannot dominate the mass balance at the ELA. Sublimation occurs whenever the temperature is below 0^oC and the turbulent latent heat is negative. Typical seasonal cycles in surface temperature mean that if, even for a short while, the temperature touches 0^oC at any time during the year, the sublimation happening in the non-melt season (i.e. the rest of the year) is already more than enough to ablate the available accumulation. Therefore the annual-mean surface temperature at the ELA must be lower, and therefore the ELA must be higher.

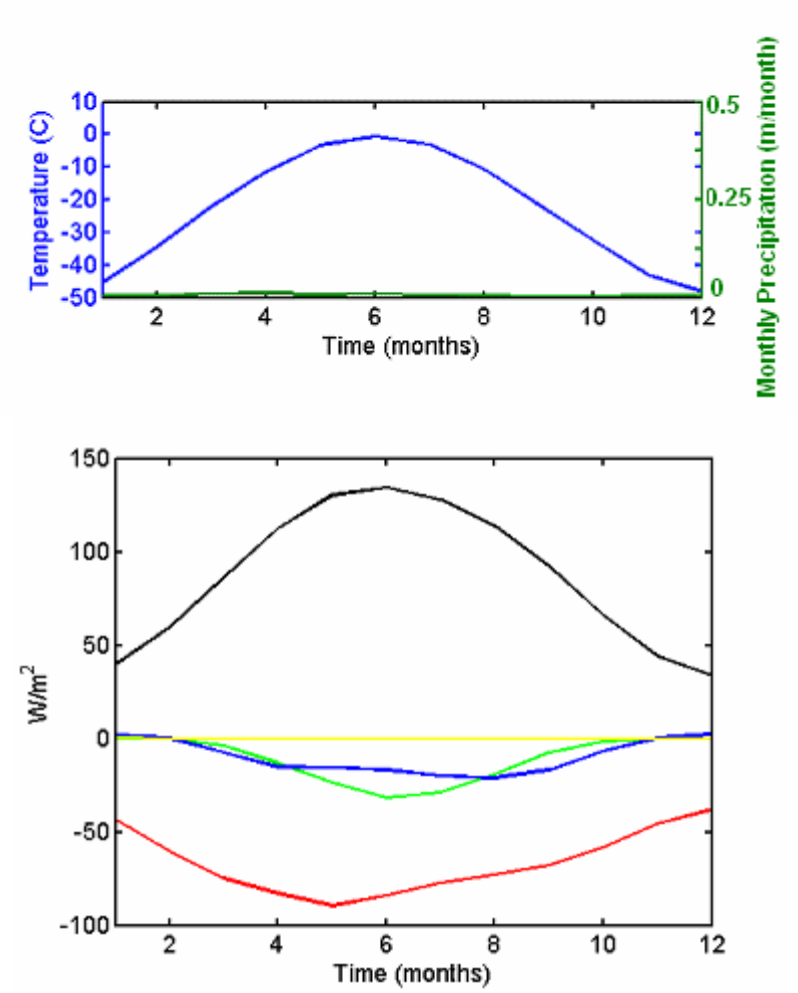

Figure 2.8: As in Figure 2.7, but for grid point B (Figure 2.5) in a sublimation-dominated region.

Figure 2.8 (bottom panel) shows how this operates at point B. Annual averaged values of the separate energy components are in Table 2.3. Averaged over the annual cycle, the net solar radtion is 90 W m^{-2}. This is chiefly balanced by the net longwave radiation (-63 W/m2). Making up the balance is sensible heat flux (-11 W/m2), and latent heat flux (-16 W/m2). This latent heat flux suffices to sublimate the accumulation and so achieve mass balance. This picture agrees

with studies on tropical glaciers. Particularly where accumulation rates and the seasonal cycles in air temperature are low, sublimation will come to dominate the mass balance (e.g., Wagnon et al., 2003; Molg and Hardy, 2004). Again, since the radiative fluxes dominate the surface energy balance at the ELA, changes in surface and air temperatures, cloudiness, and C_1 will likely influence the sublimation. Unlike melt-dominated regions, relative humidity and wind speed are also likely to be important because these variables influence the turbulent latent heat flux, which supplies all energy for sublimation. Again, sensitivity tests to changes in these variables are discussed in detail in Section 2.5.

To summarize the results above, the spatial pattern in the modeled ELAs is closely tied to the total accumulation. In particular, at the ELA, sublimation is the process of ablation in regions where precipitation is very low. In regions where precipitation is high, ablation occurs via melt at the ELA. Radiative fluxes dominate the energy balance in all regions, which is an indication that ablation will likely be most sensitive to changes in air and surface temperatures, cloudiness, and C_1 (which includes the influence of clouds). Additionally, humidity and wind may be important in sublimation regions since turbulent latent heat provides the energy available for ablation. I will show in Section 2.5 that melt regions are indeed insensitive to changes in humidity and wind, and that ablation is most sensitive to changes in temperature, cloudiness, and C_1.

Importantly, the magnitude and relative importance of the energy balance components at the ELA compare favorably with studies on individual glaciers (Calanca and Heuberger, 1990; Kayastha et al., 1999; Molg and Hardy, 2004). Additionally, the magnitude of the model parameters does not change the sensitivity of the ELAs to changes in climate (Appendix B). These results, together with the reasonable pattern in ELAs, suggest that the SEBM model is performing well and capable of capturing the sensitivity of ELAs to a change in climate at a regional scale.

2.4.4 Positive Degree Day Approach

As noted in Section 2.1 and 2.2, the positive degree day method is commonly used for determining ablation on regional scales (e.g., Braithwaite, 2002; Casal et al., 2004). Glacier melt is assumed to be proportional to the integral over the annual cycle of near-surface air temperatures that are above zero. The constant of proportionality is known as the melt-factor, which is an empirically-derived parameter. A particular strength of the SEMB approach is that the melt factors can be calculated directly, since both the seasonal cycle in near-surface air temperature and melting are outputs from the model. In regions where sublimation dominates and the temperatures remain below zero at the ELA, PDDs are not defined. Lower down on large glaciers, surface temperatures might reach zero, permitting melting at some point during the year.

Figure 2.9 shows histograms of the melt factors calculated within the three regions for grid points at which PDDs exceed zero at the ELA (50 % of total grid points). Melt factors vary between approximately 5 and 18 mm d^{-1} C^{-1} for all of Central Asia (between 25 and 60 N and 65 and 112 E), with the mean equal to 11 mm d^{-1} C^{-1}. The mean for the western, northern, and eastern zones are 12, 9, and 10 mm d^{-1} C^{-1}, respectively. While there is both regional variability and a sizable spread in melt factors across the region, the values agree well with those measured in the area. For example, Nepalese and Chinese researchers have measured the melt factors in the southern Himalayas and the Tien Shan and report melt factors ranging between 5 and 16 mm d^{-1} $^{o}C^{-1}$ (e.g., Kayastha, 2002; Zhang et al., 2006).

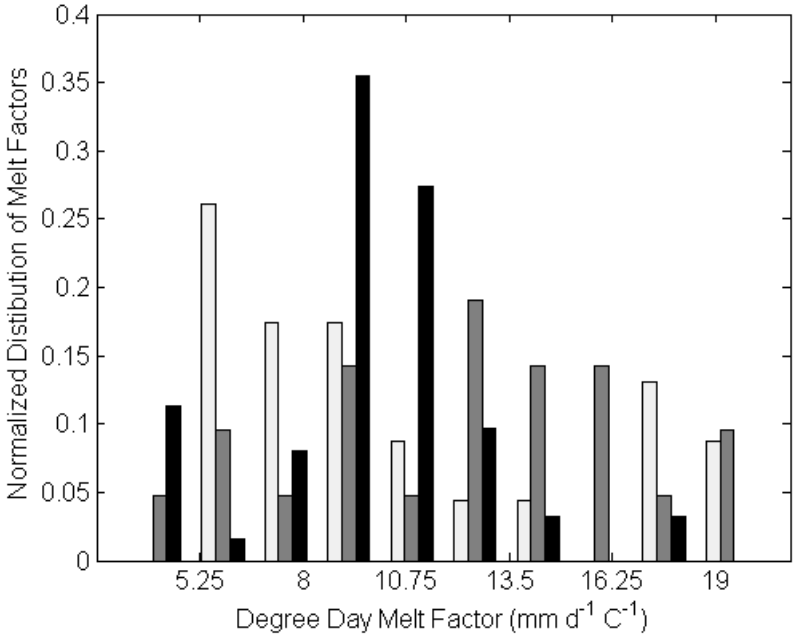

Figure 2.9: Normalized distribution of melt factors, calculated using the SEMB model, across the western (dark gray), northern (light gray), and eastern (black) zones. Mean melt factors for the western, northern and eastern zones are 12, 9, and 10 mm d^{-1} C^{-1}, respectively.

The comparison of melt factors from the SEMB model and the empirically-determined coefficients gives two pieces of information. First, the general approximate agreement between the SEMB-derived melt factors with observations suggests that the SEMB model is calculating realistic ablation rates, given the large scale forcing. Second, there is no fundamental reason the melt-factor should be constant in space or time. However studies that use the PDD method on a regional scale have to make that assumption. The histograms in Figure 2.9 give a sense of how melt factors actually vary in space, and suggests care be taken if the magnitude of the answer being sought would lie within the range of uncertainty suggested by Figure 2.9.

To this point I have shown that regional patterns in climate give rise to regional patterns in both ELAs and the dominant ablation mechanisms. From these results it follows that regional patterns in glacier ELA sensitivity to changes in climate should be expected as well.

2.5 Spatial patterns of glacier sensitivity to climate and model parameters

The SEMB model can be used to explore the sensitivity of ELAs to climate variability. The measure of climate variability I use is one standard deviation of the interannual variability of an atmospheric variable, within each reanalysis grid point. This measure normalizes these sensitivity tests against a common measure of characteristic variability for each atmospheric variable.

Figure 2.10a,b shows the mean annual precipitation and standard deviation (σP) from the reanalysis output, and averages in each of the three zones are given in Table 2.4. The regional patterns of mean and standard deviation are quite similar.

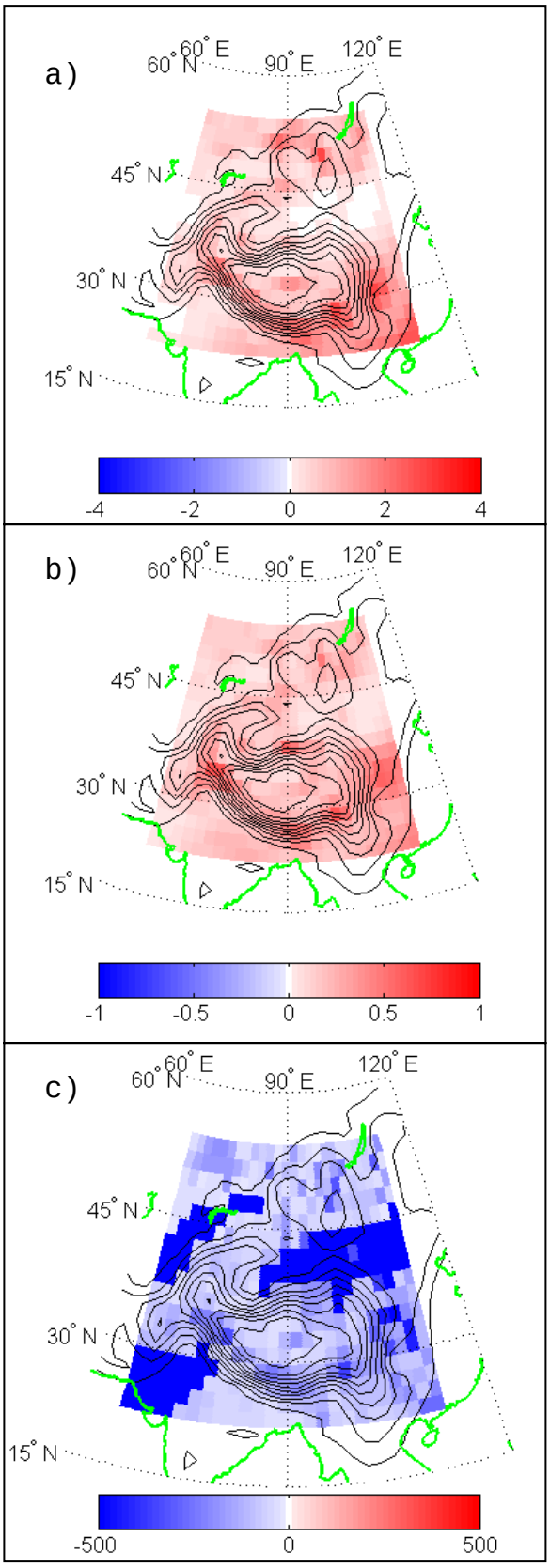
a)
60° E
90° E
120° E
60° N
45° N
30° N
15° N
-4
-2
0
2
4
b)
60° E
90° E
120° E
60° N
45° N
30° N
15° N
-1
-0.5
0
0.5
1
c)
60° E
90° E
120° E
60° N
45° N
30° N
15° N
-500
0
500

Figure 2.10: a) Mean annual precipitation (m yr^{-1}), b) standard deviation in annual precipitation (m yr^{-1}), and c) ΔELA for one standard deviation change in precipitation (m).

Table 2.4: Mean values of the energy balance components, total accumulation (which equals total ablation at the ELA), and fractional contribution of melt to total ablation for the five month melt season at point A, seven month sublimation season at point A, and all twelve months at point B.

Energy Balance Component or Ablation	**Melt Season at Point A**	**Sublimation Season at Point A**	**Point B**
Total Ablation/Total Accumulation (m/yr)	3.5		.15
Net Shortwave Radiation (W/m^2)	100	88	90
Net Longwave Radiation (W/m^2)	-53	-81	-63
Turbulent Latent Heat Flux (W/m^2)	1	-3	-16
Turbulent Sensible Heat Flux (W/m^2)	2	-4	-11
Latent Energy Flux for Melting (W/m^2)	40	0	0
Fractional Contribution of Melt to Total Ablation	99.5		0

The change in the ΔELA for a change in precipitation equal to σP is calculated at each grid point across the model domain. The complicated response of glacier ELAs is strikingly illustrated in Figure 2.10c. The pattern in Figure 2.10c is not a simple function of the magnitude of σP. In particular, regions where sublimation dominates are acutely sensitive to even small changes in precipitation. This is despite the fact that the standard deviation in precipitation in the sublimation regions is much less than in the melt regions (Figure 2.10b and Table 2.4). For example, the average change in ΔELA in the northern zone, a region dominated by sublimation, is 550m for σP equal to 0.1 m/yr. By comparison, in the melt dominated region of the eastern zone, the average change in ΔELA is only 130m for σP equal to 0.7 m/yr. Thus the sensitivity of the ELA to a change in precipitation depends on the dominant ablation process and the mean annual

precipitation. This is illustrated in Figure 2.11 of the ELA sensitivity to changes in precipitation (shown in red) versus mean annual precipitation. In sublimation-dominated regions, the change in ELA is large in regions where mean annual precipitation is low. The difference in the sensitivity of ELAs to changes in precipitation between the sublimation and melt regions arises because of the large difference between the latent heat of sublimation and that of melt. The pattern in ΔELAs within melt and sublimation regions strongly resembles the pattern in the one sigma precipitation (Figure 2.10b,c), with the largest changes in ELAs occurring where precipitation changes are also greatest (Figure 2.11).

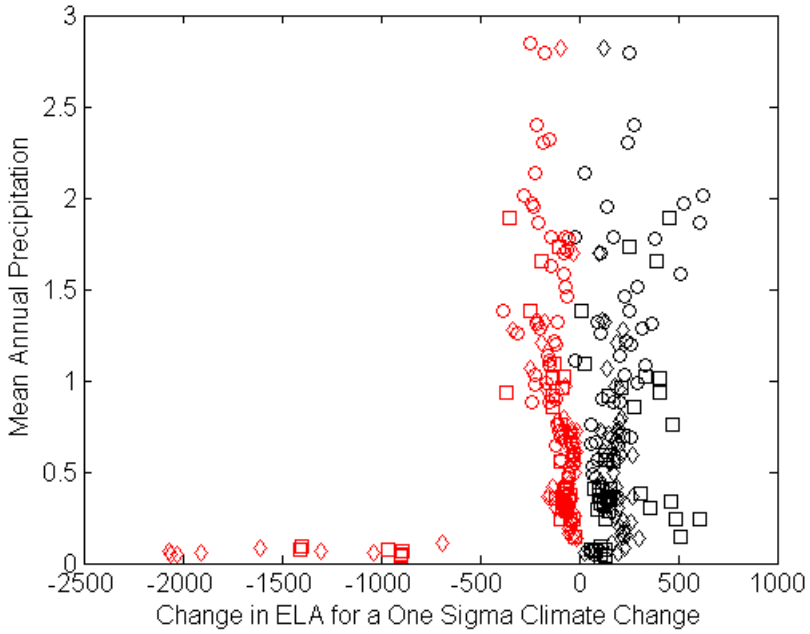

Figure 2.11: Scatter plot of the change in ELA (m) for a change in precipitation (red) and summer temperature (black) versus mean annual precipitation (m/yr) for reanalysis grid points within the three zones. The shapes indicate grid points in the eastern zone (circles), western zone (squares), and northern zone (diamonds). The figure highlights the acute sensitivity of ELAs in low precipitation regions (where sublimation dominates) to changes in precipitation.

As in the case with precipitation, the sensitivity of the ELAs to changes in relative humidity and wind speed also changes depending on the dominant ablation process (Table 2.4). ΔELAs for a sigma change in humidity and wind are small in all regions. However, sublimation-dominated regions are more sensitive to changes in humidity and wind than melt-dominated regions. These results highlight the fact that sublimation-dominated regions are generally more sensitive to even small changes in climate than melt-dominated regions are. It is important to note that for a change in climate, larger changes in humidity might be possible. Also, the energy fluxes are nonlinear combinations of atmospheric variables and day-to-day fluctuations in relative humidity are much greater than the interannual variability. These variations won't necessarily average to the monthly values. This suggests that sublimation regions are likely to be sensitive to assumptions in the formulation of the SEMB model.

Changes in shortwave radiation incident at the surface are controlled mainly by changes in cloudiness. Thus ΔELA for a one standard deviation increase in absorbed shortwave radiation is a test of the sensitivity of the ELA to the influence of clouds on downwelling shortwave radiation. The sensitivity of ELAs to a one standard deviation change in shortwave radiation is nearly uniform across Central Asia (Table 2.4), but is of secondary importance to typical interannual variability in precipitation in all regions.

The sensitivity tests to changes in individual variables clearly demonstrate that a one standard deviation change in climate results in spatial patterns in ELA changes. However, radiation effects on ELAs, such as the changes in solar radiation, cannot be completely decoupled in this model because I prescribe the seasonal cycle in air temperature (T_{amp}) using reanalysis output. This is necessary in order to get a unique solution for the annual average air temperature at the ELA. So for example, if a change in clouds leads to a change in T_{amp}, that dependency is not factored in the sensitivity analysis.

An alternative to perturbing individual climate variables is to composite atmospheric variables for years when mean summer (JJA) air temperatures are anomalously warm (chosen here to be those exceeding one standard deviation above the mean). Changes in ELAs for anomalously warm summers provide a test of the ELA sensitivity to changes in ablation. The relative importance of those variables influencing the radiative fluxes can then be evaluated separately as well.

The variables examined in the composite analysis are incident shortwave radiation, relative humidity, wind speed, atmospheric pressure, downwelling longwave constant (C_1), lapse rate in air temperature, and the amplitude in the seasonal cycle (T_{amp}). The mean summer air temperature, σT_a, and ΔELA for the anomalously warm summers are shown in Figure 2.12. Averages over the

northern, western, and eastern zones are presented in Table 2.4. Figure 2.12c highlights the result that a pattern in ΔELA occurs in response to conditions during years when summer air temperatures are anomalously warm, with the largest change in ELA generally in regions where σT_a is largest. Importantly, melt-dominated regions are far more sensitive to interannual variability in temperature than in precipitation. In particular, ΔELAs for a change in temperature are approximately twice that for changes in precipitation. In contrast, ELAs in sublimation regions are more sensitive to interannual variability in precipitation than in temperature.

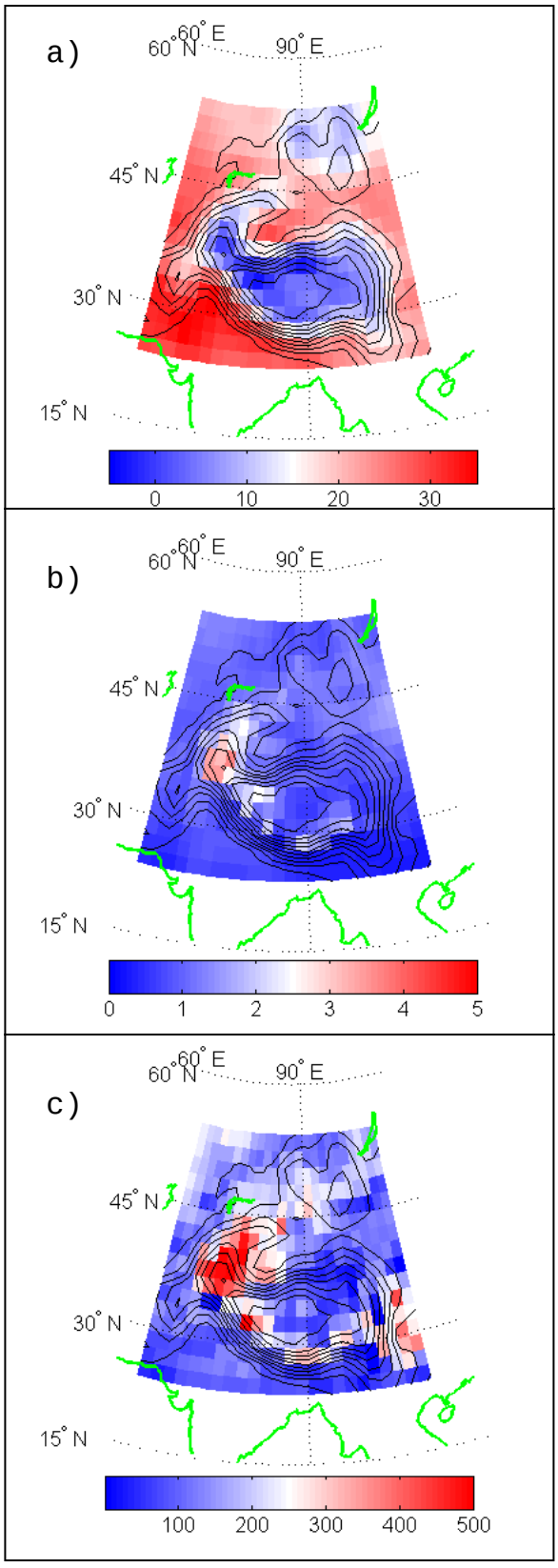
a)
60° N
60° E
90° E
45° N
30° N
15° N
0
10
20
30
b)
60° N
60° E
90° E
45° N
30° N
15° N
0
1
2
3
4
5
c)
60° N
60° E
90° E
45° N
30° N
15° N
100
200
300
400
500

Figure 2.12: a) Mean summertime (JJA) surface air temperature (^{o}C), b) standard deviation in summertime air temperature (^{o}C), and c) ΔELA for mean change in atmospheric variables when summertime temperatures are one standard deviation above the mean (m).

Together, the atmospheric variables conspire to give rise to the changes in ELA seen. Sensitivity tests suggest that incident shortwave radiation, C_1, and T_{amp} have the greatest influence on changes in ELAs during anomalously warm years. I therefore focus discussion on those three variables.

Changes in shortwave radiation and C_1 are driven by changes in cloudiness (Figure 2.13b-d). In particular, an increase in clouds has a tendency to warm the climate through an increase in downwelling longwave radiation (increase in C_1) and cool the climate through a decrease in shortwave radiation (increased albedo). The changes in cloudiness in the NCEP reanalysis output show that, in some regions, the influence of clouds on the longwave radiation tends to be greater than the decreased albedo, thereby causing a net warming when cloud fraction increases. For example, in the Taklamakan desert and the high elevation regions of the interior of the Tibetan Plateau and the Western Zone, warmest summers occur when cloud fraction is anomalously high because the increased longwave radiation is greater than the decreased shortwave radiation. The reverse is true over the more southerly regions, including the southern Himalayas, and the continental interior, where clouds have a cooling tendency due to the increased albedo. While there is likely significant uncertainty in changes in cloud fraction and type in the reanalysis output, these results highlight the idea that glacier ELAs are sensitive to the influence of clouds on the shortwave and longwave radiation. This is perhaps not surprising since my analysis of the surface energy balance at

the ELA suggests that net radiation dominates the energy balance at the surface (discussed in Section 2.4).

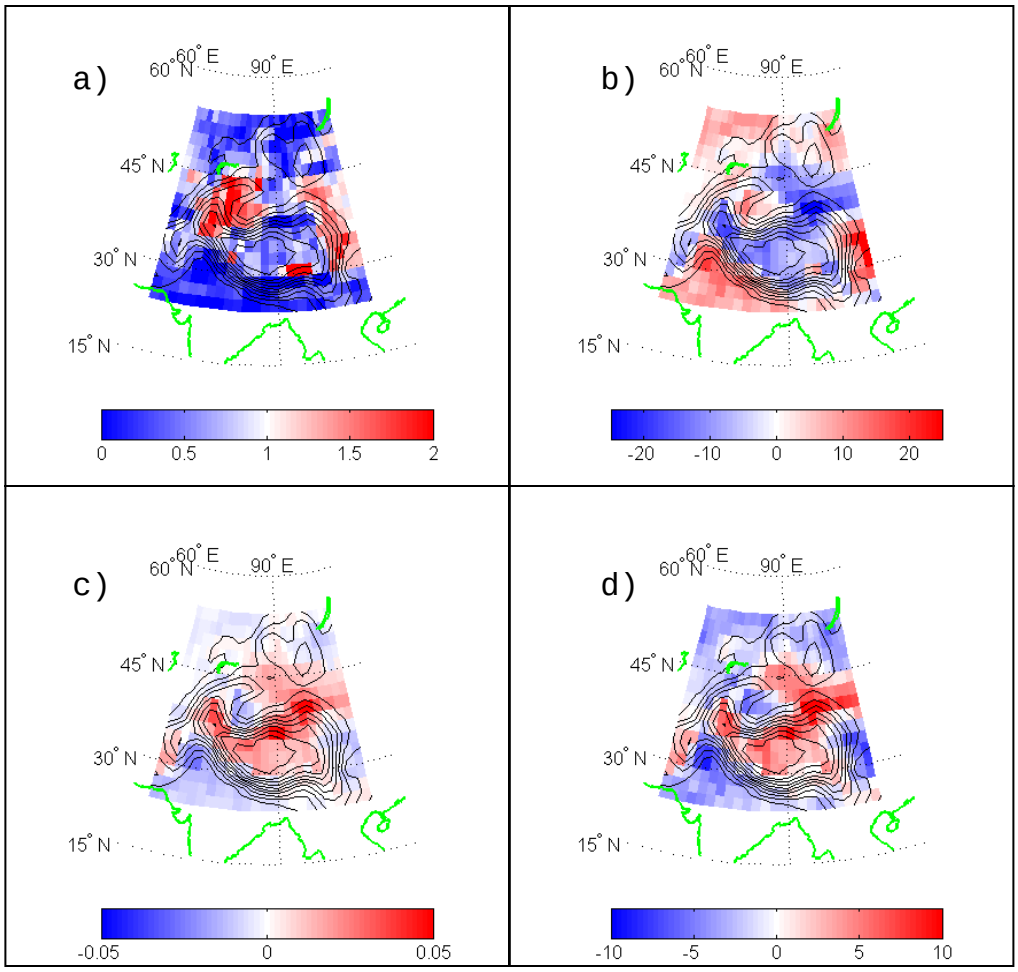

Figure 2.13: All panels are the change for anomalously warm summers minus average summers: a) amplitude in the seasonal cycle (^{o}C), b) incident shortwave radiation at the surface (W m^{-2}), c) downwelling longwave radiation constant (C_1), and d) cloud fraction (%).

A comparison of the pattern in ΔT_{amp} (Figure 2.13a) to ΔELAs (Figure 2.12c) indicates that ΔELAs increase with increasing ΔT_{amp}. This illustrates the importance of the seasonal cycle in air temperature in calculating ablation as well

as suggesting the value of a more complete sensitivity test, which calculate air temperatures independently at each time step rather than being constrained, as here, by prescribing T_{amp}. This is discussed further in Section 2.6.

The pattern in ELA sensitivities is the result of both the magnitude in the change in climate and the differing sensitivity of the ELA to the dominant ablation process. Generally, for modern interannual variability, all melt regions are more sensitive to changes in temperature than precipitation. Changes in temperature are governed by changes in cloudiness and the amplitude in the seasonal cycle in air temperatures. My results suggest that ELAs in regions dominated by sublimation are more sensitive to changes in precipitation, humidity, and wind than those dominated by melt. These regions are also likely to be more sensitive to the model formulation than the regions dominated by melt. Given the sensitivity of the sublimation-dominated regions to numerous atmospheric quantities and model formulation, these regions are flagged as particularly complicated regions.

2.6 Summary and Discussion

2.6.1 Summary

A surface-energy and mas-balance model has been developed to explore the relationship between glacier equilibrium-line altitudes (ELAs) and climate at a

regional scale. The model is applied to central Asia because of its wide range of climatic conditions.

I have shown that the model captures the pattern in absolute ELAs quite well, the seasonal cycle in energy balance terms are comparable to studies on individual glaciers in Central Asia, and the proportionality factor relating melt to positive degree days (calculated using the surface energy- and mass-balance model) is within the range of those reported for individual glaciers within the area (Calanca and Heuberger, 1990; Kayastha et al., 1999; Kayastha et al., 2002; Zhang et al, 2006). In addition, the magnitude of the model parameters does not significantly influence the sensitivity of the ELA to changes in climate (Appendix B). These results together suggest that the SEBM model performs well and is capable of capturing the sensitivity of ELAs to a change in climate at a regional scale.

With this model in hand, I am able to address the two questions posed in the introduction of this paper: (1) can we understand the relative importance of accumulation and ablation in controlling mass balance of glaciers at regional scales, and (2) how do the observed patterns of glacier response reflect regional changes in climate? I summarize the main conclusions in the context of these two questions.

Firstly, the spatial patterns in climate across Central Asia produce a spatial pattern in the dominant ablation process. In particular, where precipitation is low, ablation at the ELA is dominated by sublimation. Conversely, where precipitation is high, ablation at the ELA is dominated by melt and surface run-off.

Secondly, the ELA sensitivity to changes in climate is strongly tied to the dominant ablation process. In regions dominated by melt, the ELA is far more sensitive to ablation than accumulation. The change in ELA for anomalously warm summers in all regions is governed by changes in cloud fraction (and the associated changes in shortwave and longwave radiation) and the amplitude in the seasonal cycle in air temperature. Sublimation regions however, are far more sensitive to changes in precipitation than to changes in ablation. Additionally, ELAs in sublimation-dominated regions are more sensitive to changes in humidity and wind speed than are ELAs in melt-dominated regions.

There is a fairly narrow transition of only one or two reanalysis grid points between the sublimation dominated and melt dominated areas. This suggests ELA sensitivity in those transitional regions can quickly change in response to small changes in climate. Glaciers in these regions are close to a threshold where a small change in climate would result in rapid growth or demise of the glacier. Further sensitivity tests focused specifically on these regions would give insights

into likely climates where glaciers are close to a threshold and the magnitude of climate changes required to push these glaciers from sublimation to melt-dominated regimes, or vice versa.

2.6.2 Discussion

This study developed a framework capable of assessing the sensitivity of ELAs to changes in climate at a regional-scale, and at a first-order level of detail. Importantly, I have demonstrated that, for the level of my approach, uncertainty in model parameters and climate variables will not change the main conclusions. For example, precipitation in the Himalaya is known to vary significantly from place to place (e.g., Anders et al., 2006). The coarse resolution of the reanalysis climatology used here obviously does not adequately capture patterns in orographic precipitation. It is conceivable that the magnitude in total precipitation and interannual precipitation variability in the reanalysis output could be off by a factor of two or more. Regardless, regions of high precipitation will be dominated by melt, and the energy balance at the surface will be dominated by radiative fluxes. I therefore do not anticipate the regional-scale answers to change.

Any single glacier will be susceptible to numerous local factors, and may respond differently to climate than the larger-scale patterns would suggest. Capturing

ELA sensitivities at smaller spatial scales would require a higher level of accuracy in the driving terms and ELA model than the current model formulation allows. For example, latent heat flux due to melt percolation and refreeze is ~10-20 W m^{-2}. A change in albedo equal to 0.1 would result in a change in shortwave radiation of the same order magnitude. Thus a model capable of higher accuracy would necessarily include all variables that would have a similar or greater influence on the energy balance as albedo variations. An atmospheric column model with internally derived snowpack would be capable of this level of detail. The next logical step to this study is to apply such a model to selected grid points within the larger region of interest here and to test the sensitivity of the ELAs at smaller scales. This would give insight into how different the sensitivity of any single glacier may be within the larger regions.

There are many potential applications of the SEMB model. First, as I have shown, it can be used to ascertain the relative importance of sublimation versus melt and to test the sensitivity of glaciers to possible changes in climate at a regional scale anywhere in the world. Care must be taken to be sure that the model parameters chosen are appropriate for the region of interest. Second, the model can be used to test the tendency of the ELA to changes in forcings, such as changes in CO_2 or orbitally induced changes in solar insolation. For example, I use this same model to calculate changes in ELA between present day and the

mid-Holocene (when downwelling solar insolation was at a relative maximum) and to reconcile the pattern in ELA changes with the changes in climate in Central Asia (Rupper et al., 2007). I am also keen to use this model to determine what atmospheric variables have contributed the most to the regional changes in ELA seen around the globe over the last Century. Finally, it may be possible to couple this model to simple glacier length models to test the sensitivity of glacier length to changes in bed geometry as well as climate.

Numerous studies have focused on diagnosing the response of glaciers to changes in climate. The framework developed in this study extends previous work by revealing spatial scales of climate-driven dependencies of glaciers. By applying the model to modern interannual climate variability, I was able to determine the patterns of ELA sensitivity across the vastly differing climates across Central Asia, and diagnose why those patterns emerge. The sensitivity of ELAs to modern interannual climate variability can be used as an analog for understanding past changes in glacier mass balance, as well as a predictor of the response of glaciers to future changes in climate. For example, the analysis of modern interannual climate variability provides insight into the magnitude of climate changes required by the paleoclimate data and highlights which climate variables are likely to be the most important predictors of the fate of glaciers under global-warming conditions. Importantly, for both past and future scenarios, where

patterns in climate persist, patterns in ELAs and ELA sensitivities should be the expectation as well.

2.7 Notes to Chapter Two

Anders A, Roe G, Hallet B, Montgomery D, Finnegan N, Putkonen J, 2006: Spatial Patterns of Precipitation and Topography in the Himalaya, *In* Willett SD, Hoovius N, Brandon MT, and Fisher DM, eds., Tectonics, climate and landscape evolution. GSA Special Paper 398, Chapter 3: 39-53.

Arendt AA, Echelmeyer KA, Harrison WD, Lingle CS, Valentine VB, 2002: Rapid wastage of Alaska glaciers and their contribution to rising sea level. Science, 297 (5580): 382-386.

Bolton, D, 1980: The computation of equivalent potential temperature. Monthly Weather Review, 108: 1046-1053.

Bradley RS, 2000: Past global changes and their significance for the future. Quaternary Science Reviews, 19 (1-5): 391-402.

Braithwaite RJ, 1995: Positive degree-day factors for ablation on the Greenland ice-sheet studied by energy-balance modeling. Journal of Glaciology, 41 (137): 153-160.

Braithwaite RJ, Raper SCB, 2002: Glaciers and their contribution to sea level change. Physics and Chemistry of the Earth, 27 (32-34): 1445-1454.

Braithwaite RJ, Zhang Y, Raper SCB, 2003: Temperature sensitivity of the mass balance of mountain glaciers and ice caps as a climatological characteristic. Zeitschrift Fur Gletscherkunde und Glazialgeologie, 38 (1), 35-61.

Calanca P, Heuberger R, 1990: Glacial Climate Research in the Tianshan. Zürcher Geogrische Schriften, 39, 60-72.

Casal TGD, Kutzbach JE, Thompson LG, 2004: Present and past ice-sheet mass balance simulations for Greenland and the Tibetan Plateau. Climate Dynamics, 23 (3-4): 407-425.

Denton GH, Hendy CH, 1994: Younger Dryas age advance of Franz-Josef glacier in the Southern Alps of New Zealand. Science, 264 (5164): 1434-1437.

Duguay, CR, 1993: Radiation modeling in the mountainous terrain – Review and status. Mountain Research and Development, 13 (4): 339-357.

Fountain AG, Lewis KJ, Doran PT, 1999: Spatial climatic variation and its control on glacier equilibrium-line altitude in Taylor Valley, Antarctica. Global and Planetary Change, 22 (1-4): 1-10.

Gillespie A, Molnar P, 1995: Asynchronous maximum advances of mountain and continental glaciers. Reviews of Geophysics, 33 (3): 311-364.

Gillespie A, Rupper S, and Roe G, 2003: Climatic interpretation from mountain glaciations in Central Asia. Geological Society of America, Abstracts with Program 35(6).

Grove JM, Switsur R, 1994: Glacial geological evidence for the medieval warm period. Climatic Change, 26 (2-3): 143-169.

Haeberli W, Frauenfelder R, Hoelzle M, Maisch, 1999: On rates and acceleration trends of global glacier mass changes. Geografiska Annaler Series A-Physcial Geography, 81A (4): 585-591.

Hagen JO, Kohler J, Melvold K, Winther JG, 2003: Glaciers in Svalbard: mass balance, runoff and freshwater flux. Polar Research, 22 (2): 145-159.

Hastenrath S, 1994: Recession of tropical glaciers. Science, 265 (5180): 1790-1791.

Hoinkes H, Steinacker R, 1975: Parameterization of climate-glacier-relation. Rivista Italiana Di Geofisica E Scienze Affini, 1: 97-104 Suppl. I.

Kalnay E, Kanamitsu M, Kistler R, Collins W, Deaven D, Gandin L, Iredell M, Saha S, White G, Woollen J, Zhu Y, Chelliah M, Ebisuzaki W, Higgins W, Janowiak J, Mo KC, Ropelewski C, Wang J, Leetmaa A, Reynolds R, Jenne R, Joseph D, 1996: The NCEP/NCAR 40-year reanalysis project. Bulletin of the American Meteorological Society, 77 (3): 437-471.

Kaser G, Hardy DR, Molg T, Bradley RS, Hyera TM, 2004: Modern glacier retreat on Kilimanjaro as evidence of climate change: Observations and facts. International Journal of Climatology, 24 (3): 329-339.

Kaufman DS, Porter SC, Gillespie, AR, 2004: Quaternary alpine glaciation in Alaska, the Pacific Northwest, Sierra Nevada, and Hawaii, in Gillespie AR, Porter SC, and Atwater BF, eds., The Quaternary Period in the United States, Developments in Quaternary Science Volume 1, Elsevier Press, 77-103.

Kayastha RB, Ohata T, Ageta Y, 1999: Application of a mass-balance model to a Himalayan glacier. Journal of Glaciology, 45 (151): 559-567.

Kayastha, RB, Ageta Y, Fujita K, 2002: Use of Positive Degree-day Method For Calculating Snow/ice Melting and Discharge From Glacierized Basins In Nepal. EGS XXVII General Assembly, abstract #3520.

Kessler MA, Anderson RS, Stock GM, 2006: Modeling topographic and climatic control of east-west asymmetry in Sierra Nevada glacier length during the Last Glacial Maximum. Journal of Geophysical Research, 111 (F2): Art. No. F02002.

Kistler R, Kalnay E, Collins W, Saha S, White G, Woollen J, Chelliah M, Ebisuzaki W, Kanamitsu M, Kousky V, van den Dool H, Jenne R, Fiorino M, 2001: The NCEP-NCAR 50-year reanalysis: Monthly means CD-ROM and documentation. Bulletin of the American Meteorological Society, 82 (2): 247-267.

Lowell TV, Heusser CJ, Andersen BG, Moreno PI, Hauser A, Heusser LE, Schluchter C, Marchant DR, Denton GH, 1995: Interhemispheric correlation of late Pleistocene glacial events. Science, 269 (5230:1541-1549.

Meier, M, 1984: Contribution of small glaciers to global sea-level. Science, 226 (4618): 1418-1421.

Molg T, Hardy DR, 2004: Ablation and associated energy balance of a horizontal glacier surface on Kilimanjaro. Journal of Geophysical Research, 109 (D16): Art. No. D16104.

Oerlemans J, 2005: Extracting a climate signal from 169 glacier records. Science, 308 (5722): 675-677.

Ohmura A, 2001: Physical basis for the temperature-based melt-index method. Journal of Applied Meteorology, 40 (4): 753-761.

Paterson, 1999: Physics of Glaciers. Pergamon/Elsevier Science Inc.

Paul F, Kaab A, Maisch M, Kellenberger T, Haeberli W, 2004: Rapid disintegration of Alpine glaciers observed with satellite data. Geophysical Research Letters, 31 (21): Art. No. L21402.

Plummer M, Phillips F, 2003: A 2-D numerical model of snow/ice energy balance and ice flow for paleoclimatic interpretation of glacial geomorphic features. Quaternary Science Reviews, 22(14): 1389-1406.

Porter SC, 1975: Equilibrium-line altitudes of late Quaternary glaciers in southern Alps, New Zealand. Quaternary Research, 5 (1): 27-47.

Porter SC,1977: Present and past glaciation threshold in the Cascade Range, Washington, U. S. A.: topographic and climatic controls, and paleoclimatic implications. Journal of Glaciology, 18, 101-116.

Porter SC, Orombelli G, 1985: Glacier contraction during the middle Holocene in the western Italian Alps – evidence and implications. Geology, 13(4): 296-298.

Reichert BK, Bengtsson L, Oerlemans J, 2002: Recent glacier retreat exceeds internal variability. Journal of Climate, 15 (21): 3069-3081.

Ren DD, Karoly D, 2006: Comparison of glacier-inferred temperatures with observations and climate model simulations. Geophysical Research Letters, 33 (23): Art. No. L23710.

Rupper SB, Roe G, and Gillespie G, 2007: Spatial patterns of Holocene glacier advance and retreat in Central Asia. In preparation.

Wagnon P, Sicart JE, Berthier E, Chazarin JP, 2003: Wintertime high-altitude surface energy balance of a Bolivian glacier, Illimani, 6340 m above sea level. Journal of Geophysical Research, 108 (D6): Art. No. 4177.

Wallace J, Hobbs W, 2005: Atmospheric Science: An Introductory Survey. Academic Press.

Zhang Y, Shiyin L, Yongjian D, 2006: Observed degree-day factors and their spatial variation on glaciers in western China. Annals of Glaciology, 43, 301-306.

Chapter Three

SPATIAL PATTERNS OF HOLOCENE GLACIER ADVANCE AND RETREAT IN CENTRAL ASIA

3.1 Introduction and Motivation

Reconstructions of climate that extend back beyond the modern instrumental record usually must be based on sparse data sets of proxy variables that only indirectly reflect climate. The farther back in time, the more sparse the data tend to be. In part for this reason the paleoclimate community has focused a great deal of attention on trying to identify global-scale phenomena, and on making associations between widely separated proxy climate records. For example, there are ongoing debates over the global nature of paleoclimatic events such as the Little Ice Age, Dansgaard-Oeschger events, and the Younger Dryas (Lowell et al., 1995; Broecker, 2003; Roe and Steig, 2004; Wunsch, 2006). By comparison, the idea that climate variability tends to be expressed in spatial patterns is central to modern climate dynamics (e.g., ENSO, PDO, AO). There are instances where this is the case in the past as well. For example, while the Laurentide and Fenno-Scandinavian ice sheets covered large parts of North America and Europe, there is little evidence for substantial ice over Siberia or Alaska. This is most likely the result of large spatial patterns in and regional sensitivity to accumulation and/or

temperature (e.g., Pollard, 2000). The extent to which climate changes are regional as apposed to global, and the mechanisms driving those changes, are important for understanding the climate swings of the past.

Many proxy indicators reflect complex combinations of climate fields as well as non-climatic factors. For example, the width and density of tree rings reflect a complex biological response to such variables as temperature, precipitation, CO_2 fertilization, soil conditions, and fire frequency (Briffa et al., 1996, 1998, 2000). Proper characterization and interpretation of past climate variability therefore necessitates not only good cross-dating of different records, but also an understanding of how the proxy data in question reflects particular aspects of climate.

Glaciers are a particularly attractive proxy record for two reasons. First, geomorphic evidence of glacier advances are widespread across much of the northern hemisphere land masses. Second, glaciers are excellent recorders of properties of the atmosphere, retreating and advancing directly in response to changes in accumulation and ablation. Thus histories of glacier variability are some of the most useful records of paleoclimate. In many parts of the world, the glacier history is the primary descriptor of the climate history beyond the instrumental record, particularly where glacier deposits are widespread and confidently dated. This is true, for example, in the Pacific coast of the United

States, South America, New Zealand, the European Alps, and Asia (e.g., Porter, 1977; ; Porter, 1985; Gillespie and Molnar, 1995; Lowell et al., 1995; Kaufman et al., 2004). Therefore, reconciling the glacier histories with the climate mechanisms driving them is essential.

The glacier history in Central Asia is a very promising one to distinguish between global and regional climate change. Until the early 1990's it was generally assumed that alpine glacier advances in Central Asia were synchronous with those of high-latitude ice sheets (e.g., Anderson and Prell, 1993, Emeis et al., 1995, Kuhle, 1998). As more extensive and reliable numerical dates have become available, it has become evident that alpine advances were not only asynchronous with glacier advances in other regions of the world, but that there was also regional variability within Asia itself (e.g., Gillespie and Molnar, 1995; Schafer et al., 2002; Finkel et al., 2003; Wei et al., 2006). The observed spatial patterns of glacier variability in Central Asia prompt three questions:

- First, can we understand the relative importance of accumulation and ablation in controlling mass balance of glaciers over large regions?
- Second, are the reconstructed spatial patterns of glacier response consistent with regional changes in climate?
- Finally, do the reconstructed spatial patterns in glacier advances actually reflect patterns in climate change, or do they result from

regional variability in mass-balance sensitivities to relatively uniform changes in a particular climate variable?

Although the glacier record in Asia extends throughout the last glacial cycle, I use the Holocene period to begin addressing these issues. This is because climate boundary conditions (i.e., greenhouse-gas concentrations, sea-level, ice-sheet extent) were close to their present state, making direct comparison with modern observed climate variability possible. Therefore I focus this paper on reconciling the early-Holocene glacier record with climate, and do so by analyzing output from a suite of general circulation models (GCMs). This study differs from previous work on Holocene Central Asia (e.g., Dong, 1998; Joussaume et al., 1999; Bush, 2002), by including quantification of glacier mass balance and a detailed diagnosis of the model physics underlying the comparisons. The results show that glacier advances and retreats throughout Central Asia are dominated by changes in temperature.

3.2 Background

3.2.1 Cetral Asian Glaciers

Glaciers are found across central Asia in a diverse range of climates, ranging from the intense monsoon of the southern Himalaya, to the extreme dryness of the

eastern flank of the Karakorum and the extreme seasonal cycle (40 °C) of the Mongolian Altai. It might be expected that these diverse climate regimes are likely to respond differently to uniform changes in climate forcing (e.g., summertime solar insolation). Since glaciers respond to the changes in climate, it is not surprising to find a diverse glacier history in these regions as well.

Glacier histories are often characterized in terms of equilibrium-line altitudes (ELAs). The ELA is the altitude on a glacier at which annual accumulation equals annual ablation. In general, a glacier advances if the ELA lowers, and retreats if it rises. Changes in ELA are considered one of the most useful glaciological measures for reconstructing climate changes (e.g., Porter, 1976; Paterson, 1999; Fountain et al. 1999). In particular, ELA is a common variable that can be compared directly from one region to the next. Also, ELAs are more directly related to climate itself than glacier length, which depends on ice dynamics, bed geometry, and a myriad of other variables (Fountain et al, 2004; Paterson, 1999). Changes in the ELA of any single glacier provide a history of the local climate. If those ELA variations are correlated across extensive glaciated regions, they can be interpreted as the history of the regional climate.

Some uncertainty will obviously attend ELA reconstructions, as the exact value depends on the method used (i.e., accumulation area ratio, toe-headwall area ratio; e.g., Benn and Owen, 1998). These uncertainties, and their impact on

interpretation, will be addressed in more detail in the discussion section of this paper. I emphasize that for the purpose of this paper, it is not crucial for the changes in ELA to be reconstructed precisely: I am primarily interested in relating the broader patterns of glacier response to the climate. This signal is clear across Asia and the changes in an individual glacier's ELA are therefore less important.

On the basis of the pattern of ELA changes in Central Asia, Gillespie et al. (2003) identified three regions that capture the spatial and temporal variability of the glaciers in Central Asia (Figure 3.1). These three zones have distinct glacier histories, which are summarized briefly below (but see also Gillespie et al. (2003) for more detail).

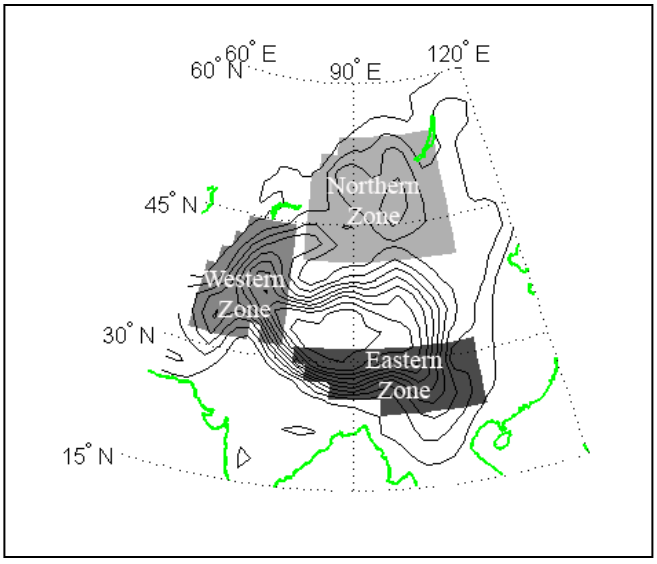

Figure 3.1: Central Asian Zones: Shaded areas of gray represent the general outline of the eastern, western, and northern zones, as defined by the glacier history. These are the regions over which statistics are calculated for each zone (Table 3.1). Contours show the 500 m NCEP-NCAR reanalysis elevation increments; the 0 contour not shown. Coast lines are in gray.

The western zone extends from the Kyrgyz Tien Shan south to the Karakoram and east to central Tibet. In this region the largest advances occurred during the pre-LGM (30 – 70 ka) with little evidence for large advances during the Last Glacial Maximum (LGM) (e.g., Phillips et al., 2000; Clark et al., 2001; Owen et al., 2002; Finkel et al., 2003; Koppes et al., 2003; Barnard et al., 2004; Abramowski et al., 2006). In contrast, the glaciers in the northern zone (central Mongolia to the Tien Shan of Xinjiang, China) advanced during the LGM, synchronously with the high-latitude ice sheets, although there are published dates that push the western boundary of this zone closer to the Mongol border (e.g., Merle et al., 2000; Clark et al., 2001; Shi, 2002). Although there is evidence for large pre-LGM and LGM advances in the southern Himalayas around the areas of eastern Nepal and Tibet (southern zone), evidence for a large early Holocene (9 ka) advance distinguishes it from the rest of Central Asia (e.g., Schafer et al, 2002; Shi, 2002; Owen et al., 2003; Wei et al., 2006). The pre-LGM glacier advance in the region is consistent with the strong sensitivity of these glaciers to local summertime temperatures and the insolation swings which were largest during the early part of the glacial cycle.

The ELA reconstructions available are still quite sparse; therefore smaller regions with homogeneous histories that differ from their neighbors cannot be ruled out. Nonetheless the size of the three regional zones (~3 x 10^6 km^2) are consistent with the spatial scale expected of major regional climate patterns, as found both for observations of the present climate and for models of past climate (discussed

below and in Rupper and Roe, 2007). These zones are therefore a convenient framework for characterizing the glacier and climate histories.

I focus on explaining the relationship between Central Asian climate and early Holocene glacier history. I also place particular emphasis on understanding the advance of glaciers in the eastern zone. The early Holocene glacier history in the eastern zone is unusual as the glaciers advanced despite it being a time of a relative maximum in insolation during the Northern Hemisphere summer (e.g., Crowley and North 1988).

3.2.1 Previous Work

The climate of the mid-Holocene has been the focus of numerous modeling studies (e.g., Kutzbach, 1988; Dong et al., 1998; Hall and Valdes, 1997; Vettoretti et al., 1998; Joussaume et al., 1999; Braconnot, 2002). These studies consistently show that, in response to the changes in incoming solar insolation, the summer (JJA) temperatures in the interior of Central Asia (northern and western zones) increased by approximately 2-6 °C compared to modern values (e.g., Joussaume et al., 1999). In climate model simulations, this increase in temperature enhances the land-sea temperature contrast, thereby intensifying the Indian summer monsoon. The models predict large increases in precipitation over India and the southern Himalaya (the southern zone) in response to this increased intensity of

the monsoon (Joussaume et al., 1999). Several studies have compared these climate changes to the available paleoclimate proxy data and noted the early Holocene glacier advance in the southern Himalaya (e.g., Kutzbach, 1988; Bush, 2002). A few papers focus specifically on explaining the Himalayan glacier advance (Benn and Evans, 1996; Finkel et al., 2003; Owen et al., 2003). All of these studies suggest that the advance of the glaciers in the southern Himalaya was a result of the increase in monsoonal precipitation during the mid-Holocene.

However glaciers respond to both annual precipitation and summer (melt season) temperatures. Therefore, a response of a glacier to the predicted changes in precipitation and temperature will depend on its sensitivity to both variables. For example, Kayastha et al. (1999) clearly show that glacier AX010 in the Nepalese Himalaya is sensitive to both temperature and precipitation. Given this fact from the modern climate, both the increase in monsoonal precipitation and the increase in summer insolation must be accounted for in understanding what the glacial history of the region reflects.

I test the sensitivity of Central Asian glaciers to changes in both precipitation and insolation using a suite of general circulation model (GCM) simulations and two mass-balance models. The GCM simulations for 6 ka and the present day (discussed below) are used to describe the simulated changes in mid-Holocene temperatures and precipitation in the three zones. The climate model output is

then used as input in the two mass-balance models. The first mass-balance model utilizes the traditional approach to estimating mass balance by assuming ablation is proportional to temperature. The second mass-balance model is a self-consistent surface energy-balance model (Rupper and Roe, 2007).

3.3 Holocene Climate

The GCM data used in this study were acquired from the Paleoclimate Model Intercomparison Project (PMIP), which has archived output from multiple atmospheric GCM integrations with the appropriate conditions for several time periods, including the present day and 6 ka (Bonfils et al., 1998). The simulations for 6 ka are atmospheric GCMs forced by fixed sea surface temperatures. No single model simulation can be regarded as an accurate simulation of a past climate. However where agreement is found between different models it provides confidence in the robustness of the simulations, and provides a means to test how sensitive Central Asian glaciers are to possible climate changes. In particular, the integrations for 6 ka allow a test of the sensitivity of Central Asian climate and glaciers to changes in incoming solar insolation.

In my analysis of the climate models, I focus on precipitation and temperature because of the important link between these two variables and glacier mass balance. In presenting results, I give a table showing the spread in the climates

simulated by the different models. For the most part there is a high degree of agreement between models in the simulated changes. In showing maps of the simulated changes, I focus therefore on one GCM, ECHAM3. Importantly, the consistency between model simulations suggests robustness of the climate response to changes in insolation forcing.

Summertime (JJA) temperatures increase by 2-6 °C as compared to the modern in the northern and western zones (Table 1, Figure 3.2). This is a direct result of the increase in summer insolation in these regions and is consistent with the continentality of these areas. In contrast to this, the temperature in the eastern zone actually decreased by 0.5 to 2 °C despite the increase in summertime insolation. As I will show in Section 3.4, this decrease in temperatures is important for explaining the glacier response in the southern Himalaya. The reasons for this response are examined closely in Section 3.5.

Table 3.1: Values are the mean change in summertime (Jun, Jul, Aug) temperature (ΔT_a), annual precipitation (ΔP), equilibrium-line altitude (ΔELA), and fractional contribution of the change in ELA due to ΔT_a only to the total ΔELA ($\Delta ELA:\Delta T_a$). Bold values are the changes averaged over the individual zones (Figure 3.1) in the ECHAM3 GCM simulation. Values in parentheses are the range in mean values across all GCM simulations.

	Units	**Eastern Zone**	**Western Zone**	**Northern Zone**
ΔT_a	°C	**-1** (-0.5 to -2)	**2** (2 to 4)	**3** (2 to 6)
ΔP	mm yr^{-1}	**500** (300 to 750)	**-50** (-200 to 200)	**90** (0 to 150)
ΔELA	m	**-300** (-100 to -400)	**400** (200 to 500)	**450** (200 to 500)
$\Delta ELA: \Delta T_a$	%	**75** (70-85)	**98** (90 to 100)	**98** (95 to 100)

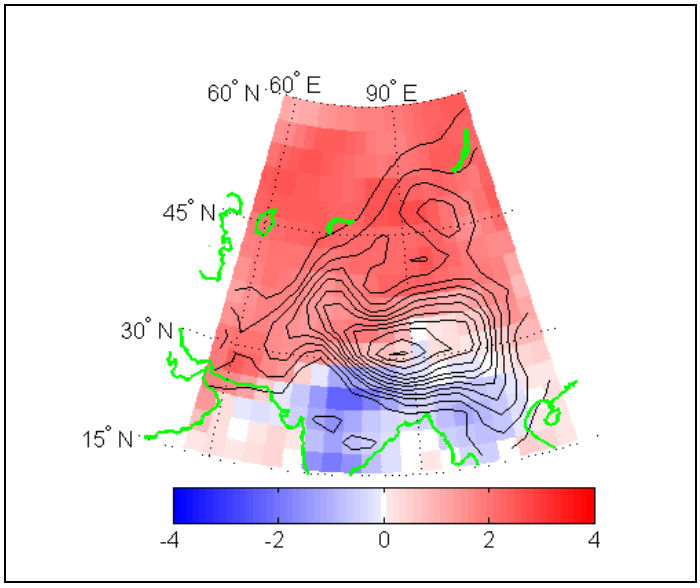

Figure 3.2: Change in summertime (Jun, Jul, Aug) air temperature (K) for 6ka as compared to present day.

The changes in precipitation in response to the increase in incoming solar insolation are also different in the three regions (Figure 3.3). In the northern zone the change in precipitation at 6 ka as compared to present-day was negligible to slightly positive (0 to 150 mm/yr) (Table 3.1). The tendency of the models towards a slight increase in precipitation may be due to the increase in temperature. For constant relative humidity, moisture content increases with temperature, as given by the Clausius-Clayperon relation (e.g., Wallace and Hobbs, 2005). In the western zone, the changes in precipitation are also small but quite variable, and even the sign of the changes is not consistent between models (-200 to 200 mm/yr) (Table 3.1). I have not diagnosed the reasons for this variability in detail, though it is likely due to model differences in the response of springtime precipitation associated with storms originating in the Mediterranean

(Hoskins and Hodges, 2002). However, I will show below that the glaciers are not sensitive to these changes in precipitation. Therefore, this inter-model variability does not change my main conclusions. Compared to the small changes in precipitation in the northern and western zones, changes in precipitation in the eastern zone are substantial, ranging between 300 and 750 mm/yr, increasing in all models. These results agree with other studies which also show an increase in precipitation at 6 ka as a result of an increase in monsoon intensity and/or duration (e.g., Joussaume et al., 1999).

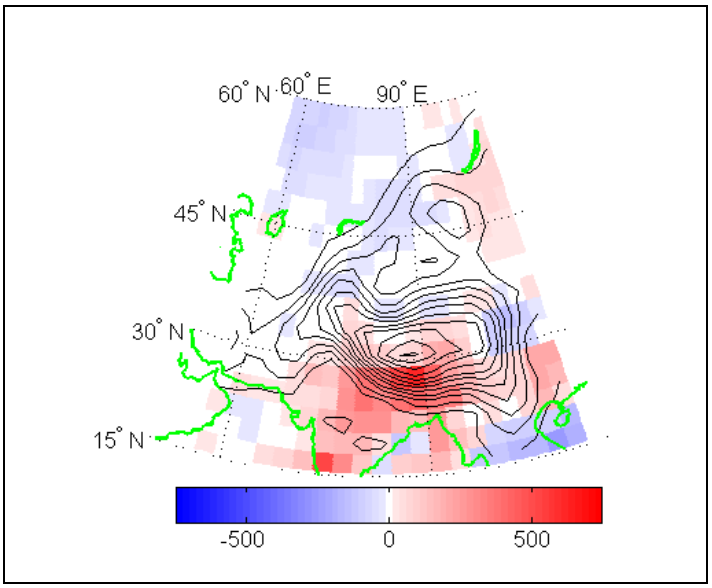

Figure 3.3: As in Figure 3.2, but for a change in annual accumulation (mm/yr).

There are two important results from the analysis of precipitation and temperature changes in Central Asia. First, with the exception of precipitation changes in the western zone, all the GCMs show broadly similar results for precipitation and

temperature changes. This reinforces confidence that the GCM simulated climate changes are a robust response of the climate to the changes in insolation forcing. Second, the GCMs show spatial variability in the temperature and precipitation changes across Central Asia in response to a relatively uniform increase in incoming solar insolation. This suggests that even a uniform change in forcing, such as increasing greenhouse gases, should result in spatial patterns in climate. Because glaciers respond to changes in temperature and precipitation, this spatial variability in temperature and precipitation changes should result in corresponding patterns of glacier variability across Central Asia. The next section focuses on whether the patterns in climate are sufficient to explain the geologic data.

3.4 ELA calculations

To understand the impact of the modeled climate changes on glacier mass balance, the GCM output is converted into ELA changes, using two different methods. The first, discussed below, is an ELA perturbation model following Ambach and Kuhn (1985), modified to use the positive degree day (PDD) model for ablation, following Braithwaite, 1995. The second model is a surface energy-balance model (Rupper and Roe, 2007), which is discussed briefly in Section 3.4.1. Both models solve for the change in ELA for a given change in climate.

PDDs are the sum of daily mean air temperatures (T_a) that are above zero.

$$PDD = \sum H(T_a), \qquad 3.1$$

where H is equal to 0 for $T_a \leq 0$ and is equal to T_a for $T_a > 0$; the sum is taken over the calendar year. Thus PDD has units of °C days. I determine PDDs using the monthly mean GCM output by calculating the daily-mean air temperature (T_a) as

$$T_a = \bar{T}(z) + T_{amp} \cos(2\pi \frac{t}{365}). \qquad 3.2$$

$\bar{T}$ is the mean annual air temperature, t is the day of the year, T_{amp} is the amplitude in the seasonal cycle in air temperature determined using the monthly GCM output. Total ablation (A_b) is then equal to PDD times a melt factor. The results presented below are for a melt factor equal to 10 mm/^{o}C days, the mid point of the modeled and empirically-derived range in melt factors from Rupper and Roe (2007) and measured values (Kayastha et al., 1999, Zhang et al., 2006). While the magnitude of the modeled ELA changes is affected by the choice of melt factor, the basic pattern of the ELA response does not change.

In Equation 3.3, accumulation equals ablation at the ELA. For a change in A_c or A_b a 1st-order Taylor Series expansion in the vertical direction can be used to

calculate the change in the ELA that would result from a change in accumulation or temperature.

$$\Delta A_c = \Delta A_b + \frac{\partial A_b}{\partial z} \Delta z \qquad 3.3$$

where Δ refers to the change from a reference climate.

The input variables on the right-hand side of Equation 3.3 are the change in ablation and the gradient in ablation. The vertical gradient in ablation is calculated by: (1) varying $\overline{T}$ about the climatological temperature lapse rate (2) calculating the change in ablation at the different elevations along the lapse rate (using Equations 3.1 and 3.2), and (3) dividing by the change in elevation. The climatological lapse rate is calculated using NCEP-NCAR reanalysis annual average air temperatures at 750 and 500 hPa (Kalnay et al., 1996). The lapse rates are then interpolated to the same grid as the GCMs.

Strictly, the left-hand side of Equation 3.3 (ΔA_c) should include both the gradient in accumulation about the ELA and the change in accumulation. However, the gradient in accumulation can be neglected for typical ELA changes, so is not included in the ELA calculations. Therefore, ΔA_c is simply change in accumulation.

ELA changes are calculated for the given changes in climate across the entire model domain. I am therefore effectively asking "if there were a glacier here, what would its change in ELA be?" Given this approach to estimating ELA changes, and the coarse resolution of the GCM grid (typically between 2.5° to 5°), two issues arise. First, the smoothed topography makes it difficult to differentiate between precipitation and snow. I choose to assume that precipitation would all be snow, thus A_c equals total annual precipitation. This errs on the side of maximizing sensitivity to model accumulation, but does not change my results below. Second, Anders et al. (2006) show that precipitation in the Himalayas varies significantly on scales much smaller than the GCM grid resolution. These GCMs therefore do not capture orographic precipitation adequately. I test the sensitivity of my results to the grid scale by calculating the ELA using model output and data at different resolutions. In particular, I use a simple algorithm (Appendix A) to seek the position of the ELA using temperature and precipitation from the present-day GCM simulations. I do the same using the highe- resolution precipitation and temperature data from Legates and Willmott (1990a, 1990b). While the 0.5°-grid resolution is still too coarse to capture orographic precipitation, it does provide a means to test the sensitivity of the results to changes in spatial resolution. The basic pattern in ELAs is similar regardless of resolution.

3.4.1 Modeled ELA changes

The pattern of ELA changes calculated by converting climate changes to ELA changes using Equation 3.3 is similar for all GCMs. In Table 3.1, I summarize the results for all models; in the figures discussed below, I show results only for one GCM, the ECHAM3.

The simulated changes in precipitation and temperature at 6 ka as compared to the present day produces a pattern in ELA changes across Central Asia (Figure 3.4). In the eastern zone, the change in climate results in a lowering of ELAs by approximately 300 m and a lifting elsewhere by 200 to 500 m. If only precipitation changes are included (i.e., temperature held fixed), ELAs in the east are lowered by only 75 m (Figure 3.4a,b). Thus changes in precipitation account for less than 30% of the total modeled change in ELA in the eastern zone. In the northern and western zones, changes in precipitation account for even less (at most 5%) of the total change in ELA. Thus, for the range of changes in temperature and precipitation predicted by the GCMs, ELAs in all regions are most sensitive to changes in temperature; and except in the eastern zone, precipitation changes are nearly negligible. In all zones, the largest uncertainty in the calculated ELA changes is the ablation term (i.e., the value chosen for the melt factor). However, for the full range of melt factors the dominance of the temperature pattern still applies.

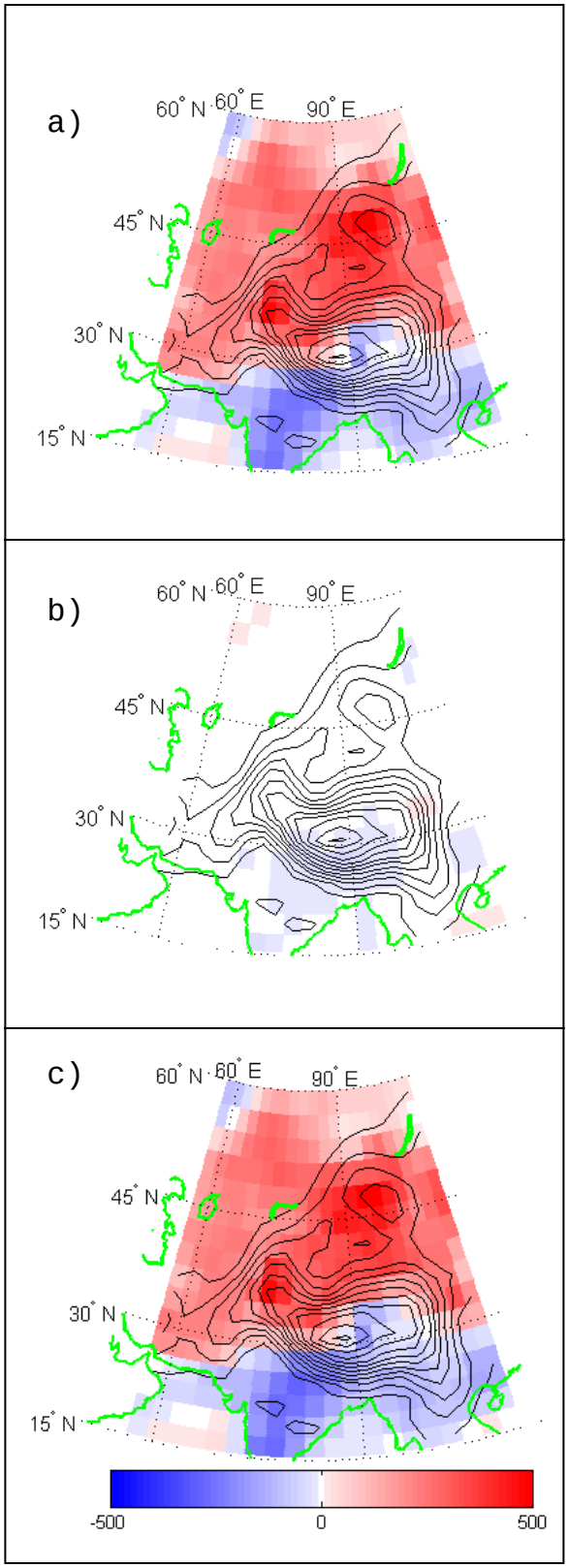
a)
60° N
60° E
90° E
45° N
30° N
15° N
b)
60° N
60° E
90° E
45° N
30° N
15° N
c)
60° N
60° E
90° E
45° N
30° N
15° N
-500
0
500

Figure 3.4: Change in equilibrium-line altitude (m) at 6ka as compared to the present day calculated using the PDD approach. ELA changes are for a: a) change in temperature only, b) change in accumulation only, and c) change in both temperature and accumulation. These figures illustrate the result that the ELAs in Central Asia are most sensitive to changes in temperature.

The calculated ELA changes predict that glaciers would have been bigger during the Holocene compared to present-day in the eastern zone, while glaciers in the north and west were smaller. This is consistent with the paleoclimate record, in which geologic evidence shows a significant advance in the eastern zone during the Holocene and glaciers equal to or smaller than modern glaciers in the north and west.

3.4.2 Energy balance results

The simple PDD method assumes that ablation is directly related to temperature. Physically, of course, it is the net heat input that is actually responsible for the melting or sublimation of snow and ice. A surface energy-balance model is needed to calculate the heat available for ablation. Such models are self-consistent representations of all the surface heat fluxes, and have often been used to study the energy balance at particular glaciers (e.g., Kayastha, 1999; Molg and Hardy, 2004). For the application to regional-scale climate patterns, I use the surface energy- and mass-balance model (SEMB model) presented in Rupper and Roe (2007). Applying the model to this study serves two purposes. First, it provides a check on the answers derived from the PDD method. Second, the analysis of the surface energy fluxes leads to important new insights that help explain the cooling of temperatures in the eastern zone.

A complete description of the SEMB model is given in Rupper and Roe (2007). Briefly, for a specified climate forcing at a given grid point, the SEMB model seeks the altitude at which a glacier surface would be in both mass and energy balance over the annual cycle. By definition, this is the ELA. The inputs from the climate model are the annual cycles in downwelling shortwave radiation, air temperature (at the climate model surface), wind, atmospheric pressure, and relative humidity. The SEMB model parameterizes the surface albedo and the downwelling longwave radiation. Sensible and latent heat fluxes are calculated in terms of the specific humidity, wind speed, assumed roughness lengths, and temperature difference between the surface and the overlying air.

The energy-balance algorithm seeks a surface temperature for a given air temperature that balances the absorbed short-wave radiation at the surface. When the surface temperature is less than zero, sublimation occurs. When the surface temperature is greater than or equal to zero, the surface temperature is reset to zero and the energy balance recalculated. The excess energy is then used to calculate the total melt. In this way the total ablation is calculated for a given mean annual air temperature. In the mass-balance algorithm, the model seeks the elevation at which the mean annual air temperature results in a total annual ablation (calculated using the energy balance method above) that exactly equals the total annual accumulation.

The SEMB model involves some significant simplifying assumptions, but it does capture the behavior of how the different surface energy fluxes adjust to balance the radiative forcing. Rupper and Roe (2007) show that the framework is suitable for characterizing how the ELA depends on regional climate patterns and can, for example, identify regions where sublimation or melt dominate the mass balance at the ELA. Such results give insight into which atmospheric variables the ELA is most sensitive to.

I use monthly time steps over the annual cycle, which are sufficient to represent the typical magnitude of the observed energy fluxes at glacier surfaces, and their seasonal cycles (Rupper and Roe, 2007). I use the output from the climate models at the present day and 6 ka to calculate the change in ELA predicted by the model, and to analyze the reasons for the predicted change.

I present the results from the ECHAM3 model for comparison to the PDD results presented above. As with the PDD approach, the change in climate at 6 ka as compared to the present day produces a pattern in ELA changes across Central Asia (Figure 3.5a). The overall pattern in ELA changes using the surface energy-balance approach is generally very similar to that of the PDD approach. Where the two methods disagree is in regions where the ablation is dominated by the sublimation term. This includes small portions of the northern and western zones. ELA changes calculated using SEMB model are much larger in these regions than

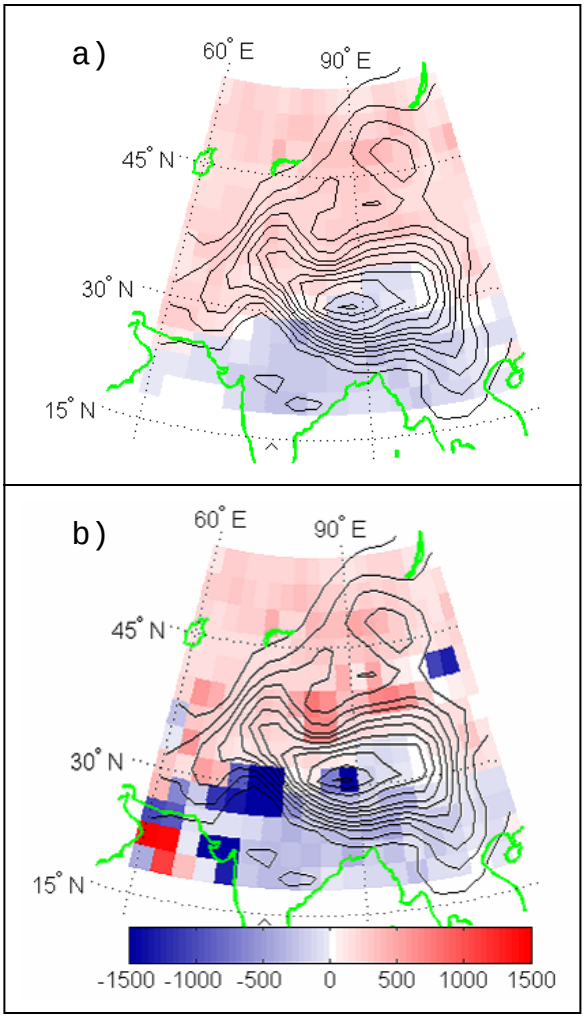

Figure 3.5: Change in ELA (m) at 6 ka minus the present day, calculated using the surface energy- and mass-balance model after Rupper and Roe (2007). Panel (a) is the change in ELA for a change in ablation only. Panel (b) is the change in ELA for the simulated changes in both accumulation and ablation. (Note scale is different than in Figure 3.4).

elsewhere in Central Asia. When sublimation dominates the mass balance, large changes in surface temperature are necessary for sublimation alone to bring the system back into mass balance, which results in large changes in ELAs. Therefore sublimation regions are very sensitive to even small change in precipitation. ELAs in regions dominated by sublimation, calculated using the

PDD approach, should be interpreted with caution (See Rupper and Roe, 2007, for a detailed discussion of the reasons for melt versus sublimation).

To facilitate further comparison of the surface energy-balance model results to the PDD method, the ELA changes averaged over each of the three zones are presented. In the eastern zone, the change in climate results in a lowering of ELAs by approximately 350 m. Elsewhere in Central Asia (excluding sublimation regions), ELAs increase by approximately 450 m. The relative importance of ablation versus accumulation in determining the ELA changes can be analyzed by computing the changes in ELAs while neglecting the change in precipitation (Figure 3.5 (b)). That is, ELA changes are calculated for a change in ablation only. In this case, the ELAs in the east lower by approximately 250 m, more than 70 % of the total ELA change. Thus changes in precipitation account for less than 30% of the total change in ELA (similar to the results reported for the PDD approach). Outside of the eastern zone and excluding the sublimation dominated regions, changes in precipitation account for at most 5% of the total change in ELA (again comparable to the results using the PDD method). In contrast to these melt-dominated regions, sublimation-dominated regions are very sensitive to changes in precipitation with precipitation changes accounting for 50% to 80% of the total ELA change.

The results suggest that where melting dominates, the PDD approach adequately captures the physics included in the full energy-balance model. Where sublimation dominates, however, the PDD approach greatly underestimates the sensitivity of the ELA to small changes in precipitation. These results indicate that for the typical changes in atmospheric variables predicted by the GCM's, glaciers in the melt-dominated regions are most sensitive to those changes that conspire to change temperature. Therefore the surface energy-balance model confirms the result that the pattern in ELA changes across Central Asia (for the 6 ka minus the present-day results) is primarily a result of the pattern in temperature changes, with the exception of the sublimation-dominated regions.

3.5 Explaining the temperature changes

The decrease in temperature in the eastern zone during the mid-Holocene has not previously been addressed or explained. Since this decrease plays an important role in the modeled ELA changes, it is important to understand the cause. Insight into these temperature changes is gained through a discussion of modern variability in monsoonal temperatures and precipitation, and analysis of the radiation balance in the GCM integrations.

Both the seasonal cycle and the interannual variability of the modern Indian monsoon suggest a reason for the model results of lower temperatures over the

eastern zones at 6 ka. When the monsoon rains begin every year, temperatures cool over India, and years with a strong monsoon are also years with greater than average cloudiness and lower than average surface air temperature (e.g., Ramanathan, 1987; Collins et al., 1996; Wilcox and Ramanathan, 2001). The climate model output at 6 ka suggests that an analogous situation occurs during the mid-Holocene. The models all predict increased cloudiness (as well as albedo) along with the decreased temperatures at 6ka as compared to the present day (Figure 3.6a).

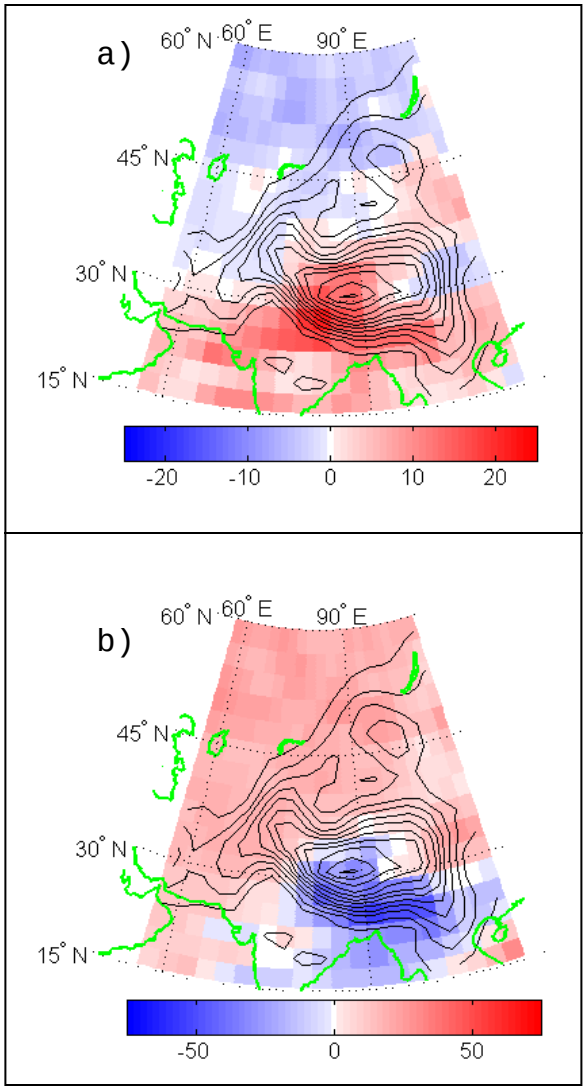

Figure 3.6: Change in (a) cloud fraction (%) and (b) shortwave radiation (W/m^2) for 6 ka as compared to the present day.

The connection between the changes in radiation and the temperature response at the surface can be seen by analyzing the terms in the surface energy balance. As the results are again broadly similar for all GCM's, the results for one model, ECHAM3, are presented here. Figure 3.6b shows the difference between 6 ka and

present-day shortwave radiation along with the change in cloud fraction (Figure 3.6a), which allows for comparison of the pattern in shortwave radiation changes to the change in cloud fraction. Figure 3.7a-c presents the changes in longwave radiation and sensible and latent heat fluxes. Together these figures show that in the central and western portion of the Himalaya there is a decrease in both shortwave radiation (-40 W/m^2) and latent heat (-45 W/m^2). Therefore, both an increase in cloud fraction and an increase in evaporation contribute to the surface cooling. In the far eastern portion of the Himalaya there is no significant change in the latent heat, only in the shortwave radiation. Thus the cooling in the far eastern Himalaya can be attributed to the decrease in shortwave radiation (-50 W/m^2) due to the increased albedo (increased cloud fraction) compared to the present day. Therefore, the surface cooling across the eastern zone is due in part to an increase in evaporation as well as an increase in cloudiness. Finally, in the northern and western zones, the increase in summer temperatures is a direct result of the increased shortwave radiation reaching the surface (30 W/m^2).

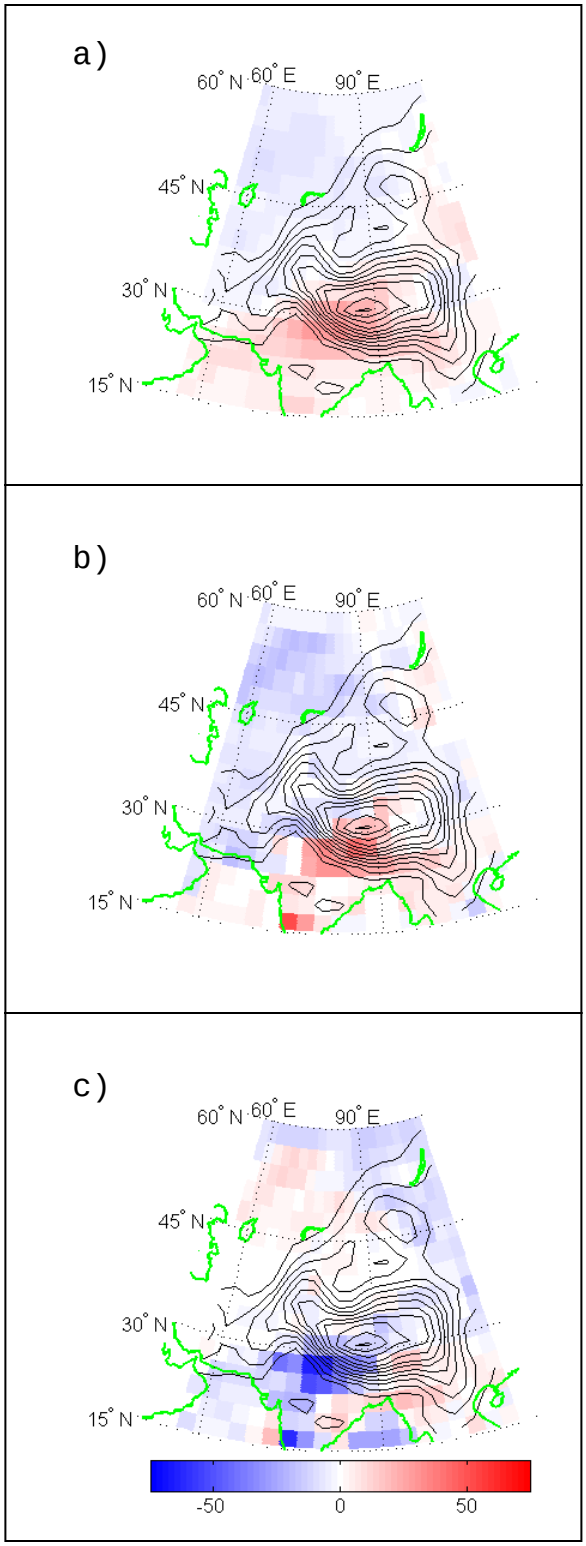

Figure 3.7: Change in (a) longwave radiation, (b) sensible heat flux, and (c) latent heat flux (all in W/m^2) for 6 ka as compared to the present day.

In summary, these results suggest that the advance of glaciers in the Southern Himalaya is a result of a combination of factors. Enhanced monsoon intensity and/or duration led to an increase in precipitation as well as a decrease in temperature via increased cloud fraction (decreased shortwave radiation) and evaporation. Thus, glaciers in the eastern region are influenced by changes in the monsoons and the associated changes in both temperature and precipitation. These results contradict previous work suggesting that Holocene glacier advances in the southern Himalaya were due to increased precipitation only. The lack of glacier advance in the northern and western zones is due to the large increase in average summer temperatures, a direct result of the increase in incoming summer insolation, consistent with other results showing a strong sensitivity of continental climates to changes in radiation (e.g., Felzer et al. 1995).

3.5 Summary and Discussion

Central Asian glacier history provides a unique opportunity to reconcile regional scale glacier changes with the climate mechanisms driving them. In particular, the advance of glaciers in the southern Himalaya in the early Holocene is in contrast to the smaller alpine glaciers in the western and northern regions of Central Asia (e.g., Gillespie and Molnar, 1995, Gillespie et al., 2003).

Previous studies attribute this southern Himalayan Holocene glacier advance to an increase in monsoonal precipitation (e.g., Benn and Evans, 1998; Bush, 2002; Finkel et al., 2003). Although a substantial increase in precipitation is evident during the early and mid-Holocene in GCM simulations (e.g. Joussaume et al., 1999), my results show that this is only a small part of the story. I use two different mass-balance models to quantify the change in ELA for simulated changes in mid-Holocene climate. The first of these models uses a positive degree day approach to estimate ablation (Braithwaite, 1995) and a modified version of the Ambach and Kuhn (1985) ELA perturbation method to calculate changes in ELA. As such, this model was used to assess the relative importance of temperature and precipitation on ELA changes in Central Asia. The second model is a self-consistent surface energy- and mass-balance model that incorporates changes in all relevant atmospheric variables (Rupper and Roe, 2007). Eighteen GCM simulations using boundary conditions appropriate for the present day and 6 ka were acquired from PMIP and used as input in the ELA models. While assumptions and simplifications in the model formulations must be made, due in large part to the coarse grid (2.5° to 5°) and temporal resolution (monthly) of the GCM output, these were found not to significantly change the main conclusions. The pattern in ELA changes using both models were consistent for those regions where melt dominates total ablation, suggesting the PDD approach is appropriate in melt regions.

Both ELA models clearly show that the lowering of ELAs in the southern Himalayas, a region dominated by melt, is largely due to a decrease in summer temperatures during the Holocene, and that the increase in precipitation accounts for, at most, 30% of the total ELA changes. In the melt-dominated regions of the western and northern zones, both ELA models show a rise in ELAs in response to a general increase in temperatures. Importantly, these results suggest that there is regional variability in the climate's response to the increase in northern hemisphere summer insolation, and that the regional variability in glacier changes in Central Asia is largely explained by the resulting temperature pattern in the melt-dominated regions. Sublimation dominates the ablation in portions of the northern and western zones. In these sublimation-dominated regions, the mass and energy-balance model shows that ELAs are acutely sensitive to changes in precipitation. Thus the sensitivity of the ELAs to changes in climate depends on the dominant ablation process.

Through a detailed evaluation of the energy balance at the surface, I was able to explain the pattern in temperature changes in Central Asia. The increase in summer temperatures in the more northern regions of Central Asia is a direct radiative response to the increase in solar insolation at 6 ka, and is consistent with other studies showing temperatures in continental interiors slave to radiation changes (e.g., Felzer et al. 1995). The temperature decrease in the more southern regions, on the other hand, is a dynamic response to the increase in temperatures

in the interior. In particular, the increase in land-sea temperature contrast intensifies the monsoonal circulation. This results in an increase in precipitation as well as a substantial increase in cloudiness over the southern region. The decrease in summer temperatures is the result of both a decrease in shortwave radiation due to the increase in cloudiness (and a resulting increase in albedo) and an increase in evaporative cooling.

The results presented in this study are for climate changes at 6 ka while the largest Holocene glacier advances occurred earlier in the Holocene, ~9 ka. It is important to discuss the validity of the results in light of this time discrepancy. The boundary conditions around 9 ka were similar to that for 6 ka but with small remnants of the ice sheets remaining at higher latitudes, and larger increases in Northern Hemisphere summer insolation. I compared my results to one GCM simulation under boundary conditions appropriate for 9 ka, the CCM0 AGCM. The patterns in climate and ELA changes for 9 ka were very similar to those for 6 ka, but with larger magnitude changes in both. The mechanisms giving rise to the climate and ELA changes are also the same for 9 ka and 6 ka. Therefore, it is reasonable to use the PMIP suite of GCM simulations for 6 ka to understand the early Holocene glacier advances.

The consistency between all GCMs reinforces confidence that the model results are a robust response of the climate to the changes in insolation forcing. In the

case for Central Asia, spatial patterns in climate occur in response to a relatively uniform increase in solar insolation at the top of the atmosphere. The patterns in glacier advances across Central Asia are a result of the spatial variability in the climate response. This suggests that spatial patterns in climate and glaciers should be expected even in cases where there is a uniform change in forcing (e.g., increasing CO_2). In addition, and in contrast to previous work, my results suggest that the advance of glaciers in the Southern Himalaya is a result of a combination of factors, not just increased precipitation. These glacier records, therefore, highlight the need for a good physical model to test the sensitivity of a given climate proxy to climate change. Such models can be used to determine whether a suggested mechanism that is consistent with the record is a) a unique answer, and b) of sufficient magnitude to impart the recorded signal.

3.6 Notes to Chapter Three

Abramowski U, Bergau A, Seebach D, Zech R, Glaser B, Sosin P, Kubik PW, Zech W, 2006: Pleistocene glaciations of Central Asia: results from Be-10 surface exposure ages of erratic boulders from the Pamir (Tajikistan), and the Alay-Turkestan range (Kyrgyzstan). Quaternary Science Reviews, 25 (9-10): 1080-1096.

Ambach W, Kuhn M, 1985: Accumulation gradients in Greenland and mass balance response to climatic changes. Z Gletscherkd Glazialgeol, 21, 311-317.

Anders A, Roe G, Hallet B, Montgomery D, Finnegan N, Putkonen J, 2006: Spatial Patterns of Precipitation and Topography in the Himalaya, *In* Willett SD, Hoovius N, Brandon MT, and Fisher DM, eds., Tectonics, climate and landscape evolution,GSA Special Paper 398, Chapter 3: 39-53.

Anderson DM, Prell WL, 1993: A 300 kyr record of upwelling off Oman during the late Quaternary – evidence of the Asian southwest monsoon. Paleoceanography, 8 (2): 193-208.

Benn DI, Owen LA, 1998: The role of the Indian summer monsoon and the mid-latitude westeries in Himalayan glaciation: review and speculative discussion. Journal of the Geological Society, 155 (2): 353-363.

Barnard P, Owen L, Finkel R, 2004: Style and timing of glacial and paraglacial sedimentation in a monsoon-influenced high Himalayan environment, the upper Bhagirathi valley, Gavhwal Himalaya. Sedimentary Geology, 165, 199-221.

Bonfils CJ, Lewden D, Taylor KE, 1998: Documentation of the PMIP models. PMCI Report.

Braconnot P, Loutre MF, Dong B, Joussaume S, Valdes P, 2002: How the simulated change in monsoon at 6 ka BP is related to the simulation of the modern climate: results from the Paleoclimate Modeling Intercomparison Project. Climate Dynamics, 19 (2) :107-121.

Braithwaite RJ, 1995: Positive degree-day factors for ablation on the Greenland ice-sheet studied by energy-balance modeling. Journal of Glaciology, 41 (137): 153-160.

Broecker WS, 2003: Does the trigger for abrupt climate change reside in the ocean or in the atmosphere? Science, 300 (5625): 1519-1522.

Bush ABG, 2002: A comparison of simulated monsoon circulations and snow accumulation in Asia during the mid-Holocene and at the Last Glacial Maximum. Global and Planetary Change, 32 (4): 331-347.

Clark D, Gillespie A, Bierman P, Caffee M, 2001: Glacial asynchrony in the Kunlun Shan, northwestern Tibet. Abstracts with Programs – Geological Society of America, 33 (6): 441.

Collins WD, Valero FPJ, Flatau PJ, Lubin D, Grassl H, Pilewskie P, Spinhirne J, 1996: The radiative effects of convection in the Tropical Pacific. Journal of Geophysical Research, 101(D10):14999-15012.

Crowley TJ, North GR, 1988: Abrupt climate change and extinction events in earth history. Science, 240 (4855): 996-1002.

Dong GR, Wang GY, Li XZ, Chen HZ, Jin J, 1998: Palaeomonsoon vicissitudes in eastern desert region of China since last interglacial period. Science in China Series D-Earth Sciences, 41 (2): 215-224.

Emeis KC, Anderson DM, Doose H, Kroon D, Schulzbull D, 1995: Sea-surface temperatures and the history of monsoon upwelling in the northwest Arabian Sea during the last 500,000 years. Quaternary Research, 43 (3): 355-361.

Felzer B, Oglesby RH, Shao H, Webb T, Hyman DE, Prell WL, and Kutzbach JE, 1995: A systematic study of GCM sensitivity to latitudinal changes in solar-radiation. Journal of Climate, 8 (4): 877-887.

Finkel RC, Owen, L, Barnard P, Caffee M, 2003: Beryllium-10 dating of Mount Everest moraines indicates a strong monsoon influence and glacial synchroneity throughout the Himalaya. Geology, 31 (6): 561-564.

Fountain AG, Lewis KJ, Doran PT, 1999: Spatial climatic variation and its control on glacier equilibrium line altitude in Taylor Valley, Antarctica. Global and Planetary Change, 22 (1-4): 1-10.

Gillespie A, Molnar P, 1995: Asynchronous maximum advances of mountain and continental glaciers. Reviews of Geophysics, 33 (3): 311-364.

Gillespie A, Rupper S, and Roe G, 2003: Climatic interpretation from mountain glaciations in Central Asia. Geological Society of America, Abstracts with Program 35(6).

Hall NMJ, Valdes PJ, 1997: A GCM simulation of the climate 6000 years ago. Journal of Climate, 10 (1): 3-17.

Hoskins BJ, Hodges KI, 2002: New perspectives on the Northern Hemisphere winter storm tracks. Journal of the Atmospheric Sciences, 59 (6) 1041-1061.

Joussaume S, Taylor KE, Braconnot P, Mitchell JFB, Kutzbach JE, Harrison SP, Prentice IC, Broccoli AJ, Abe-Ouchi A, Bartlein PJ, Bonfils C, Dong B, Guiot J, Herterich K, Hewitt CD, Jolly D, Kim JW, Kislov A, Kitoh A, Loutre MF, Masson V, McAvaney B, McFarlane N, de Noblet N, Peltier WR, Peterschmitt JY, Pollard D, Rind D, Royer JF, Schlesinger ME, Syktus J, Thompson S, Valdes P, Vettoretti G, Webb RS, Wyputta U, 1999: Monsoon changes for 6000 years ago: Results of 18 simulations from the Paleoclimate Modeling Intercomparison Project (PMIP). Geophysical Research Letters, 26 (7): 859-862.

Kalnay E, Kanamitsu M, Kistler R, Collins W, Deaven D, Gandin L, Iredell M, Saha S, White G, Woollen J, Zhu Y, Chelliah M, Ebisuzaki W, Higgins W, Janowiak J, Mo KC, Ropelewski C, Wang J, Leetmaa A, Reynolds R, Jenne R, Joseph D, 1996: The NCEP/NCAR 40-year reanalysis project. Bulletin of the American Meteorological Society, 77 (3): 437-471 MAR 1996

Kaufman DS, Porter SC, Gillespie AR, 2004: Quaternary alpine glaciation in Alaska, the Pacific Northwest, Sierra Nevada, and Hawaii, in Gillespie AR, Porter SC, and Atwater BF, eds., The Quaternary Period in the United States, Developments in Quaternary Science Volume 1, Elsevier Press, 77-103.

Kayastha RB, Ohata T, Ageta Y, 1999: Application of a mass-balance model to a Himalayan glacier. Journal of Glaciology, 45 (151): 559-567.

Koppes MN, Gillespie AR, Burke RM, Thompson SC, Clark DH, 2003: Late Quaternary glaciation in northern Central Asia. XVI INQUA Congress, Programs with Abstracts, Reno, July, p. 156.

Kuhle M, 1998: Reconstruction of the 2.3 million km(2) late Pleistocene ice sheet on the Tibetan Plateau and its impact on the global climate (vol 45, pg 71, 1998). Quaternary International, 47-8: 173-182.

Kutzbach JE, Gallimore RG, 1988: Sensitivity of a couples atmosphere atmosphere mixed layer ocean model to changes in orbital forcing at 9000 years bp. Journal of Geophyscial Researach, 93 (D1): 803-821.

Legates DR, Willmott CJ, 1990a: Mean seasonal and spatial variability in gauge-corrected, global precipitation. International Journal of Climatology, 10 (2): 111-127.

Legates DR, Willmott CJ, 1990b: Mean seasonal and spatial variability in global surface air-temperature. Theoretical and Applied Climatology, 41 (1-2): 11-21.

Lowell TV, Heusser CJ, Andersen BG, Moreno PI, Hauser A, Heusser LE, Schluchter C, Marchant DR, Denton GH, 1995: Interhemispheric correlation of late Pleistocene glacial events. Science, 269 (5230:1541-1549.

Merle J, Carson R, Cady J, Hinz N, 2000: Quaternary geology of the Tengis_Shishid Gol region, Khovsgo, Mongolia. Anonymous Abstracts with Programs- Geological Society of America, 33 (3): 67.

Molg T, Hardy DR, 2004: Ablation and associated energy balance of a horizontal glacier surface on Kilimanjaro. Journal of Geophysical Research, 109 (D16): Art. No. D16104.

Owen LA, Kamp U, Spencer JQ, Haserodt K, 2002: Timing and style of Late Quaternary glaciation in the eastern Hindu Kush, Chitral, northern Pakistan: a review and revision of the glacial chronology based on new optically stimulated luminescence dating. Quaternary International, 97-8: 41-55.

Owen LA, Finkel RC, Haizhou M, Spencer JQ, Derbyshire E, Barnard PL, Caffee MW, 2003: Timing and style of Late Quaternary glaciation in northeastern Tibet. Geological Society of America Bulletin, 115 (11): 1356-1364.

Paterson, 1999: Physics of Glaciers. Pergamon/Elsevier Science Inc.

Phillips WM, Sloan VF, Shroder JF, Sharma P, Clarke ML, Rendell HM, 2000: Asynchronous glaciation at Nanga Parbat, northwestern Himalaya Mountains, Pakistan. Geology, 28 (5): 431-434.

Porter SC, 1975: Equilibrium-line altitudes of late Quaternary glaciers in southern Alps, New Zealand. Quaternary Research, 5 (1): 27-47.

Porter SC,1977: Present and past glaciation threshold in the Cascade Range, Washington, U. S. A.: topographic and climatic controls, and paleoclimatic implications. Journal of Glaciology, 18, 101-116.

Porter SC, Orombelli G, 1985: Glacier contraction during the middle Holocene in the western Italian Alps – evidence and implications. Geology, 13(4): 296-298.

Ramanathan Y, 1987: Cumulus parameterization in a case-study of a monsoon depression. Monthly Weather Review, 108 (3): 313-321.

Roe GH, Steig EJ, 2004: Characterization of millennial-scale climate variability. Journal of Climate, 17 (10): 1929-1944.

Rupper and Roe, 2007: Glacier changes and regional climate: a mass and energy balance approach. In preparation.

Schafer JM, Tschudi S, Zhao ZZ, Wu XH, Ivy-Ochs S, Wieler R, Baur H, Kubik PW, Schluchter C, 2002: The limited influence of glaciations in Tibet on global climate over the past 170 000 yr. Earth and Planetary Science Letters, 194 (3-4): 287-297.

Shi Y, 2002: Characteristics of late Quaternary monsoonal glaciation on the Tibetan Plateau and in East Asia. Quaternary International, 97-8: 79-91.

Vettoretti G, Peltier WR, McFarlane NA, 1998: Simulations of mid-Holocene climate using an atmospheric general circulation model. Journal of Climate, 11 (10): 2607-2627.

Wei Z, Zhijiu C, Yanghua L, 2006: Review of the timing and extent of glaciers during the last glacial cycle in the bordering mountains of Tibet and in East Asia. Quaternary International, 154-155: 32-43.

Wilcox EM, Ramanathan V, 2001: Scale dependence of the thermodynamic forcing of tropical monsoon clouds: Results from TRMM observations. Journal of Climate, 14 (7): 1511-1524.

Wunsch C, 2006: Abrupt climate change: An alternative view. Quaternary Research, 65 (2): 191-203.

Zhang Y, Shiyin L, Yongjian D, 2006: Observed degree-day factors and their spatial variation on glaciers in western China. Annals of Glaciology, 43, 301-306.

Chapter Four

SPATIAL PATTERNS IN CENTRAL ASIAN CLIMATE AND EQUILIBRIUM-LINE ALTITUDES AT THE LAST GLACIAL MAXIMUM

4.1: Motivation and Introduction

Whereas focusing on the Holocene primarily addresses how ELAs change in response to changes in insolation, the LGM provides a test for how ELAs change in response to changes in CO2, SSTs, and land-surface topography and albedo. I provide a summary of the general circulation model (GCM) simulations and LGM boundary conditions used in this chapter. A description of results from previous studies on climate changes 21 ka in response to the large changes in ocean and land-surface boundary conditions can be found in Chapter 1.

I use the PMIP GCM simulations for 21 ka and present-day (Bonfils et al., 1998). All 17 PMIP GCMs use the same specified boundary conditions for 21 ka (Table 1.1). These boundary conditions include atmospheric CO_2 equal to 200 ppm, Peltier (1994) ice sheet reconstructions, 21 ka orbital parameters (Berger and Loutre, 1991), and vegetation and albedo equal to present day for grid points with no ice/snow cover. Nine models compute SSTs by coupling atmospheric GCMs to a slab-ocean model. Eight models use fixed SSTs. This suite of models

provides a means to test how sensitive Central Asian glaciers are to possible climate changes.

4.2: Glacier History

Chapters 1 through 3 present details on the glacier history in Central Asia. Here I briefly recap this history, focusing on the LGM in the western, northern, and eastern zones (Figures 1.1 and 2.1).

The western zone includes the Kyrgyz Tien Shan south to the Karakoram and east to central Tibet. Significant work has been done in this region to define the timing of Quaternary glaciations. In much of this region, evidence of large LGM advances is lacking. Owen et al. (2002) report dates for two minor valley glaciations in the Karakoram at Pakistan's northern most tip. The dates, 25.7-21.8 ka and 18.4-15.3 ka, bracket the LGM, but the glaciers were smaller than the pre-LGM advances. Near Mt. Everest, just east of the western zone, Finkel et al. (2003) report evidence of two smaller advances also bracketing the LGM. There is also evidence suggesting that the LGM moraines in the Kyrgyz Tien Shan were actually restricted to the cirques, close to the modern glaciers (Koppes et al., 2003). At most sites in western Central Asia there is inconclusive evidence for large glacier advances during the LGM (e.g. Koppes et al., 2003, Phillips et al., 2000, Clark et al., 2001, Owen et al, 2001, and Barnard et al., 2004). In summary

then, it appears that there is substantial evidence of a large pre-LGM advance (Chapter 1), deposits indicating many large valley and piedmont glaciers dating to that period, while LGM glaciers were much smaller than these earlier advances.

The northern zone is defined by the area from central Mongolia to China's Xinjiang Tien Shan. While large pre-LGM advances are evident, there is also evidence of substantial LGM advances as well. This contrasts with the western zone, where it appears that the advances early in the last ice age cycle were far larger than at the LGM. For example, there is evidence of large advances at the LGM near the Jarai and Tingis rivers in the Darhad Basin of northern Mongolia, headwaters of the Ynesei River (Merle et al., 2000), and in the Die Han Je Le Gou drainage in the Xingian Tien Shan (Clark et al., 2001). There is also evidence that glaciers advanced during the LGM in western Xingiang, Daxigou in the Tien Shan, and the Karlik Shan were at least as large as the pre-LGM advances in the region. Throughout the northern region, maximum changes in ELA values increase with latitude, from 500 m in the Tien Shan to 1000-1200 m north of 51^{o} N (e.g. Shi, 2002). The LGM and maximum change in ELA's differ by only 25-100 m.

The glacier history in the eastern zone, Nepal and eastern Tibet, is not as clearly defined as the other two zones. However, there are several studies where dates are convincing and can be used to begin to understand the glacier history of the

regions. In particular, Owen et al. (2003) demonstrate convincingly that the largest advance in the Anyemaqen and Nianbaoyeze mountains were pre-LGM. However, Schafer et al (2002) show that the largest advance at Kanchenjunga occurred during the LGM. Thus there is evidence that both LGM and pre-LGM glacier advances were extensive. Maximum changes in ELA values in eastern Tibet and the Himalaya increase from west to east as well as from north to south, ranging from 300-500 m on the plateau to >1000 m near Namche Barwa (Shi, 2002).

In summary, the LGM advances in the western zone were small, often restricted to cirques. LGM advances in the northern zone were substantial, probably equal to or larger than pre-LGM advances. It is not clear whether the pre-LGM or LGM advances were larger in the eastern zone, though the current evidence suggests both were large. Since glaciers advance and retreat in response to changes in climate, the spatial pattern in glacier ELAs and length changes at the LGM suggest spatial patterns in climate also occurred. The two main goals of this chapter are to 1) reconcile the pattern in ELA changes with the climate changes, and 2) test the sensitivity of ELAs to changes in LGM boundary conditions.

I test the sensitivity of Central Asian glaciers to changes in both precipitation and ablation using the PMIP suite of GCM simulations and two mass-balance models. The first mass-balance model utilizes the traditional approach to estimating mass

balance by assuming ablation is proportional to temperature. The second mass-balance model applies a self-consistent surface energy-balance model (Rupper and Roe, 2007). Detailed descriptions of both mass-balance models and the PMIP GCM simulations are provided in Chapters 2 and 3. This chapter utilizes the same models and approach to analyzing and diagnosing the changes in ELAs for simulated LGM climates as for the Holocene in Chapter 3. In the next sections I describe first the simulated changes in mid-Holocene temperatures and precipitation in the three zones, and second the change in ELAs that result from these changes in climate.

4.3 GCM Simulation of Temperature and Precipitation

In my analysis of the GCMs, I focus on precipitation and temperature because of the important link between these two variables and glaciers. In presenting the results, I show maps from 6 GCM simulations which represent the spread in the results. The results presented include three atmospheric GCMs with fixed SSTs (BMRC-2, ECHAM-3, LMCELMD-5) and three with computed SSTs (CCC2-0, GFDL, UKMO). Table 4.1 lists the mean changes in temperature and precipitation averaged over each of the zones separately. Importantly, there is less consistency between the model simulations at 21 ka than in simulations at 6 ka, particularly for precipitation. This is discussed below and in Section 4.5. Despite the spread between models, these GCMs can nonetheless be used to

evaluate the range of predicted climate response to LGM boundary conditions. Below I present the changes in precipitation and temperature at 21 ka as compared to present-day, as well as important differences between the models.

Table 4.1: Changes in climate variables and ELAs averaged for all GCM simulations for the eastern, western, and northern zones. T is the mean summer (JJA) air temperature, P is mean annual precipitation, ELA is the equilibrium-line altitude, IV is the index of variability (absolute values of the standard deviation divided by the mean change).

	Model Approach	Units	Eastern Zone	Western Zone	Northern Zone
ΔT		^{o}C	-3	-4	-4
IV for T		---	1	0.5	0.6
ΔP		m yr^{-1}	-0.1	-0.01	-0.08
IV for P		---	>2	>2	0.25
ΔELA	PDD	m	-500	-1000	-1000
ΔELA for ΔT only	PDD	m	-440	-900	-910
ΔELA	SEMB	m	-700	-1200	-1200
ΔELA for ablation change only	SEMB	m	-600	-1100	-1100

4.3.1 Patterns in Temperature Changes

All the GCMs simulate a decrease in summertime (JJA) temperatures in the northern and western zones (1-10 K) (Figure 4.1a-f). In contrast to this general decrease in temperatures, the temperature changes are more variable along the southern Himalaya, including in the eastern zone, ranging between +3 °C and -5

°C. Figure 4.2a shows the mean temperature change across the 12 highest resolution GCMs (see also Table 4.1 for averages over each zone). The output for all 12 models was linearly interpolated to the ECHAM3 grid, and then averaged at each grid point. The mean of the models shows a decrease in temperature everywhere with the magnitude of the temperature change generally increasing with increasing latitude and over the Tibetan Plateau. The spread in the model results is illustrated in Figure 4.2b of the standard deviation divided by the absolute value of the mean summertime (JJA) temperature change for all model simulations at each grid point. The values represent an index of how consistent the modeled temperatures are, and are hereafter referred to as the index of variability. An index of variability less than one (blue color in Figure 4.2b) indicates regions where the standard deviation in summertime temperature across the models is small relative to the mean change in summertime temperature and suggests consistency in the model simulations. Conversely, where the index of variability is greater than one (red colors in Figure 4.2b) the spread in modeled temperature changes is large. For most of Central Asia the index of variability is less than 1, suggesting that the simulated changes in temperature are greater than the spread, indicating a fairly robust response of the simulated temperatures to changes in boundary conditions at 21 ka. A small portion of the eastern Himalayas is more variable, which corresponds to the region which showed the greatest variability in the panels in Figure 4.1. As I will show in Section 4.4, the patterns in temperature changes are important for explaining the modeled ELA

changes across Central Asia. The reasons for the temperature response and spread are examined closely in section 4.5.

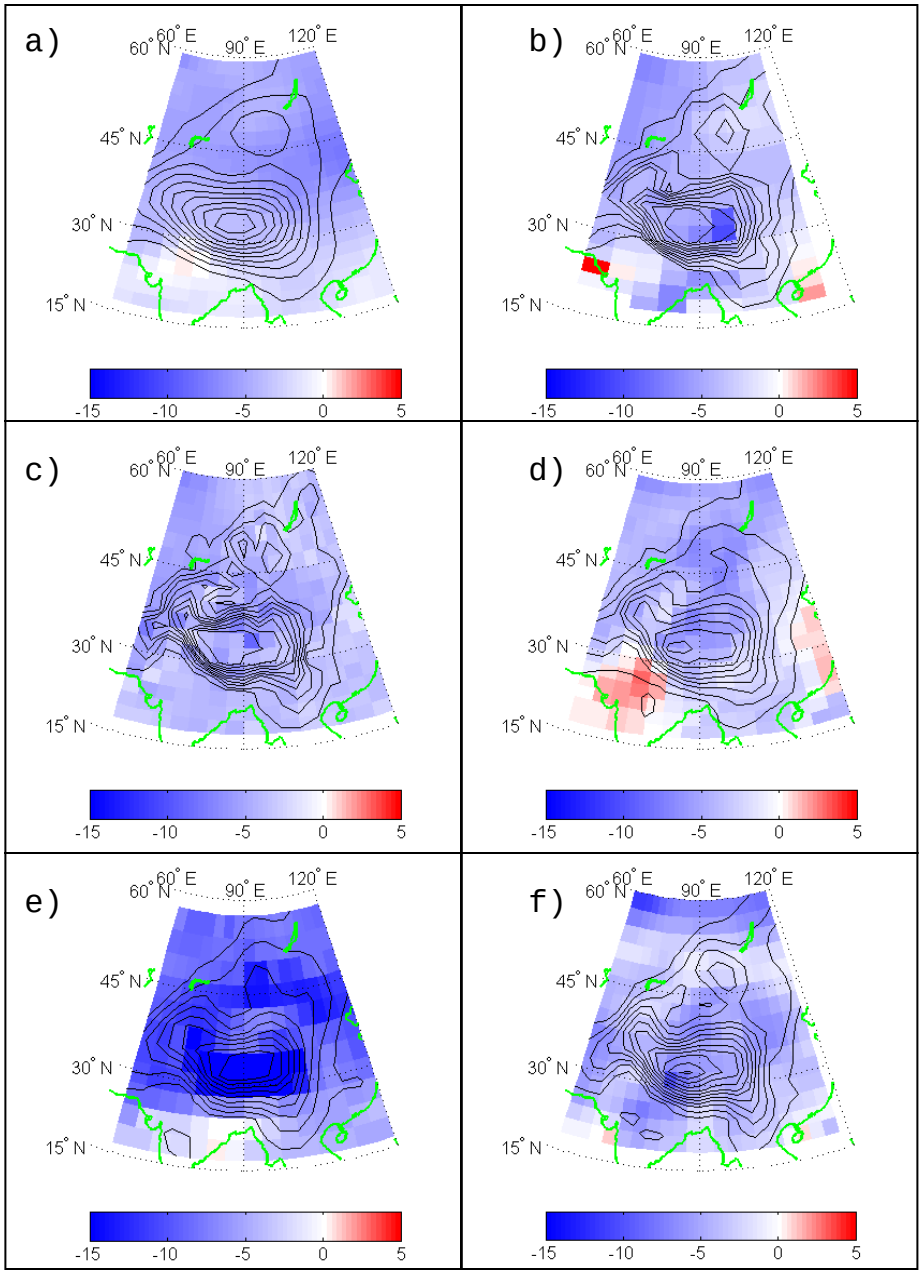

Figure 4.1: Change in mean summertime (JJA) temperature (°C) at 21 ka as compared to present day for a) GFDL, b) LMCELMD-5, c) UKMO, d) BMRC-2, e)CCC2-0, and f) ECHAM-3.

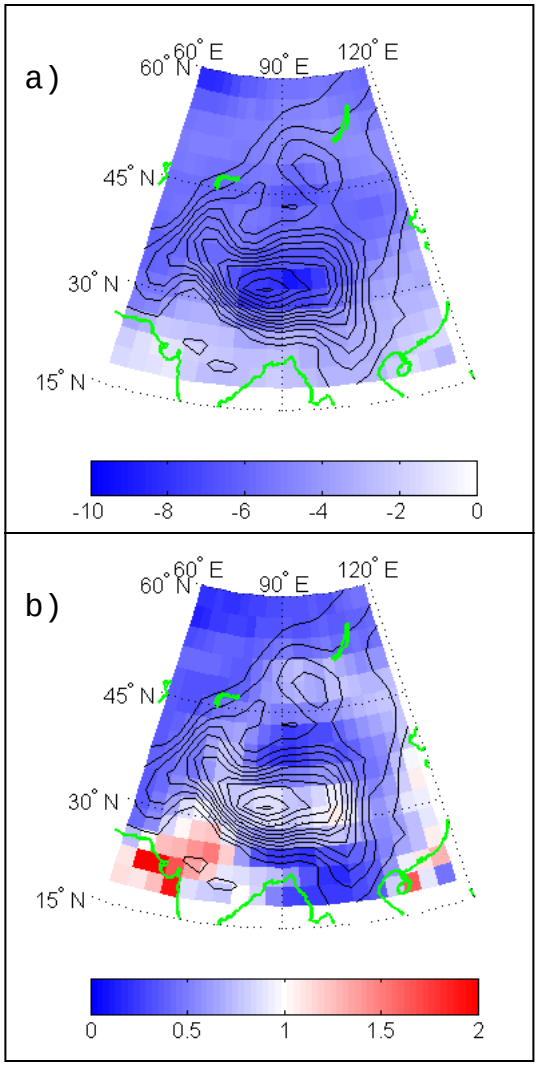

Figure 4.2: Mean change in summertime (JJA) temperature (°C) for 12GCMs (a), and the standard deviation divided by the absolute values of the mean (the index of variability) for summertime temperature change for the 12 GCMs (b). Each GCM used in calculating the mean and standard deviations were interpolated to the ECHAM-3 grid.

4.3.2 Patterns in Precipitation Changes

There is a large spread in the GCM simulated changes in annual precipitation for much of Central Asia, with the exception of the northern zone. Annual precipitation decreases in all GCMs in the northern zone (Figure 4.3), averaging

between 25 and 250 cm/yr. Precipitation changes in the western and eastern zones are highly variable from model to model, and even the sign of the change is not consistent. This may be due to differences in modeled changes in the Mediterranean storm track (western zone) and the Indian summer monsoon in response to LGM boundary conditions. While the mean of all models (Figure 4.4a and Table 4.1) shows a decrease in precipitation in the north and west and an increase in the east, the index of variability is large in the western and eastern zones (Figure 4.4b), highlighting these regions as having the greatest variability between models. In comparison, the decreased precipitation in the north is a robust response of the climate to conditions at 21 ka (index of variability less than one). The tendency of the models towards a decrease in precipitation is likely due to the decrease in temperature. For constant relative humidity, moisture content increases with temperature, as given by the Clausius-Clayperon relation (e.g., Wallace and Hobbs, 2005).

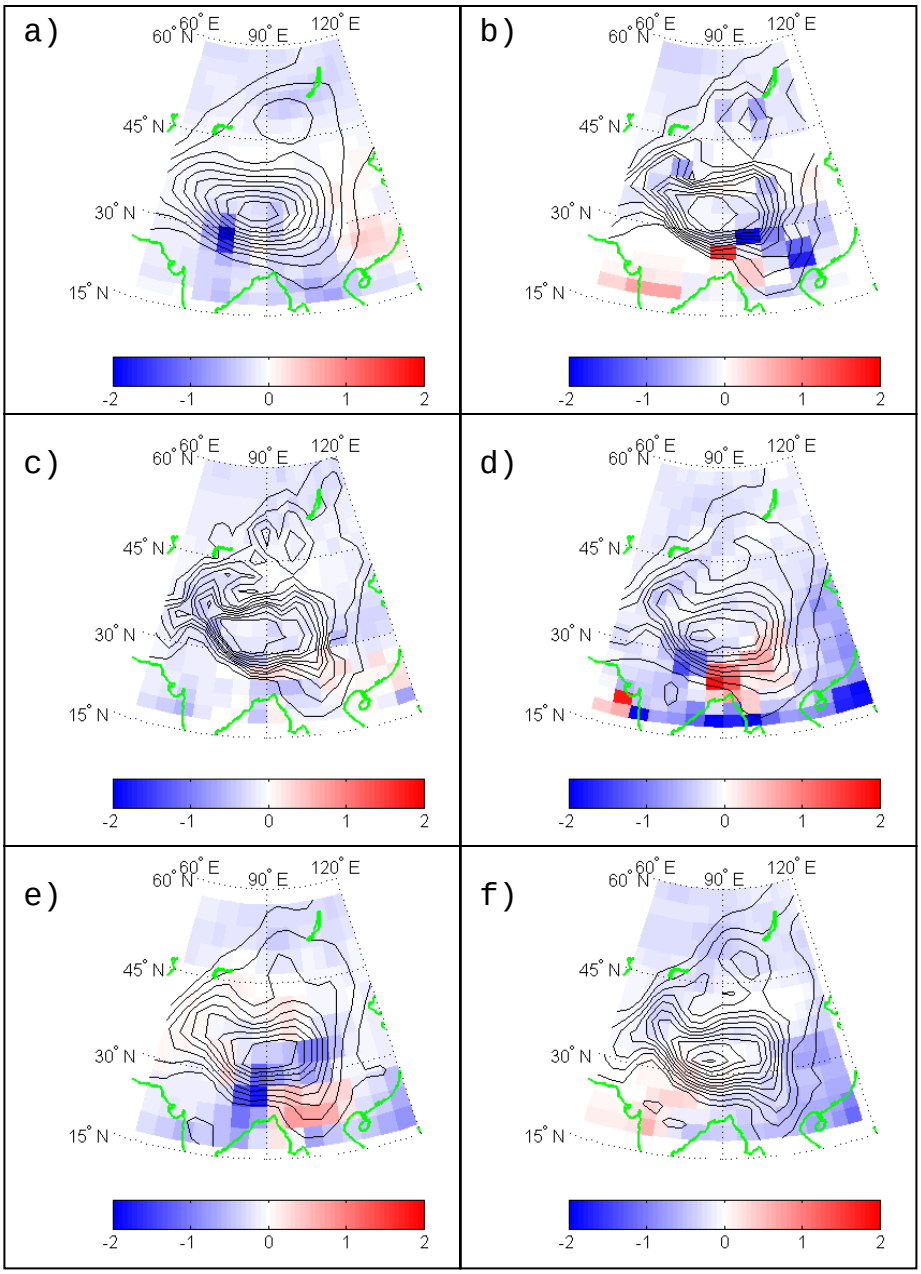

Figure 4.3: Change in annual precipitation (m yr^{-1}) for 21 ka as compared to the present day for a) GFDL, b) LMCELMD-5, c) UKMO, d) BMRC-2, e) CCC2-0, and f) ECHAM-3.

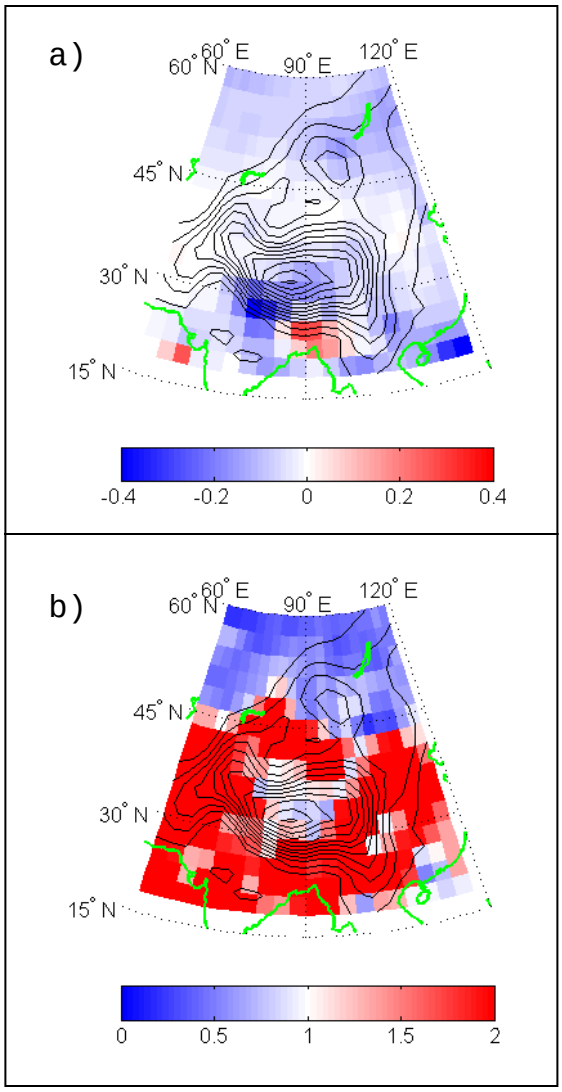

Figure 4.4: As in Figure 4.2, but for the change in precipitation (m/yr).

Three important results can be gleaned from the above discussion of temperature and precipitation changes in Central Asia. Firstly, the simulated temperature changes are consistent for the northern and western zones, an indication that the GCM summertime temperatures are a robust response of the climate to changes in LGM boundary conditions. The temperature changes in the southern Himalaya

(including the western most part of the eastern zone) are variable between the models. This suggests that there is a high degree of uncertainty in the response of the climate in the monsoon regions to LGM boundary conditions. There is a large spread in precipitation changes across much of Central Asia, except the northern zone. Thus precipitation changes are far more uncertain than temperature changes. Second, despite the variability between the GCM simulations, all GCMs produce spatial patterns in temperature and precipitation changes across Central Asia in response to the changes in boundary conditions. Finally, glaciers respond to changes in temperature and precipitation. Therefore the spatial patterns in temperature and precipitation changes should impart patterns in ELA changes across Central Asia.

4.4: Spatial Pattern in ELA Changes

To understand the impact of the simulated climate changes on glacier mass balance, the GCM output must be converted into changes in ELA. To do this I use two different models. The first is an ELA perturbation model following Ambach and Kuhn (1989), modified to use the positive degree day (PDD) model for ablation (Braithwaite, 1995). The second model is a surface energy- and mass-balance model (Rupper and Roe, 2007). Refer to Chapters 2 and 3 for detailed descriptions of both models.

4.4.1 Modeled ΔELAs: PDD Approach

In this section I discuss the results of converting climate changes to ELA changes using the PDD approach. There are important discrepancies between the patterns of ELA changes for the different GCMs; I therefore present figures for the same six GCMs discussed in Section 4.3 (Figure 4.5). Average ELA changes for the three separate zones are listed in Table 4.1. The largest discrepancy between models occurs in the southern Himalayas. Even the sign of the ELA changes is not consistent between models in this region, ranging between -1000 m and 500 m. This coincides with the same region where the sign of the temperature changes was also different between the models. All models predict a lowering of ELAs in the northern and western zones, but the pattern of this lowering is different for different models. For example, the ΔELAs for the GFDL GCM generally increase with latitude (Figure 4.5a). By comparison, the ΔELAs for the LMCDEL-5 GCM shows the largest change over the interior of the Tibetan Plateau and decreasing changes at higher latitudes (Figure 4.5b). Therefore, while the sign of the ELA changes are consistent, the pattern of ELA changes is different between the models. The pattern in ELA changes is reminiscent of the pattern in temperature changes. To determine how important the patterns in temperature change are, the change in ELA is calculated for change in temperature only (no change in precipitation). If only the temperature changes, the ELA changes for all three zones are approximately 80-90% of the total ELA

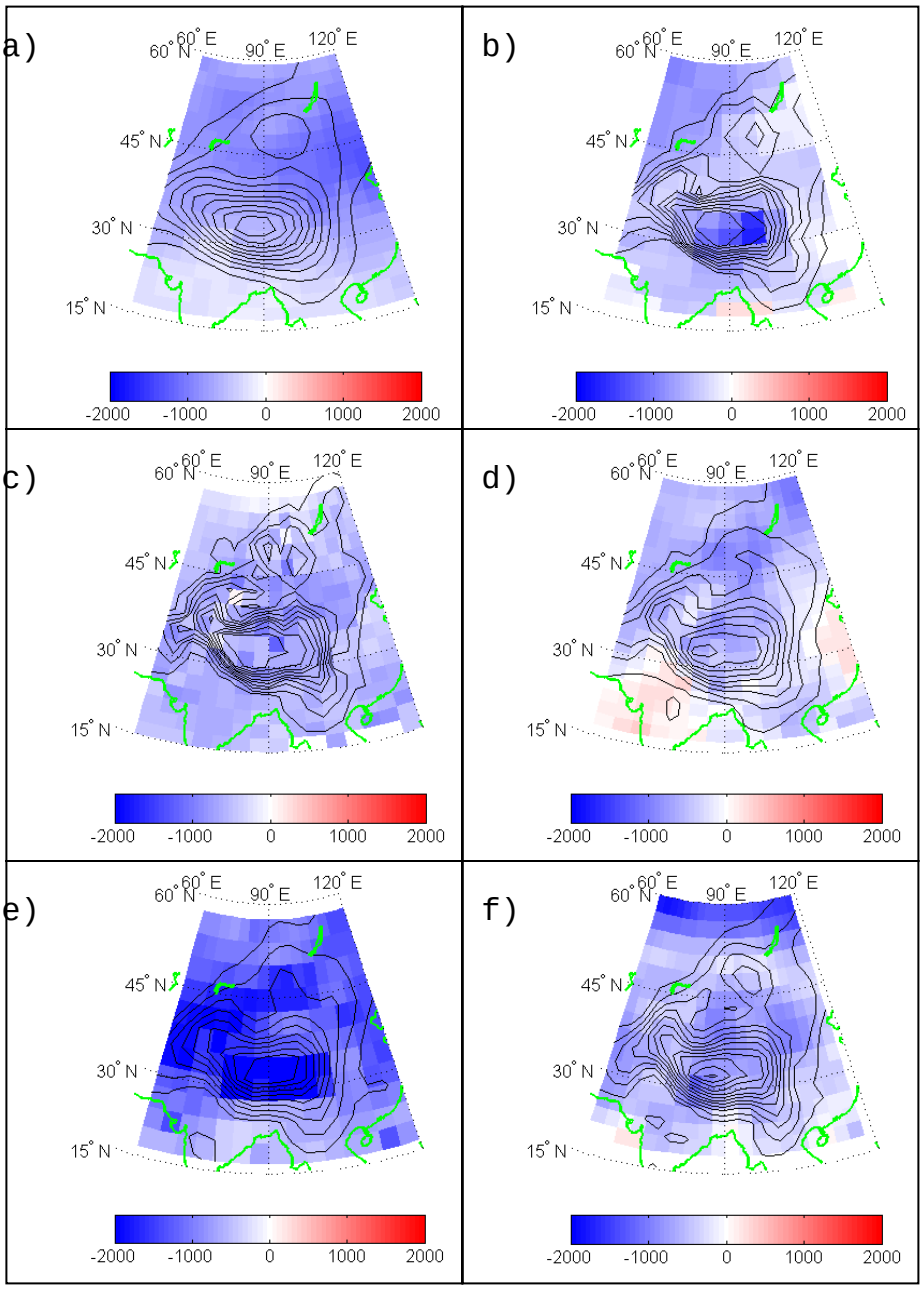

Figure 4.5: Changes in ELAs for present-day minus 21 ka, calculated using the PDD approach to ablation: a) GFDL, b) LMCELMD-5, c) UKMO, d) BMRC-2, e) CCC2-0, and f) ECHAM-3.

change (Table 4.1). Therefore precipitation accounts for at most 20% of the total change in ELAs. This highlights the fact that, despite some differences in the

magnitude of the ELA response, ELAs across Central Asia are most sensitive to the simulated changes in temperature.

4.4.2 Modeled ΔELAs: Surface-Energy and Mass-Balance Approach

The simple PDD method assumes that ablation is directly related to temperature. Physically, of course, it is a net input of heat that is actually responsible for the melting or sublimation of snow and ice. For the application to regional-scale climate patterns, I use the surface energy- and mass-balance model (SEMB model) presented in Rupper and Roe (2007). Applying the model to this study serves two purposes. Firstly, it provides check on the answers derived from the PDD method. Secondly, as a by product, the analysis of the surface energy fluxes can be used to explain the temperature patterns across Central Asia.

I use the output from the climate models at present-day and 21 ka to calculate the change in ELA predicted by the model, and to analyze the reasons for the predicted change. Again, there is a large spread between models, therefore I present the results from the 6 GCM used in Sections 4.3, for comparison to the PDD results presented above. As is the case with the PDD approach, the change in climate at 21 ka as compared to modern produces a pattern in ELA changes across Central Asia (Figure 4.6). The overall pattern in ELA changes using the surface energy-balance approach is very similar to that of the PDD approach for

each of the models. Where the two methods disagree is in regions where sublimation dominates the ablation (Figure 2.4). ELA changes are larger in these regions than elsewhere in Central Asia. As discussed in Chapter 3, there is a high degree of uncertainty in ELA changes, calculated using the PDD approach, in regions where sublimation dominates.

To facilitate further comparison of the surface energy-balance model results to the PDD method, I model the ELA changes for a change in ablation only (Table 4.1). If precipitation does not change, the change in ELAs in all melt-dominated regions account for more than 80% of the total change in ELA. In contrast to these melt-dominated regions, sublimation-dominated regions are very sensitive to changes in precipitation with precipitation changes accounting for 50% to 75% of the total ELA change.

These results are consistent with the results presented in Chapter 3 for the Holocene. In particular, where melt dominates, the results suggest that the PDD approach can adequately capture the effect of the surface energy- and mass-balance model. Where sublimation dominates, the ELA is extremely sensitive to small changes in precipitation, and caution should be used when applying the PDD approach. These results indicate that for the typical changes in atmospheric variables predicted by the GCM's, the glaciers in melt-dominated regions are most sensitive to those atmospheric variables that control summer temperature.

Therefore, the surface energy- and mass-balance model confirms the result that the patterns in ELA changes across Central Asia (for 6 ka minus present-day) are primarily a result of the pattern in temperature changes, with the exception of the sublimation regions.

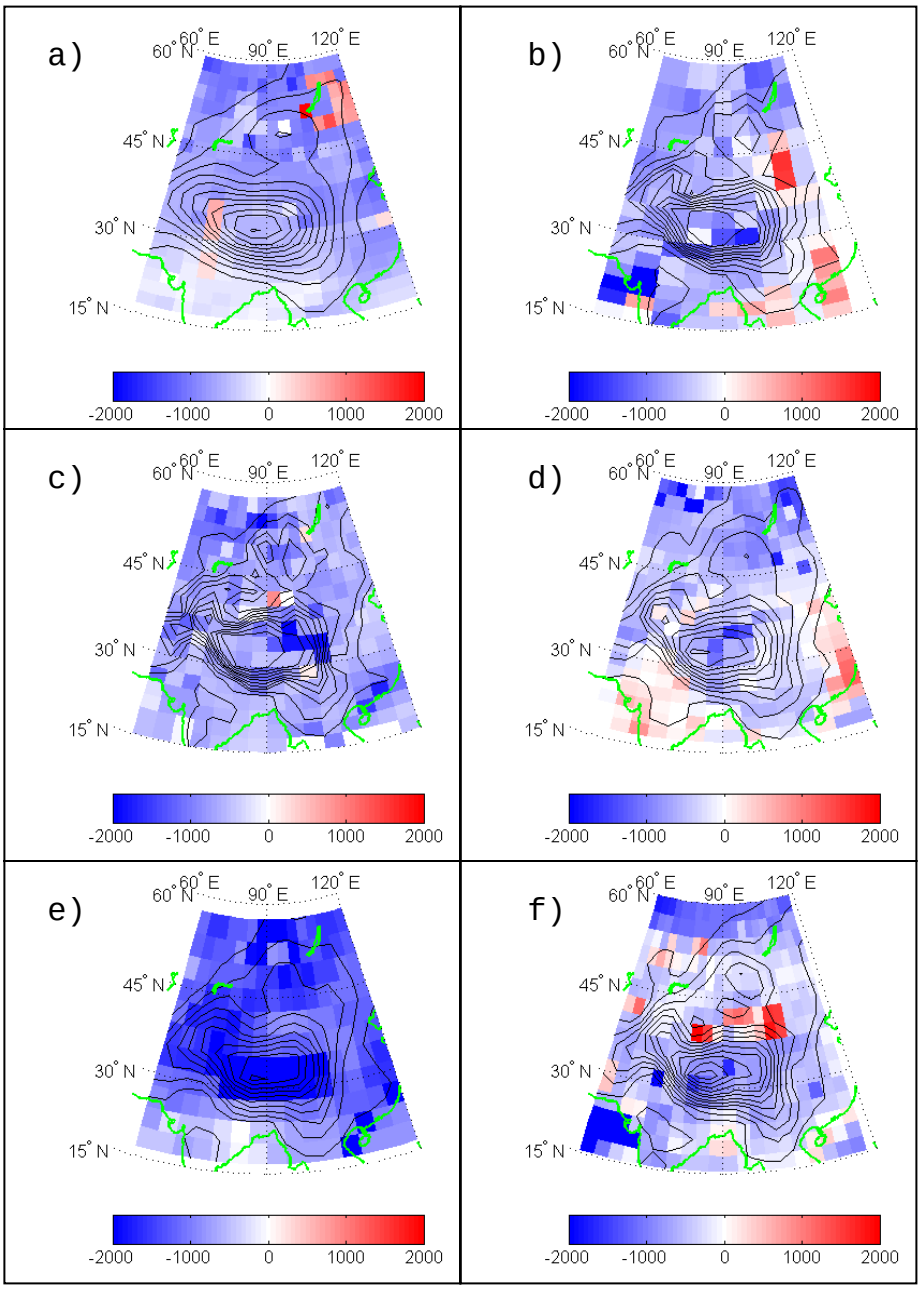

Figure 4.6: Change in ELA for 0 ka minus 21 ka, calculated using the SEMB model: a) GFDL, b) LMCELMD-5, c) UKMO, d) BMRC-2, e) CCC2-0, and f) ECHAM-3.

4.6 Patterns in Temperature and Energy Balance Components

Since the pattern in temperature changes play an important role in the modeled ELA changes, it is important to understand why these changes occur. Insight into these temperature changes is gained through further discussion of the SEMB model results above, and an analysis of the radiation balance in the GCM integrations.

The SEMB model includes all the relevant energy balance components, but does not include dynamical horizontal heat flux convergence. The temperature changes used in the PDD model do include the heat flux convergence. My finding that the patterns in ELA changes are similar between these two mass-balance models suggests that dynamic heat flux convergence is at best only a small contributor to the discrepancies between the GCMs. This is consistent with observations of the modern climate in which dynamic heat flux convergence is only a small term in the local energy budget in summertime climates (e.g., Peixoto and Oort, 1992)

The connection between the changes in radiation and the temperature response at the surface can be seen by analyzing the terms in the surface energy balance. Figures 4.7 and 4.8 show the mean changes in the energy balance components for all models and the variability in the models. The decrease in temperatures in the

northern and western zones is due to the decrease in the longwave radiation flux (Figure 4.7b). This is consistent with the results in Chapter 3 that suggested continental interiors are slave to changes in radiative forcing. In addition, the index of variability is less than one for these regions, suggesting the change in longwave radiation predicted by these models is robust. This radiative cooling is due, at least in part, to a decrease in cloud faction (Figure 4.9a). The role of clouds is discussed further after presentation of the energy balance results for the eastern zone.

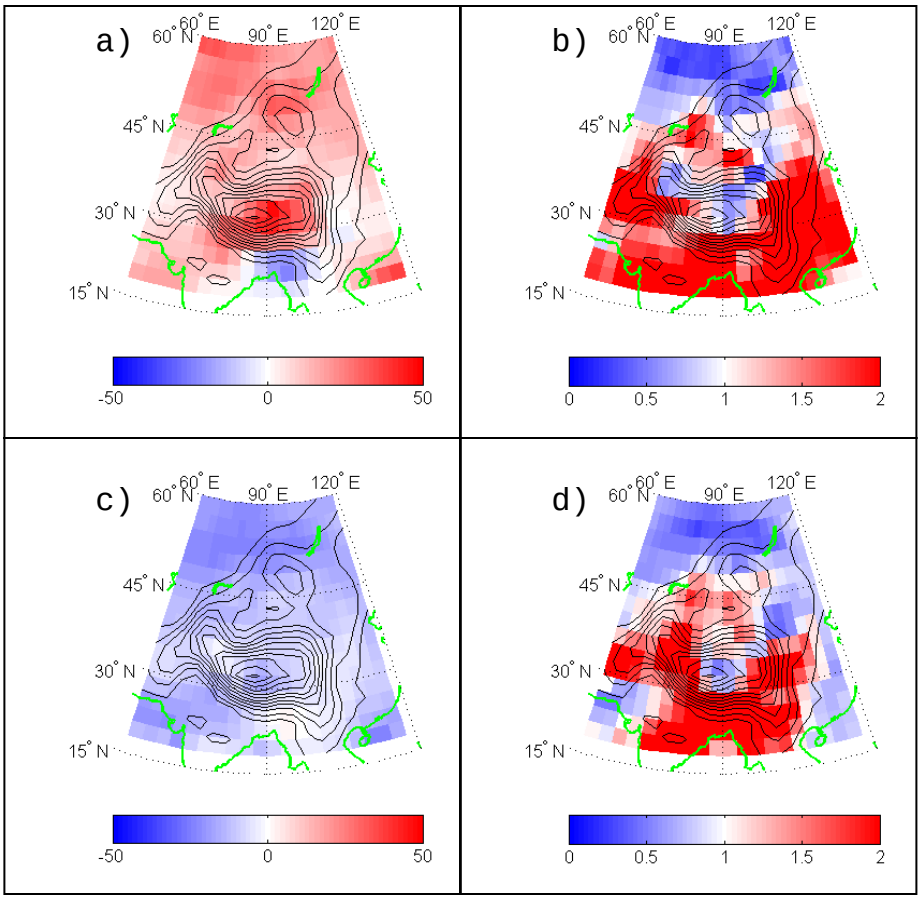

Figure 4.7: The mean and index of variability for 12 GCMs for changes in summertime shortwave radiation (W m^{-2}) (a,b) and summertime longwave radiation (W m^{-2}) (c,d).

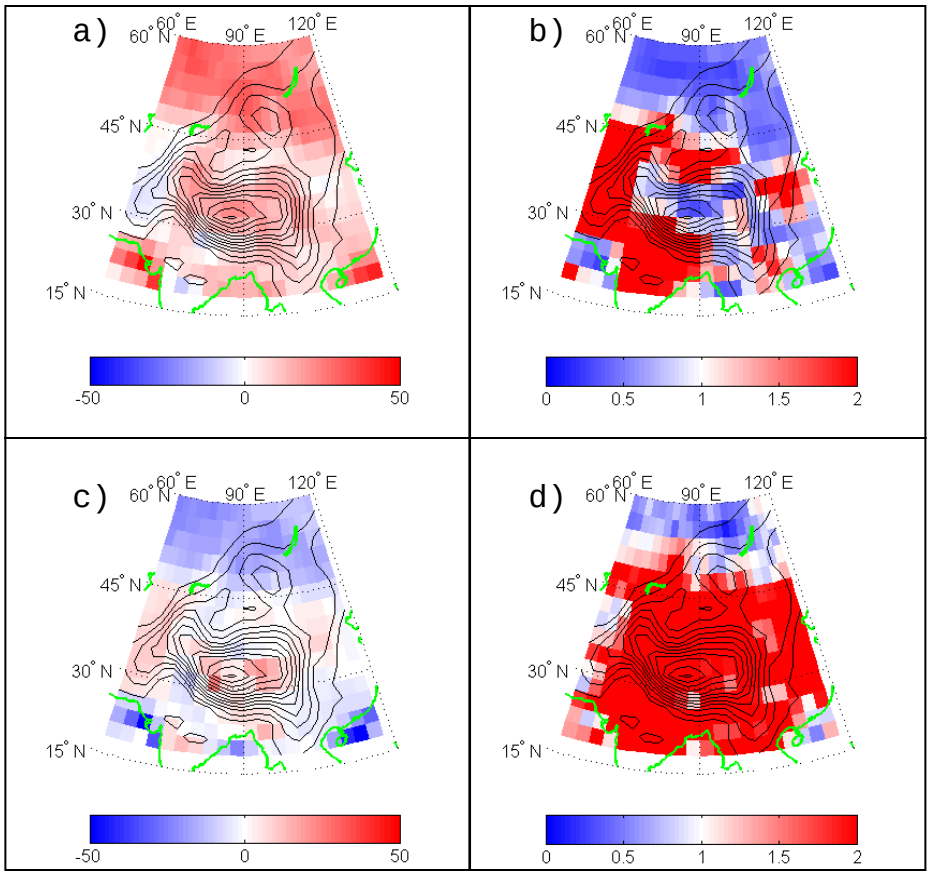

Figure 4.8: The mean change and index of variability for 12 GCMs for changes in summertime latent heat flux (W m^{-2}) (a,b) and summertime sensible heat flux (W m^{-2}) (c,d).

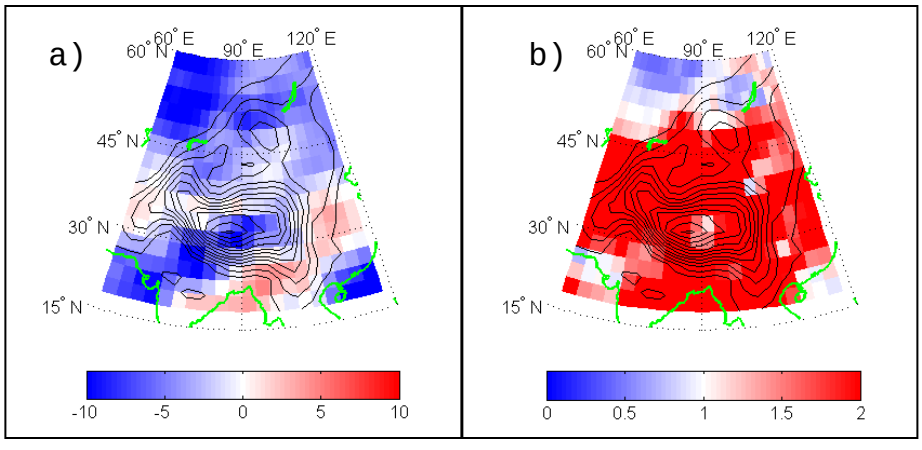

Figure 4.9: The mean change in cloud fraction (%, a) and the index of variability for summertime cloud fraction (b) for 12 GCMs.

On average, the temperature decrease in the eastern zone is largely due to the increase in cloud fraction, which decreases the incident shortwave radiation (Figure 4.7a). However, the result in the southern Himalayas is more variable than in the northern and western zones. In particular, even where the sign of the temperature change is consistent, the reason for that change varies from model to model. In some simulations for example, the decrease in temperature is largely due to a decrease in longwave radiation. In others, the decrease in temperature is due to a decrease in shortwave radiation. In a few instances, such as the BMRC-2 GCM, there is even an increase in temperature resulting from a large increase in shortwave radiation (decrease in cloud fraction). Results in Chapters 2 and 3 highlight the idea that changes in temperature and precipitation in the eastern zone and the southern Himalayas are due to the dynamic response of the monsoon to radiative changes in the continental interior. The variability in the temperature changes and causes of those changes between models suggests that the response of the monsoon to LGM boundary conditions is highly variable between models. I do not diagnose the reasons for the monsoon variability in the GCMs. However, in modern climate, the monsoon intensity and duration is influenced by numerous factors, some of which include the land-sea temperature contrast, snow cover, and the El Nino Southern Oscillation (Barnett et al., 1988; Cohen and Rind, 1990; Wang et al., 2000; Gong et al., 2002; Barlow et al., 2002; Tippett et al., 2003). The monsoon response in the GCMs to LGM boundary conditions therefore likely depends on the exact response of these factors to LGM boundary conditions. For

example, differences in snow pack between the GCMs, and differences in the atmospheric circulation sensitivity to changes in snow pack, will give rise to differences in monsoon induced changes in precipitation and temperature.

The differences in the pattern in temperature changes discussed in Section 4.3 are due, at least in part, to the large variability in cloud fraction. Figure 4.9b illustrates the variability in cloud fraction between the models. For much of Central Asia, the index of variability is greater than one. The differences in cloud fraction, and the resulting influence on the shortwave and longwave radiation fluxes, gives rise to the variability in the pattern in temperature changes across Central Asia. Therefore, while the decrease in CO_2 at the LGM will tend to cool the climate, variability in cloudiness between different models can either amplify or diminish this cooling.

The analysis of the energy balance components gives rise to 3 important results. First, the pattern in temperature changes across Central Asia are the result of the pattern in longwave and shortwave radiation fluxes. In the northern and western zones, the decrease in cloud fraction decreases the downwelling longwave radiation resulting in a general cooling across those zones. In the eastern zone, the temperature change is variable between the models due to variability in both the shortwave and longwave radiation fluxes. Second, the model differences in

simulated temperature and radiative fluxes are due, at least in part, to the differences in cloud fraction changes between the models.

4.7: Summary and Discussion

4.7.1 Summary

I have shown that the decrease in temperature in the northern zone for 21 ka compared to present day is consistent for all PMIP GCM simulations. This suggests that the temperature changes are a robust response of climate to changes in LGM boundary conditions. This temperature decrease is due to a large decrease in longwave radiation flux. In the eastern zone and the western Himalayas, the changes in temperature are more variable between the models, and the causes of these temperature changes also varies from one model to the next. This suggests that the response of the monsoon regions to changes in LGM boundary conditions is more variable between models. The pattern in temperature changes for all regions is due, at least in part, to the pattern in cloud fraction.

Precipitation changes in the western and eastern zones are also highly variable between models, again suggesting uncertainty in the monsoonal response to changes in LGM boundary conditions. In the northern zone, the decrease in

precipitation is robust and probably due to the decrease in temperatures, and is consistent with the decrease in clouds.

The pattern in climate changes gives rise to patterns in ELA changes. In particular, I have shown that the changes in ELAs across Central Asia are due to the changes in temperature. This result is confirmed by both the simpler PDD approach to estimating ablation and the surface energy and mass-balance model.

4.7.2 Discussion

The records of past ELAs suggest that in the northern zone ELAs at the LGM were lower than today and at least as large as during the pre-LGM (e.g., Merle et al., 2000; Clark et al., 2001; Shi, 2002). By comparison, ELAs in the western zone at the LGM were smaller than at the pre-LGM and probably restricted to cirques (e.g., Koppes et al., 2003; Phillips et al., 2000; Clark et al., 2001; Owen et al., 2001; Barnard et al., 2004). All GCMs indicate large decreases in temperature in western zone. This results in a large lowering of modeled ELAs in the west which is contrary to the geomorphic evidence of glacier length and ELA changes. Assuming that the paleo-ELAs in the western zone are reliable, the GCMs are overestimating the temperature decrease in the western region. This may be due to the large uncertainty in clouds in that region. It is also possible that sublimation was more important in that region than the SEMB model suggests –

in that case even small changes in precipitation would have a large impact on ELAs.

While the paleoclimate data highlight regions where GCMs may be less reliable, the GCMs and ELA model results can point to regions where more paleoclimate data are needed to accurately reconstruct past climates. For example, some studies suggest that LGM glaciers in the eastern zone were extensive while others find evidence of large LGM glaciers lacking (e.g., Schafer et al.,2002; Shi, 2002; Owen et al., 2003). Modeled temperature and ELA changes are also most variable in the eastern zone of Central Asia. These results suggest that there is a great need for additional dates in the eastern zone in order to reconstruct both the glacial and climate histories in that region.

As in the case for the early Holocene, there are conflicting explanations of glacier advances at the LGM in the eastern zone (Chapter 1.4.2). While there is variability in modeled ELA changes to changes in simulated climates, my results suggest that changes in ELAs in the Southern Himalaya are the result of changes in temperature, not monsoonal precipitation. These glacier records, therefore, highlight the need for a good physical model to test the sensitivity of a given climate proxy to climate change.

The consistency between all GCM simulations for 6 ka reinforces confidence that the model results are a robust response of the climate to the changes in insolation forcing. Conversely, the inconsistency between GCM simulations for 21 ka in the Southeast Asian monsoon region suggests the models are less reliable when there are large changes in boundary conditions. It has been shown that the monsoon has a complicated dependency on numerous factors such as the land-sea temperature contrast, snow cover, and ENSO (Barnett et al., 1988; Cohen and Rind, 1990; Wang et al., 2000; Gong et al., 2002; Barlow et al., 2002; Tippett et al., 2003). Understanding the exact reasons for the variability between GCMs will necessarily require diagnosing the model changes and sensitivity to those factors that influence the intensity and duration of the monsoon. These results, therefore, suggest an important area where further research is needed.

4.8 Notes to Chapter Four

Ambach W, Kuhn M, 1985: Accumulation gradients in Greenland and mass balance response to climatic changes. Z Gletscherkd Glazialgeol, 21, 311-317.

Barlow M, Cullen H, Lyon B, 2002: Drought in Central and Southwest Asia: La Nina, the warm pool, and Indian Ocena precipitation. Journal of Climate, 15: 697-700.

Barnard P, Owen L, Finkel R, 2004: Style and timing of glacial and paraglacial sedimentation in a monsoon-influenced high Himalayan environment, the upper Bhagirathi valley, Gavhwal Himalaya. Sedimentary Geology, 165: 199-221.

Barnett T, Dumenil L, Schlese U, Rockner E, 1988: The effect of Eurasian snow cover on global climate. Science, 239: 504-507.

Berger A, Loutre MF, 1991: Insolation values for the climate of the last 10,000,000 years. Quaternary Science Reviews, 10 (4): 297.

Bonfils CJ, Lewden D, Taylor KE, 1998: Documentation of the PMIP models. PMCI Report.

Braithwaite RJ, 1995: Positive degree-day factors for ablation on the Greenland ice-sheet studied by energy-balance modeling. Journal of Glaciology, 41 (137): 153-160.

Clark D, Gillespie A, Bierman P, Caffee M, 2001: Glacial asynchrony in the Kunlun Shan, northwestern Tibet. Abstracts with Programs – Geological Society of America, 33 (6): 441.

Gong G, Entekhabi D, Cohen J, 2002: Modeled northern hemisphere winter climate response to realistic Siberian snow anomalies. Journal of Climate, 16: 3917-3932.

Koppes MN, Gillespie AR, Burke RM, Thompson SC, Clark DH, 2003: Late Quaternary glaciation in northern Central Asia. XVI INQUA Congress, Programs with Abstracts, Reno, July, p. 156.

Merle J, Carson R, Cady J, Hinz N, 2000: Quaternary geology of the Tengis_Shishid Gol region, Khovsgo, Mongolia. Anonymous Abstracts with Programs- Geological Society of America, 33 (3): 67.

Owen LA, Gualtieri L, Finkel RC, Caffee MW, Benn DI, Sharma MC, 2001: Cosmogenic radionuclide dating of glacial landforms in the Lahul Himalaya, northern India: defining the timing of Late Quaternary glaciation. Journal of Quaternary Science, 16 (6): 555-563.

Owen LA, Finkel RC, Haizhou M, Spencer JQ, Derbyshire E, Barnard PL, Caffee MW, 2003: Timing and style of Late Quaternary glaciation in northeastern Tibet. Geological Society of America Bulletin, 115 (11): 1356-1364.

Peixoto JP, Oort AH, 1992: Physics of Climate. American Institute of Physics, New York: 520.

Peltier W, 1994: Ice-age paleotopography. Science, 265 (5169): 195-201.

Phillips WM, Sloan VF, Shroder JF, Sharma P, Clarke ML, Rendell HM, 2000: Asynchronous glaciation at Nanga Parbat, northwestern Himalaya Mountains, Pakistan. Geology, 28 (5): 431-434.

Rupper and Roe, 2007: Glacier changes and regional climate: a mass and energy balance approach. In preparation.

Schafer JM, Tschudi S, Zhao ZZ, Wu XH, Ivy-Ochs S, Wieler R, Baur H, Kubik PW, Schluchter C, 2002: The limited influence of glaciations in Tibet on global climate over the past 170 000 yr. Earth and Planetary Science Letters, 194 (3-4): 287-297.

Shi Y, 2002: Characteristics of late Quaternary monsoonal glaciation on the Tibetan Plateau and in East Asia. Quaternary International, 97-8: 79-91.

Tippett M, Barlow M, Lyon B, 2003: Statistical correction of Central Southwest Asia winter precipitation simulations. International Journal of Climatology, 23: 1421-1433.

Wang B, Wu R, Fu X, 2000: Pacific-East Asian teleconnectoin: How does ENSO affect East Asian climate? Journal of Climate, 13: 1517-1536.

Chapter Five

GLACIER CHANGES AND REGIONAL CLIMATE: A SYNOPSIS

5.1 Summary

A surface-energy and mass-balance (SEMB) model has been developed to explore the relationship between glacier equilibrium-line altitudes (ELAs) and climate at a regional scale. The model is applied to central Asia because of its wide range of climatic conditions and spatial patterns in the glacial history. Central Asia is divided into three separate zones, which are defined based on the glacial history (Figures 1.1 and 2.1).

The western zone extends from the Kyrgyz Tien Shan south to the Karakoram and east to central Tibet. In this region the largest advances occurred during the pre-LGM (30 – 70 ka) with little evidence for large advances during the Last Glacial Maximum (LGM) (e.g., Phillips et al., 2000; Clark et al., 2001; Owen et al., 2002; Finkel et al., 2003; Koppes et al., 2003; Barnard et al., 2004; Abramowski et al., 2006). In contrast, the glaciers in the northern zone (central Mongolia to the Tien Shan of Xinjiang, China) advanced during the LGM, synchronously with the high-latitude ice sheets, although there are published dates that push the western boundary of this zone closer to the Mongol border (e.g., Merle et al., 2000; Clark

et al., 2001; Shi, 2002). Although there is evidence for large pre-LGM and LGM advances in the southern Himalayas around the areas of eastern Nepal and Tibet (southern zone), evidence for a large early Holocene (9 ka) advance distinguishes it from the rest of Central Asia (e.g., Schafer et al, 2002; Shi, 2002; Owen et al., 2003; Wei et al., 2006). This dissertation focuses on explaining the ELA changes for changes in climate in these three zones for modern interannual climate variability, the mid-Holocene (6 ka), and the Last Glacial Maximum (LGM, 21 ka).

In Chapter 2 I show that the SEMB model captures the pattern in absolute ELAs quite well, the seasonal cycle in energy balance terms are comparable to studies on individual glaciers in Central Asia, and the proportionality factor relating melt to positive degree days (calculated using the SEMB model) is within the range of those reported for individual glaciers within the area (Calanca and Heuberger, 1990; Kayastha et al., 1999; Kayastha et al., 2002; Zhang et al, 2006). In addition, the magnitude of the model parameters does not significantly influence the sensitivity of the ELA to changes in climate (Appendix B). These results together suggest that the SEMB model performs well and is capable of capturing the sensitivity of ELAs to changes in climate at a regional scale.

With this model in hand, I am able to address the three questions posed in the introduction of this dissertation: (1) can we understand the relative importance of

accumulation and ablation in controlling mass balance of glaciers at regional scales, (2) how do the observed patterns of glacier response reflect regional changes in climate, and (3) do these patterns in glacier advances actually reflect patterns in climate change or are they the result of differing sensitivities to changes in a particular climate variable? I summarize my main conclusions for chapters 2-4 in the context of these three questions.

5.1.1 ELA Sensitivity to Modern Interannual Climate Variability

By applying the SEMB model to modern interannual climate variability (Chapter 2), I am able to determine the patterns of ELA sensitivity across the vastly differing climates of Central Asia, and diagnose why those patterns emerge. The spatial patterns in climate across Central Asia produce a spatial pattern in the dominant ablation process. In particular, where precipitation is low, ablation at the ELA is dominated by sublimation. Conversely, where precipitation is high, ablation at the ELA is dominated by melt and surface run-off.

The ELA sensitivity to changes in climate is strongly tied to the dominant ablation process. In regions dominated by melt, the ELA is far more sensitive to interannual variability in ablation than accumulation. The change in ELA for anomalously warm summers in all regions is governed by changes in cloud fraction (and the associated changes in shortwave and longwave radiation) and the

amplitude in the seasonal cycle in air temperature. ELAs in sublimation regions however, are far more sensitive to changes in precipitation than to changes in ablation. Additionally, ELAs in sublimation-dominated regions are more sensitive to changes in humidity and wind speed than are ELAs in melt-dominated regions.

The sensitivity of ELAs to modern interannual climate variability provides insight into the magnitude of climate changes required by the paleoclimate data. The sensitivity of ELAs in melt-dominated regions to changes in temperature (or those variables that conspire to change temperature) suggests that the paleo-ELAs are likely a record of past temperature changes as well. I reconcile the spatial pattern in ELA changes for the mid-Holocene and LGM in Chapters 3 and 4.

Eighteen GCM simulations using boundary conditions appropriate for the present day, 6 ka, and 21 ka were acquired from PMIP and used as input in two ELA models. The first of these models uses a positive degree day approach to estimate ablation (Braithwaite, 1995) and a modified version of the Ambach and Kuhn (1985) ELA perturbation method to calculate changes in ELA. As such, this model was used to assess the relative importance of temperature and precipitation on ELA changes in Central Asia. The second model is the SEMB model that incorporates changes in all relevant atmospheric variables and seeks the ELA (Chapter 2). While assumptions and simplifications in the model formulations

must be made, due in large part to the coarse grid (typically 2.5° to 5°) and temporal resolution (monthly) of the GCM output, these were found not to significantly change the main conclusions.

5.1.1 Mid-Holocene ELA and Climate Changes

In Chapter 3 I focus on explaining the relationship between Central Asian climate and early Holocene glacier history. I also place particular emphasis on understanding the advance of glaciers in the eastern zone. The early Holocene glacier history in the eastern zone is unusual as the glaciers advanced despite it being a time of a relative maximum in insolation during the Northern Hemisphere summer (e.g., Crowley and North 1988).

Both ELA models clearly show that the lowering of ELAs in the southern Himalayas, a region dominated by melt, is largely due to a decrease in summer temperatures during the Holocene, and that the increase in precipitation accounts for, at most, 30% of the total ELA changes. In the melt-dominated regions of the western and northern zones, both ELA models show a rise in ELAs in response to a general increase in temperatures. Importantly, these results suggest that there is regional variability in the climate's response to the increase in northern hemisphere summer insolation, and that the regional variability in glacier changes in Central Asia is largely explained by the resulting temperature pattern in the

melt-dominated regions. Sublimation dominates the ablation in small areas in the northern and western zones. In these sublimation-dominated regions, the SEMB model shows that ELAs are acutely sensitive to changes in precipitation. Thus the sensitivity of the ELAs to changes in climate depends on the dominant ablation process.

Through a detailed evaluation of the energy balance at the surface, I was able to explain the pattern in temperature changes in Central Asia. The increase in summer temperatures in the more northern regions of Central Asia is a direct radiative response to the increase in solar insolation at 6 ka, and is consistent with other studies showing temperatures in continental interiors slave to radiation changes (e.g., Felzer et al. 1995). The temperature decrease in the more southern regions, on the other hand, is a dynamic response to the increase in temperatures in the interior. In particular, the increase in land-sea temperature contrast intensifies the monsoonal circulation. This results in an increase in precipitation as well as a substantial increase in cloudiness over the southern region. The decrease in summer temperatures is the result of both a decrease in shortwave radiation due to the increase in cloudiness (and a resulting increase in albedo) and an increase in evaporative cooling.

The consistency between all GCMs reinforces confidence that the model results are a robust response of the climate to the changes in insolation forcing. In the

case for Central Asia, spatial patterns in climate occur in response to a relatively uniform increase in solar insolation at the top of the atmosphere. The patterns in glacier advances across Central Asia are a result of the spatial variability in the climate response. This suggests that spatial patterns in climate and glaciers should be expected even in cases where there is a uniform change in forcing (e.g., increasing CO_2). In addition, and in contrast to previous work, my results suggest that the advance of glaciers in the Southern Himalaya is a result of a combination of factors, not just increased precipitation.

5.1.2 LGM ELA and Climate Changes

Whereas focusing on the Holocene primarily addresses how ELAs change in response to changes in insolation, the LGM provides a test for how ELAs change in response to changes in CO2, SSTs, and the presence of land-ice. In Chapter 4 I focus on explaining the relationship between Central Asian climate and the LGM glacier history.

Temperatures decrease in all three zones at 21 ka relative to the present day. I show that the decrease in temperatures in the northern zone for 21 ka compared to present day is consistent for all PMIP GCM simulations. This suggests that the temperature changes are a robust response of climate to changes in LGM boundary conditions. This temperature decrease is due to a large decrease in

longwave radiation flux. In the eastern zone and the western Himalayas, the changes in temperature are more variable between the models, and the causes of these temperature changes also varies from one model to the next. This contrasts with the mid-Holocene results, where the temperature changes are robust in all three regions. The pattern in temperature changes for all regions is due, at least in part, to the pattern in cloud fraction through its influence on the radiative fluxes.

Precipitation changes in the western and eastern zones are also highly variable between models. For the eastern zone, the variability in precipitation between models again suggests uncertainty in the monsoonal response to changes in LGM boundary conditions. The variability in the western zone may be due to variability in GCM simulations of the response of the Mediterranean storm track to LGM boundary conditions. In the northern zone, the decrease in precipitation is robust and probably due to the decrease in temperatures, and is consistent with the decrease in clouds.

The pattern in climate changes at the LGM gives rise to patterns in ELA changes. In particular, I have shown that the changes in ELAs across Central Asia are due to the changes in temperature. This result is confirmed by both the simpler PDD approach to estimating ablation and the surface energy and mass-balance model.

5.2 Future Research Directions

There are numerous potential applications of the current formulation of the SEMB model. Additionally, while the current framework provides a useful tool for exploring regional-scale interactions between glaciers and climate, the results of this dissertation also point towards ways in which to expand upon this research. A few examples of applications of the SEMB and new research directions that follow from this dissertation are discussed below.

There are many potential applications of the current formulation of the SEMB model. First, it can obviously be used to ascertain the relative importance of sublimation versus melt and to test the sensitivity of glaciers to possible changes in climate at a regional scale anywhere in the world. For example, the mesoscale climate model (MM5) provides high resolution climate output. Using this model, I can test the sensitivity of glaciers in the Pacific Northwest of the United States to changes in atmospheric variables, and compare these results to the coarser resolution reanalysis climatology and GCM output. In addition there is a wealth of data on past glacier advances and retreats in the Pacific Northwest. GCM simulations can be used as input in the SEMB model to determine the mechanisms giving rise to past glacier changes and reconcile the patterns in climate changes with ELA changes. The sensitivity of ELAs to changes in the

maritime climate of the Pacific Northwest would provide an interesting comparison to the climates of the south Indian monsoon and continental interior of Central Asia. Care must be taken to be sure that the model parameters chosen are appropriate for the region of interest.

Second, I use the SEMB model to test the tendency of ELAs to changes in climate forcings and boundary conditions, such as orbitally induced changes in solar insolation 6 ka. This can be done for other times in the past as well, such as the Little Ice Age and Medievel Warm Period. The recent retreat of glaciers across the globe has been attributed to the current global warming. I am also keen to use this model to determine what atmospheric variables have contributed the most to the regional changes in ELAs seen around the globe over the last Century.

Finally, it may be possible to couple this model to simple glacier length models to test the sensitivity of glacier length to changes in bed geometry as well as climate. For example, Fountain et al. (1999) show that the differences in glacier length changes between the southern and northern areas of the Sierra Nevada are due to both patterns in climate change and differences in bed geometry. Fountain et al. (1999) apply their 2D glacier model and simple temperature-ablation model to a limited number of basins. This assumes that the chosen basins have both characteristic bed geometries and climate changes of the larger regions of interest. It may be possible to expand upon their work by taking a more regional-scale

approach akin to this dissertation. For example, it might be possible to define the regional-scale glacier bed geometry by calculating the bed geometry using a high resolution DEM and averaging that geometry per GCM grid point. In other words, I may be able to define characteristic bed geometries on a grid-scale equivalent to the climate simulations being used. Then I would be able to couple the regional-scale SEMB model to a simple glacier length model (such as that popularized by Oerlemans et al. (1998)) which incorporates the regional-scale bed geometry. In this way, I would be able to apply the same regional-scale approach to reconciling glacier changes and climate as in this dissertation, but take into account spatial patterns in glacier length due to patterns in bed geometry as well as climate.

The current formulation of the SEMB model is appropriate for the level of the approach taken in this dissertation, and in the above examples. However, any single glacier will be susceptible to numerous local factors, and may respond differently to climate than the larger-scale patterns would suggest. Capturing ELA sensitivities at smaller spatial scales would require a higher level of accuracy than the current model formulation allows. For example, latent heat flux due to melt percolation and refreeze is ~10-20 W m^{-2}. A change in albedo equal to 0.1 would result in a change in shortwave radiation of the same order magnitude. Thus a model capable of higher accuracy would necessarily include all variables that would have a similar or greater influence on the energy balance as albedo

variations. An atmospheric column model with internally derived snow pack would be capable of this level of detail. The next logical step to this study is to apply such a model to selected grid points within the larger region of interest here and to test the sensitivity of the ELAs at smaller scales to changes in these higher-order parameters. This would give insight into how different the sensitivity of any single glacier may be within the larger regions.

Interestingly, there is a fairly narrow transition of only one or two reanalysis grid points between the sublimation-dominated and melt-dominated regions of Central Asia. This suggests the ELA sensitivity in those transitional regions can quickly change in response to small changes in climate. Glaciers in these regions are close to a threshold where a small change in climate would result in rapid growth or demise of the glacier. Further sensitivity tests, using a column model coupled to a snow pack model, focused specifically on these transitional regions would give insights into likely climates where glaciers are close to a threshold and the magnitude of climate changes required to push these glaciers from sublimation to melt-dominated regimes, or vice versa.

5.3 Discussion

Numerous studies have focused on diagnosing the response of glaciers to changes in climate. This study developed a framework capable of assessing the sensitivity

of ELAs to changes in climate at a regional-scale, and at a first-order level of detail. This framework extends previous work by revealing spatial scales of climate-driven dependencies of glaciers. The results also suggest directions for future research on glacier-climate interactions.

By applying the model to modern interannual climate variability, I was able to determine the patterns of ELA sensitivity across the vastly differing climates of Central Asia, and diagnose why those patterns emerge. The sensitivity of ELAs to modern interannual climate variability can be used as an analog for understanding past changes in glacier mass balance, as well as a predictor of the response of glaciers to future changes in climate. For example, I use this same model to calculate changes in ELAs between the present day and the mid-Holocene and LGM, and to reconcile the pattern in ELA changes with the changes in climate in Central Asia (Rupper et al., 2007). In melt-dominated regions of Central Asia, the ELAs are most sensitive to changes in ablation for modern interannual climate variability, 6ka, and 21 ka. These results are in contrast to previous studies which often suggest that the glacier changes in the southern Himalayas are due to changes in monsoonal precipitation.

Paleoclimate proxy records must be used to extend the climate record beyond the modern instrumental record, which is essential for determining the mechanisms giving rise to natural climate variability. The glacier records in Central Asia

highlight the need for a good physical model to test the sensitivity of a given climate proxy to climate change. Such models can be used to determine whether a suggested mechanism that is consistent with the record is a) a unique answer, and b) of sufficient magnitude to impart the recorded signal. Importantly, the results from this dissertation suggest that for both past and future climate scenarios, where patterns in climate persist, patterns in ELAs and ELA sensitivities should be the expectation as well.

5.4 Notes to Chapter Five

Abramowski U, Bergau A, Seebach D, Zech R, Glaser B, Sosin P, Kubik PW, Zech W, 2006: Pleistocene glaciations of Central Asia: results from Be-10 surface exposure ages of erratic boulders from the Pamir (Tajikistan), and the Alay-Turkestan range (Kyrgyzstan). Quaternary Science Reviews, 25 (9-10): 1080-1096.

Ambach W, Kuhn M, 1985: Accumulation gradients in Greenland and mass balance response to climatic changes. Z Gletscherkd Glazialgeol, 21, 311-317.

Barnard P, Owen L, Finkel R, 2004: Style and timing of glacial and paraglacial sedimentation in a monsoon-influenced high Himalayan environment, the upper Bhagirathi valley, Gavhwal Himalaya. Sedimentary Geology, 165: 199-221.

Braithwaite RJ, 1995: Positive degree-day factors for ablation on the Greenland ice-sheet studied by energy-balance modeling. Journal of Glaciology, 41 (137): 153-160.

Calanca P, Heuberger R, 1990: Glacial Climate Research in the Tianshan. Zürcher Geogrische Schriften, 39, 60-72.

Clark D, Gillespie A, Bierman P, Caffee M, 2001: Glacial asynchrony in the Kunlun Shan, northwestern Tibet. Abstracts with Programs – Geological Society of America, 33 (6): 441.

Crowley TJ, North GR, 1988: Abrupt climate change and extinction events in earth history. Science, 240 (4855): 996-1002.

Felzer B, Oglesby RH, Shao H, Webb T, Hyman DE, Prell WL, and Kutzbach JE, 1995: A systematic study of GCM sensitivity to latitudinal changes in solar-radiation. Journal of Climate, 8 (4): 877-887.

Finkel RC, Owen, L, Barnard P, Caffee M, 2003: Beryllium-10 dating of Mount Everest moraines indicates a strong monsoon influence and glacial synchroneity throughout the Himalaya. Geology, 31 (6): 561-564.

Fountain AG, Lewis KJ, Doran PT, 1999: Spatial climatic variation and its control on glacier equilibrium line altitude in Taylor Valley, Antarctica. Global and Planetary Change, 22 (1-4): 1-10.

Kayastha RB, Ageta Y, Fujita K, 2002: Use of positive degree-day method for calculating snow/ice melting and discharge from glacierized basins in Nepal. EGS XXVII General Assembly, abstract #3520.

Kayastha RB, Ohata T, Ageta Y, 1999: Application of a mass-balance model to a Himalayan glacier. Journal of Glaciology, 45 (151): 559-567.

Koppes MN, Gillespie AR, Burke RM, Thompson SC, Clark DH, 2003: Late Quaternary glaciation in northern Central Asia. XVI INQUA Congress, Programs with Abstracts, Reno, July, p. 156.

Merle J, Carson R, Cady J, Hinz N, 2000: Quaternary geology of the Tengis_Shishid Gol region, Khovsgo, Mongolia. Anonymous Abstracts with Programs- Geological Society of America, 33 (3): 67.

Oerlemanns J, Anderson B, Hubbard A, Huybrechts P, Johannesson T, Knap WH, Schmeits M, Stroeven AP, van de Wall RSW, Wallinga J, Zuo Z, 1998: Modelling the response of glaciers to climate warming. Climate Dynamics, 14 (4): 267-274.

Owen LA, Kamp U, Spencer JQ, Haserodt K, 2002: Timing and style of Late Quaternary glaciation in the eastern Hindu Kush, Chitral, northern Pakistan: a review and revision of the glacial chronology based on new optically stimulated luminescence dating. Quaternary International, 97-8: 41-55.

Owen LA, Finkel RC, Haizhou M, Spencer JQ, Derbyshire E, Barnard PL, Caffee MW, 2003: Timing and style of Late Quaternary glaciation in northeastern Tibet. Geological Society of America Bulletin, 115 (11): 1356-1364.

Phillips WM, Sloan VF, Shroder JF, Sharma P, Clarke ML, Rendell HM, 2000: Asynchronous glaciation at Nanga Parbat, northwestern Himalaya Mountains, Pakistan. Geology, 28 (5): 431-434.

Rupper SB, Roe G, and Gillespie G, 2007: Spatial patterns of Holocene glacier advance and retreat in Central Asia. In preparation.

Schafer JM, Tschudi S, Zhao ZZ, Wu XH, Ivy-Ochs S, Wieler R, Baur H, Kubik PW, Schluchter C, 2002: The limited influence of glaciations in Tibet on global climate over the past 170 000 yr. Earth and Planetary Science Letters, 194 (3-4): 287-297.

Shi Y, 2002: Characteristics of late Quaternary monsoonal glaciation on the Tibetan Plateau and in East Asia. Quaternary International, 97-8: 79-91.

Wei Z, Zhijiu C, Yanghua L, 2006: Review of the timing and extent of glaciers during the last glacial cycle in the bordering mountains of Tibet and in East Asia. Quaternary International, 154-155: 32-43.

Zhang Y, Shiyin L, Yongjian D, 2006: Observed degree-day factors and their spatial variation on glaciers in western China. Annals of Glaciology, 43, 301-306.

BIBLIOGRAPHY

Abramowski U, Bergau A, Seebach D, Zech R, Glaser B, Sosin P, Kubik PW, Zech W, 2006: Pleistocene glaciations of Central Asia: results from Be-10 surface exposure ages of erratic boulders from the Pamir (Tajikistan), and the Alay-Turkestan range (Kyrgyzstan). Quaternary Science Reviews, 25 (9-10): 1080-1096.

Ambach W, Kuhn M, 1985: Accumulation gradients in Greenland and mass balance response to climatic changes. Z Gletscherkd Glazialgeol, 21, 311-317.

Anders A, Roe G, Hallet B, Montgomery D, Finnegan N, Putkonen J, 2006: Spatial Patterns of Precipitation and Topography in the Himalaya, *In* Willett SD, Hoovius N, Brandon MT, and Fisher DM, eds., Tectonics, climate and landscape evolution,GSA Special Paper 398, Chapter 3: 39-53.

Anderson DM, Prell WL, 1993: A 300 kyr record of upwelling off Oman during the late Quaternary – evidence of the Asian southwest monsoon. Paleoceanography, 8 (2): 193-208.

Araguas-Araguas L, Froehlich K, Rozanski K, 1998: Stable isotope composition of precipitation over southeast Asia. Journal of Geophysical Research, 103 (D22): 28721-28742.

Arendt AA, Echelmeyer KA, Harrison WD, Lingle CS, Valentine VB, 2002: Rapid wastage of Alaska glaciers and their contribution to rising sea level. Science, 297 (5580): 382-386.

Barlow M, Cullen H, Lyon B, 2002: Drought in Central and Southwest Asia: La Nina, the warm pool, and Indian Ocena precipitation. Journal of Climate, 15: 697-700.

Barnard P, Owen L, Finkel R, 2004: Style and timing of glacial and paraglacial sedimentation in a monsoon-influenced high Himalayan environment, the upper Bhagirathi valley, Gavhwal Himalaya. Sedimentary Geology, 165: 199-221.

Barnard P, Owen L, Finkel R, 2004: Style and timing of glacial and paraglacial sedimentation in a monsoon-influenced high Himalayan environment, the upper Bhagirathi valley, Gavhwal Himalaya. Sedimentary Geology, 165: 199-221.

Barnett T, Dumenil L, Schlese U, Rockner E, 1988: The effect of Eurasian snow cover on global climate. Science, 239: 504-507.

Benn DI, Owen LA, 1998: The role of the Indian summer monsoon and the mid-latitude westeries in Himalayan glaciation: review and speculative discussion. Journal of the Geological Society, 155 (2): 353-363.

Berger A, Loutre MF, 1991: Insolation values for the climate of the last 10,000,000 years. Quaternary Science Reviews, 10 (4): 297.

Bolton, D, 1980: The computation of equivalent potential temperature. Monthly Weather Review, 108: 1046-1053.

Bonfils CJ, Lewden D, Taylor KE, 1998: Documentation of the PMIP models. PMCI Report.

Braconnot P, Loutre MF, Dong B, Joussaume S, Valdes P, 2002: How the simulated change in monsoon at 6 ka BP is related to the simulation of the modern climate: results from the Paleoclimate Modeling Intercomparison Project. Climate Dynamics, 19 (2): 107-121.

Braconnot, P., S. Joussaume, N. de Noblet, G. Ramstein, 2000: Mid-Holocene and last glacial maximum African monsoon changes as simulated within the Paleoclimate Modeling Intercomparison project. Global and Planetary Change, 26, 51-66.Bradley R, Diaz H, Kiladis G, Eischeid J, 1987: ENSO signal in continental temperatuare and precipitation records. Nature, 327 (6122): 497-501.

Bradley RS, 2000: Past global changes and their significance for the future. Quaternary Science Reviews, 19 (1-5): 391-402.

Braithwaite RJ, 1995: Positive degree-day factors for ablation on the Greenland ice-sheet studied by energy-balance modeling. Journal of Glaciology, 41 (137): 153-160.

Braithwaite RJ, Raper SCB, 2002: Glaciers and their contribution to sea level change. Physics and Chemistry of the Earth, 27 (32-34): 1445-1454.

Braithwaite RJ, Zhang Y, Raper SCB, 2003: Temperature sensitivity of the mass balance of mountain glaciers and ice caps as a climatological characteristic. Zeitschrift Fur Gletscherkunde und Glazialgeologie, 38 (1), 35-61.

Briffa, K.R., 2000: Annual climate variability in the Holocene: interpreting the message of ancient trees. Quaternary Science Review, 19: 87-105.

Briffa, K.R., P.D. Jones, F.H. Schweingruber and T.J. Osborn, 1998: Influence of volcanic eruptions on Northern Hemisphere summer temperature over the past 600 years. Nature, 393: 450-455.

Briffa, K.R., P.D. Jones, F.H. Schweingruber, S.G. Shiyatov and E.A. Vaganov, 1996: Development of a North Eurasian chronology network: Rationale and preliminary results of comparative ring-width and densitometric analyses in northern Russia. In: Tree Rings, Environment, and Humanity. Radiocarbon 1996, J.S. Dean, D.M. Meko and T.W. Swetnam (eds.). Department of Geosciences, The University of Arizona, Tucson, 25-41.

Broecker WS, 2003: Does the trigger for abrupt climate change reside in the ocean or in the atmosphere? Science 300 (5625): 1519-1522.

Burke R, Gillespie A, Bayasgalan A, Sheinkman V, Chadwick O, 2003: Late Quaternary glaciation in northern Central Asia. XVI INQUA Congress, Programs with Abstracts, Reno, July, 156.

Bush ABG, 2002: A comparison of simulated monsoon circulations and snow accumulation in Asia during the mid-Holocene and at the Last Glacial Maximum. Global and Planetary Change, 32 (4): 331-347.

Bush ABG, 2004: Modelling of late Quaternary climate over Asia: a synthesis. Boreas, 33 (2): 155-163.

Calanca P, Heuberger R, 1990: Glacial Climate Research in the Tianshan. Zürcher Geogrische Schriften, 39, 60-72.

Casal TGD, Kutzbach JE, Thompson LG, 2004: Present and past ice-sheet mass balance simulations for Greenland and the Tibetan Plateau. Climate Dynamics, 23 (3-4): 407-425.

Chiang JCH, Biasutti M, Battisti DS, 2003: Sensitivity of the Atlantic Intertropical Convergence Zone to Last Glacial Maximum boundary conditions. Paleoceanography, 18(4): 1094.

Clark D, Gillespie A, Bierman P, Caffee M, 2001: Glacial asynchrony in the Kunlun Shan, northwestern Tibet. Abstracts with Programs – Geological Society of America, 33 (6): 441.

CLIMAP, 1981: Seasonal reconstructions of the Earth´s surface at the last glacial maximum. Map Series, Technical Report MC-36, Geological Society of America, Boulder, Colorado.

Cohen J, Rind D, 1990: The effect of snow cover on the climate. Journal of Climate, 4: 689-706.

Collins WD, Valero FPJ, Flatau PJ, Lubin D, Grassl H, Pilewskie P, Spinhirne J, 1996: The radiative effects of convection in the Tropical Pacific. Journal of Geophysical Research, 101(D10):14999-15012.

Crowley TJ, North GR, 1988: Abrupt climate change and extinction events in earth history. Science, 240 (4855): 996-1002.

Dai AG, Wigley TM, 2000: Global patterns of ENSO-induced precipitation. Geophysical Research Letters, 27 (9): 1283-1286.

Denton GH, Hendy CH, 1994: Younger Dryas age advance of Franz-Josef glacier in the Southern Alps of New Zealand. Science, 264 (5164): 1434-1437.

Dong GR, Wang GY, Li XZ, Chen HZ, Jin J, 1998: Palaeomonsoon vicissitudes in eastern desert region of China since last interglacial period. Science in China Series D-Earth Sciences, 41 (2): 215-224.

Duguay, CR, 1993: Radiation modeling in the mountainous terrain – Review and status. Mountain Research and Development, 13 (4): 339-357.

Emeis KC, Anderson DM, Doose H, Kroon D, Schulzbull D, 1995: Sea-surface temperatures and the history of monsoon upwelling in the northwest Arabian Sea during the last 500,000 years. Quaternary Research, 43 (3): 355-361.

Felzer B, Oglesby RH, Shao H, Webb T, Hyman DE, Prell WL, and Kutzbach JE, 1995: A systematic study of GCM sensitivity to latitudinal changes in solar-radiation. Journal of Climate, 8 (4): 877-887.

Finkel RC, Owen, L, Barnard P, Caffee M, 2003: Beryllium-10 dating of Mount Everest moraines indicates a strong monsoon influence and glacial synchroneity throughout the Himalaya. Geology, 31 (6): 561-564.

Fountain AG, Lewis KJ, Doran PT, 1999: Spatial climatic variation and its control on glacier equilibrium line altitude in Taylor Valley, Antarctica. Global and Planetary Change, 22 (1-4): 1-10.

Gallimore R, Kutzbach J, 1989: Effects of soil-moisture on the sensitivity of a climate model to earth orbital forcing at 9000-yr-BP. Climatic Change, 14 (2): 175-205.

Ganopolski, A., S. Rahmstorf, V. Petoukhov and M. Claussen, 1998: Simulation of modern and glacial climates with a coupled global model of intermediate complexity. Nature, 391: 351- 356.

Gillespie A, Burke R, Byasgalan A, 2001: Neoglaciation in Central Asia. Abstracts with Programs- Geological Society of America, 33 (6): 442.

Gillespie A, Molnar P, 1995: Asynchronous maximum advances of mountain and continental glaciers. Reviews of Geophysics, 33 (3): 311-364.

Gillespie A, Rupper S, and Roe G, 2003: Climatic interpretation from mountain glaciations in Central Asia. Geological Society of America, Abstracts with Program 35(6).

Gong G, Entekhabi D, Cohen J, 2002: Modeled northern hemisphere winter climate response to realistic Siberian snow anomalies. Journal of Climate, 16: 3917-3932.

Grove JM, Switsur R, 1994: Glacial geological evidence for the medieval warm period. Climatic Change, 26 (2-3): 143-169.

Haeberli W, Frauenfelder R, Hoelzle M, Maisch, 1999: On rates and acceleration trends of global glacier mass changes. Geografiska Annaler Series A-Physcial Geography, 81A (4): 585-591.

Hagen JO, Kohler J, Melvold K, Winther JG, 2003: Glaciers in Svalbard: mass balance, runoff and freshwater flux. Polar Research, 22 (2): 145-159.

Hall NMJ, Valdes PJ, 1997: A GCM simulation of the climate 6000 years ago. Journal of Climate, 10 (1): 3-17.

Harris N, 2006: The elevation history of the Tibetan Plateau and its implications for the Asian monsoon. Palaeogeography Palaeoclimatology Palaeoecology, 241 (1): 4-15.

Hastenrath S, 1994: Recession of tropical glaciers. Science, 265 (5180): 1790-1791.

Hoinkes H, Steinacker R, 1975: Parameterization of climate-glacier-relation. Rivista Italiana Di Geofisica E Scienze Affini, 1: 97-104 Suppl. I.

Hoskins BJ, Hodges KI, 2002: New perspectives on the Northern Hemisphere winter storm tracks. Journal of the Atmospheric Sciences, 59 (6) 1041-1061.

Intergovernmental Panel on Climate Change, 2001: The scientific basis.

Joussaume S, Taylor K, 2001: The paleoclimate model intercomparison project. Proceedings from the third PMIP workshop.

Joussaume S, Taylor KE, Braconnot P, Mitchell JFB, Kutzbach JE, Harrison SP, Prentice IC, Broccoli AJ, Abe-Ouchi A, Bartlein PJ, Bonfils C, Dong B, Guiot J, Herterich K, Hewitt CD, Jolly D, Kim JW, Kislov A, Kitoh A, Loutre MF, Masson V, McAvaney B, McFarlane N, de Noblet N, Peltier WR, Peterschmitt JY, Pollard D, Rind D, Royer JF, Schlesinger ME, Syktus J, Thompson S, Valdes P, Vettoretti G, Webb RS, Wyputta U, 1999: Monsoon changes for 6000 years ago: Results of 18 simulations from the Paleoclimate Modeling Intercomparison Project (PMIP). Geophysical Research Letters, 26 (7): 859-862.

Ju Y, 2004: Glacial advance/retreat and climate change in the middle part of North-Tianshan. Doctoral Thesis, pp.34-37.

Kageyama, M., P. J. Valdes, G. Ramstein, C. Hewitt and U. Wyputta, 1999: Northern hemisphere storm-tracks in present day and last glacial maximum climate simulations: a comparison of the European PMIP models. Journal of Climate, 12, 742-760.

Kageyama M, Valdes P, 2000: Impact of the North American ice-sheet orography on the Last Glacial Maximum eddies and snowfall. Geophysical Research Letters, 27 (10): 1515-1518.

Kalnay E, Kanamitsu M, Kistler R, Collins W, Deaven D, Gandin L, Iredell M, Saha S, White G, Woollen J, Zhu Y, Chelliah M, Ebisuzaki W, Higgins W, Janowiak J, Mo KC, Ropelewski C, Wang J, Leetmaa A, Reynolds R, Jenne R, Joseph D, 1996: The NCEP/NCAR 40-year reanalysis project. Bulletin of the American Meteorological Society, 77 (3): 437-471.

Kaser G, 2001: Glacier-climate interaction at low latitudes. Journal of Glaciology, 47 (157): 195-204.

Kaser G, Hardy DR, Molg T, Bradley RS, Hyera TM, 2004: Modern glacier retreat on Kilimanjaro as evidence of climate change: Observations and facts. International Journal of Climatology, 24 (3): 329-339.

Kaufman DS, Porter SC, Gillespie AR, 2004: Quaternary alpine glaciation in Alaska, the Pacific Northwest, Sierra Nevada, and Hawaii, in Gillespie AR, Porter SC, and Atwater BF, eds., The Quaternary Period in the United States. Developments in Quaternary Science, Volume 1, Elsevier Press, 77-103.

Kayastha RB, Ohata T, Ageta Y, 1999: Application of a mass-balance model to a Himalayan glacier. Journal of Glaciology, 45 (151): 559-567.

Kayastha, RB, Ageta Y, Fujita K, 2002: Use of positive degree-day method for calculating snow/ice melting and discharge from glacierized basins in Nepal. EGS XXVII General Assembly, abstract #3520.

Kessler MA, Anderson RS, Stock GM, 2006: Modeling topographic and climatic control of east-west asymmetry in Sierra Nevada glacier length during the Last Glacial Maximum. Journal of Geophysical Research, 111 (F2): Art. No. F02002.

Kistler R, Kalnay E, Collins W, Saha S, White G, Woollen J, Chelliah M, Ebisuzaki W, Kanamitsu M, Kousky V, van den Dool H, Jenne R, Fiorino M, 2001: The NCEP-NCAR 50-year reanalysis: Monthly means CD-ROM and documentation. Bulletin of the American Meteorological Society, 82 (2): 247-267.

Koppes MN, Gillespie AR, Burke RM, Thompson SC, Clark DH, 2003: Late Quaternary glaciation in northern Central Asia. XVI INQUA Congress, Programs with Abstracts, Reno, July, p 156.

Kuhle M, 1998: Reconstruction of the 2.3 million km (2) late Pleistocene ice sheet on the Tibetan Plateau and its impact on the global climate (vol 45, pg 71, 1998). Quaternary International, 47-8: 173-182.

Kutzbach JE, Gallimore RG, 1988: Sensitivity of a couples atmosphere atmosphere mixed layer ocean model to changes in orbital forcing at 9000 years bp. Journal of Geophyscial Researach, 93 (D1): 803-821.

Legates DR, Willmott CJ, 1990a: Mean seasonal and spatial variability in gauge-corrected, global precipitation. International Journal of Climatology, 10 (2): 111-127.

Lowell TV, Heusser CJ, Andersen BG, Moreno PI, Hauser A, Heusser LE, Schluchter C, Marchant DR, Denton GH, 1995: Interhemispheric correlation of late Pleistocene glacial events. Science, 269 (5230:1541-1549.

Mann ME, 2002: The value of multiple proxies. Science, 297 (5586): 1481-1482.

Meier, M, 1984: Contribution of small glaciers to global sea-level. Science, 226 (4618): 1418-1421.

Merle J, Carson R, Cady J, Hinz N, 2000: Quaternary geology of the Tengis_Shishid Gol region, Khovsgo, Mongolia. Anonymous Abstracts with Programs- Geological Society of America, 33 (3): 67.

Molg T, Hardy DR, 2004: Ablation and associated energy balance of a horizontal glacier surface on Kilimanjaro. Journal of Geophysical Research, 109 (D16): Art. No. D16104.

Oerlemans J, 2005: Extracting a climate signal from 169 glacier records. Science, 308 (5722): 675-677.

Oerlemanns J, Anderson B, Hubbard A, Huybrechts P, Johannesson T, Knap WH, Schmeits M, Stroeven AP, van de Wall RSW, Wallinga J, Zuo Z, 1998: Modelling the response of glaciers to climate warming. Climate Dynamics, 14 (4): 267-274.

Oerlemans J, Fortuin J, 1992: Sensitivity of glaciers and small ice caps to greenhouse warming. Science, 258 (5079): 115-117.

Ohmura A, 2001: Physical basis for the temperature-based melt-index method. Journal of Applied Meteorology, 40 (4): 753-761.

Owen LA, Finkel RC, Haizhou M, Spencer JQ, Derbyshire E, Barnard PL, Caffee MW, 2003: Timing and style of Late Quaternary glaciation in northeastern Tibet. Geological Society of America Bulletin, 115 (11): 1356-1364.

Owen LA, Gualtieri L, Finkel RC, Caffee MW, Benn DI, Sharma MC, 2001: Cosmogenic radionuclide dating of glacial landforms in the Lahul Himalaya, northern India: defining the timing of Late Quaternary glaciation. Journal of Quaternary Science, 16 (6): 555-563.

Owen LA, Kamp U, Spencer JQ, Haserodt K, 2002: Timing and style of Late Quaternary glaciation in the eastern Hindu Kush, Chitral, northern Pakistan: a review and revision of the glacial chronology based on new optically stimulated luminescence dating. Quaternary International, 97-8: 41-55.

Paterson, 1999: Physics of Glaciers. Pergamon/Elsevier Science Inc.

Paul F, Kaab A, Maisch M, Kellenberger T, Haeberli W, 2004: Rapid disintegration of Alpine glaciers observed with satellite data. Geophysical Research Letters, 31 (21): Art. No. L21402.

Peixoto JP, Oort AH, 1992: Physics of Climate. American Institute of Physics, New York: 520.

Peltier W, 1994: Ice-age paleotopography. Science, 265 (5169): 195-201.

Phillips WM, Sloan VF, Shroder JF, Sharma P, Clarke ML, Rendell HM, 2000: Asynchronous glaciation at Nanga Parbat, northwestern Himalaya Mountains, Pakistan. Geology, 28 (5): 431-434.

Plummer M, Phillips F, 2003: A 2-D numerical model of snow/ice energy balance and ice flow for paleoclimatic interpretation of glacial geomorphic features. Quaternary Science Reviews, 22(14): 1389-1406.

Porter SC, 1975: Equilibrium-line altitudes of late Quaternary glaciers in southern Alps, New Zealand. Quaternary Research, 5 (1): 27-47.

Porter SC, 1977: Present and past glaciation threshold in the Cascade Range, Washington, U. S. A.: topographic and climatic controls, and paleoclimatic implications. Journal of Glaciology, 18, 101-116.

Porter SC, Orombelli G, 1985: Glacier contraction during the middle Holocene in the western Italian Alps – evidence and implications. Geology, 13(4): 296-298.

Porter SC,1977: Present and past glaciation threshold in the Cascade Range, Washington, U. S. A.: topographic and climatic controls, and paleoclimatic implications. Journal of Glaciology, 18, 101-116.

Qiang XK, Li ZX, Powell CM, Zheng HB, 2001: Magnetostratigraphic record of the Late Miocene onset of the East Asian monsoon, and Pliocene uplift of northern Tibet. Earth and Planetary Science Letters, 187 (1-2): 83-93.

Ramanathan Y, 1987: Cumulus parameterization in a case-study of a monsoon depression. Monthly Weather Review, 108 (3): 313-321.

Reichert BK, Bengtsson L, Oerlemans J, 2002: Recent glacier retreat exceeds internal variability. Journal of Climate, 15 (21): 3069-3081.

Ren DD, Karoly D, 2006: Comparison of glacier-inferred temperatures with observations and climate model simulations. Geophysical Research Letters, 33 (23): Art. No. L23710.

Roe GH, Steig EJ, 2004: Characterization of millennial-scale climate variability. Journal of Climate, 17 (10): 1929-1944.

Ropelewski C, Halpert M, 1987: Global and regional scale precipitation patterns associated with the El-Nino Southern Oscillation. Monthly Weather Review, 115 (8): 1606-1626.

Rupper and Roe, 2007: Glacier changes and regional climate: a mass and energy balance approach. In preparation.

Rupper SB, Roe G, and Gillespie G, 2007: Spatial patterns of Holocene glacier advance and retreat in Central Asia. In preparation.

Schafer JM, Tschudi S, Zhao ZZ, Wu XH, Ivy-Ochs S, Wieler R, Baur H, Kubik PW, Schluchter C, 2002: The limited influence of glaciations in Tibet on global climate over the past 170 000 yr. Earth and Planetary Science Letters, 194 (3-4): 287-297.

Schotterer U, Frohlich K, Gaggeler HW, 1997: Isotope records from Mongolian and alpine ice cores as climate indicators. Climatic Change, 36 (3-4): 519-530.

Shi Y, 2002: Characteristics of late Quaternary monsoonal glaciation on the Tibetan Plateau and in East Asia. Quaternary International, 97-8: 79-91.

Tippett M, Barlow M, Lyon B, 2003: Statistical correction of Central Southwest Asia winter precipitation simulations. International Journal of Climatology, 23: 1421-1433.

Tsukamoto S, Asahi K, Watanabe T, Rink WJ, 2002: Timing of past glaciations in Kanchenjunga Himal, Nepal by optically stimulated luminescence dating of tills. Quaternary International, 97-8: 57-67.

Vettoretti G, Peltier WR, McFarlane NA, 1998: Simulations of mid-Holocene climate using an atmospheric general circulation model. Journal of Climate, 11 (10): 2607-2627.

Wagnon P, Sicart JE, Berthier E, Chazarin JP, 2003: Wintertime high-altitude surface energy balance of a Bolivian glacier, Illimani, 6340 m above sea level. Journal of Geophysical Research, 108 (D6): Art. No. 4177.

Wallace J, Hobbs W, 2005: Atmospheric Science: An Introductory Survey. Academic Press.

Wang B, Wu R, Fu X, 2000: Pacific-East Asian teleconnectoin: How does ENSO affect East Asian climate? Journal of Climate, 13: 1517-1536.

Wang J, 1981: Ancient glaciers at the head of Urumqui River, Tian Shan. Journal of Glaciology and Cryopedology, 3, 55-63.

Weaver AJ, Eby M, Augustus FF, Wiebe EC, 1998: Simulated influence of carbon dioxide, orbital forcing and ice sheets on the climate of the Last Glacial Maximum. Nature, 394 (6696): 847-853.

Wei Z, Zhijiu C, Yanghua L, 2006: Review of the timing and extent of glaciers during the last glacial cycle in the bordering mountains of Tibet and in East Asia. Quaternary International, 154-155: 32-43.

Wilcox EM, Ramanathan V, 2001: Scale dependence of the thermodynamic forcing of tropical monsoon clouds: Results from TRMM observations. Journal of Climate, 14 (7): 1511-1524.

Wunsch C, 2006: Abrupt climate change: An alternative view. Quaternary Research, 65 (2): 191-203.

Yang JP, Ding YJ, Chen RS, Liu SY, Lu AX, 2003: Causes of glacier change in the source regions of the Yangtze and Yellow rivers on the Tibetan Plateau. Journal of Glaciology, 49 (167): 539-546.

Zhang Y, Shiyin L, Yongjian D, 2006: Observed degree-day factors and their spatial variation on glaciers in western China. Annals of Glaciology, 43, 301-306.

Zhisheng A, Kutzbach JE, Prell WL, Porter SC, 2001: Evolution of Asian monsoons and phased uplift of the Himalayan Tibetan plateau since Late Miocene times. Nature, 411 (6833): 62-66.

Zhoa J, Zhou S, Cui J, Jiao K, Ye Y, Xu L, 2001: ESR dating of glacial tills at the headwaters of the Urumqui River in the Tianshan Mountains. Journal of Glaciology and Geocryology, 24, 737-743.

Appendix A

SUPPLEMENTAL SURFACE ENERGY-BALANCE EQUATIONS

The purpose of this appendix is to present all equations used in the surface energy- and mass-balance (SEMB) model that were not discussed in detail in the main body of Chapter 2. For more details on these equations, see Molg and Hardy (2004), Kayastha et al. (1999), and Wagnon et al. (2003).

A.1 Transfer coefficients

D_s is the turbulent-transfer coefficient under stable conditions used in calculations of latent and sensible heat fluxes. It is derived by converting the transfer coefficient for neutral-stability (D_n) to that for stable conditions. Several steps are required in this process, including a calculation of D_n, recalculating wind speed, determining the Richardson number, and finally applying a Richardson number correction to D_n to calculate D_s. The appropriate equations and terms are described below. See Tables 2.1 and 2.2 for a description of all variables and parameters.

The equation used to calculate the transfer coefficient for neutral-stability is

$$D_n = \frac{k^2 v}{[\ln(\frac{z}{z_o}) \ln(\frac{z}{z_{oh}})]}. \qquad \text{A.1}$$

Since wind speed is measured at a different level than humidity and air temperature, the wind speed was recalculated at the level of air temperature and humidity using this equation:

$$v = \frac{v^*}{k} \ln(\frac{z}{z_{om}}), \qquad \text{A.2}$$

The turbulent-transfer coefficient under stable conditions (D_s) is then obtained by converting the transfer coefficient for neutral-stability to that for stable conditions. This conversion is usually done in terms of either the Richardson number (Schneider, 1999, Kayastha et al., Wagnon et al.) or the Obukhov length (e.g., Gustafsson et al., 2001). I use the bulk Richardson number, Ri, here.

$$R_i = g\,(z - z_{om})\,(\frac{T_a - T_s}{T_a\, v^2}). \qquad \text{A.3}$$

A Φ–function correction based on R_i is then applied to D_n:

$$\Phi = (1 - 5R_i)^2, \text{ and} \qquad \text{A.4}$$

$$D_s = D_n \Phi. \qquad A.5$$

The basic equations used to calculate D_s in the latent heat equation are the same as for sensible heat with only one change. In Equation A.1, z_{oh} is replaced with z_{ov} (the scalar roughness length of water vapor).

Since neither profile measurements or sublimation measurements can be used here to determine the scalar roughness lengths, a scalar roughness length equal to 0.5 mm is used for all roughness lengths (after Kayastha et al. (1999) for a Himalayan glacier). This assumption that all three roughness lengths are equal follows the justification suggested by Molg and Hardy (2004). They state that when measurements of roughness values are not available and there is not enough data to calculate them via the surface renewal theory of Andreas (1987), then using similar roughness lengths is most appropriate (Sharan et al., 2003). While roughness lengths do influence the exact elevation of the equilibrium line, especially in regions dominated by sublimation, sensitivity tests show that ΔELA in response to a change in climate is not sensitive to the roughness lengths.

A.2 Vapor Pressure

e_a and e_s, in the latent heat equation, are calculated using the formula of Bolton (1980) for vapor pressure over a plane surface of pure water and the prevailing relative humidity (RH).

$$e_a = RH\ 0.622 \exp\left[\frac{A + T_a}{B\ T_a}\right]. \qquad A.6$$

e_s is assumed to be saturated with respect to a plane surface of pure water at surface temperature. Therefore, in calculating e_s, RH in Equation A.6 is equal to 100% and T_s is used in place of T_a.

A.3 Atmopheric pressure at the ELA

Again, since the model is seeking the ELA, air pressure must be calculated for the appropriate elevation. The difference in air temperature at the surface and at the ELA divided by the climatological lapse rate gives the change in elevation between the surface and the ELA. That information is then used to calculate the pressure at the ELA assuming hydrostatic balance, where

$$p = p_s \exp\left(\frac{-Z}{H}\right). \qquad A.7$$

Appendix B

ELA SENSITIVITY TO MODEL PARAMETERS

Though the exact position of the ELA is sensitive to the chosen model parameters, the sensitivity of the ELA to changes in atmospheric quantities is relatively insensitive to the model parameters. How the sensitivity of the ELA to changes in atmospheric variables (ΔELA/ΔVariable) changes for a given change in parameter (ΔParameter) is calculated by subtracting the ΔELA/ΔVariable for a modest increase in model parameter minus the standard case presented in Chapter 2. Table 2.5 shows the results as d(ΔELA/ΔVariable)/ΔParameter. In other words this is the change in ELA sensitivity to climate for a change in model parameter.

The results presented in Table B.1 show that the sensitivity of the ELA to the chosen values for surface roughness, C_1, and the temperature lapse rate is insensitive to modest changes in these variables. This is especially true in regions where melt is the mechanism of ablation at the ELA. The only parameter that influences the ELA sensitivity is the albedo. A modest change in albedo results in a small change in the ELA sensitivity in melt-dominated regions and a large change in ELA sensitivity in sublimation-dominated regions. Despite the greater sensitivity of the ELA sensitivity to the chosen albedo, the relative importance of

atmospheric variables does not change. In other words, melt-dominated regions are most sensitive to ablation and sublimation-dominated regions are most sensitive to precipitation, regardless of the exact magnitude of the snow/ice albedo. Thus the main conclusions presented in the body of Chapter 2 will not change for a different set of model parameters.

In all cases, ELAs in sublimation regions are more sensitive to the chosen parameters than melt-dominated regions. This again highlights the complexity of sublimation-dominated regions.

Table B.1: ELA Sensitivity to ΔParameters: Included in the table is a measure of how sensitive the ELA results are to a change in model parameter, including roughness heights (Z), albedo of the snow/ice surface (α), the downwelling longwave constant (C_1), and temperature lapse rate (λ). This is calculated as the difference in ELA sensitivity to a change in climate for the new parameter minus that for the original model run. These are labeled as d(ΔELA / ΔVariable) / ΔParameter. The changes applied to the parameters are an increase in albedo of 0.1, an increase in all roughness heights by 10 times, a decrease in C_1 by 0.01 (the mean standard deviation for Central Asia), and an increase in the lapse rate by 1 °C/km.

	East	**West**	**North**
Roughness heights increased 10 times			
d(ΔELA/ΔP) / ΔZ	8	6	22
d(ΔELA/ΔS) / ΔZ	-1	-2	-4
d(ΔELA/ΔRH) / ΔZ	0	1	-1
d(ΔELA/ΔV) / ΔZ	-0	-0	-3
Albedo increased by 0.1			
d(ΔELA/ΔP) / Δα	-50	-48	-143
d(ΔELA/ΔS) / Δα	10	3	9
d(ΔELA/ΔRH) / Δα	-0	-1	-4
d(ΔELA/ΔV) / Δα	-3	-7	4
Downwelling longwave emissivity decreased by 0.01			
d(ΔELA/ΔP) / ΔC_1	-8	-7	-9
d(ΔELA/ΔS) / ΔC_1	1	-7	3
d(ΔELA/ΔRH) / ΔC_1	0	0	0
d(ΔELA/ΔV) / ΔC_1	-0	-1	1
Lapse rate increased by 1 °C/km			
d(ΔELA/ΔP) / Δλ	0	1	10
d(ΔELA/ΔS) / Δλ	-0	0	-0
d(ΔELA/ΔRH) / Δλ	-0	-3	-1
d(ΔELA/ΔV) / Δλ	-0	-0	0